UNIVERSIDAD DE CHILE
FACULTAD DE CIENCIAS FÍSICAS Y MATEMÁTICAS
DEPARTAMENTO DE INGENIERÍA ELÉCTRICA

ANALYSIS AND EVALUATION OF NYQUIST-I PULSES IMPAIRED BY INTER-SYMBOL AND CO-CHANNEL INTERFERENCE

TESIS PARA OPTAR AL GRADO DE MAGÍSTER EN
CIENCIAS DE LA INGENIERÍA, MENCIÓN ELÉCTRICA

MEMORIA PARA OPTAR AL TITULO DE INGENIERO CIVIL ELÉCTRICO

JAIME ANDRÉS ARANDA CUBILLO

PROFESOR GUÍA:
DR. CESAR AUGUSTO AZURDIA MEZA

PROFESOR CO-GUÍA:
DR. SAMUEL MONTEJO SÁNCHEZ

MIEMBROS DE LA COMISIÓN:
DR. NESTOR JORGE BECERRA YOMA
DR. CARLOS ADRIÁN GUTIÉRREZ DÍAZ DE LEÓN

Este trabajo ha sido parcialmente financiado por Proyecto FONDECYT Iniciacion, Grant No. 11160517

SANTIAGO DE CHILE
2019

RESUMEN DE TESIS PARA OPTAR AL
TÍTULO DE MAGISTER EN CIENCIAS
DE LA INGENIERÍA, MENCIÓN ELÉCTRICA
RESUMEN DE LA MEMORIA PARA OPTAR AL
TÍTULO DE INGENIERO CIVIL ELÉCTRICO
POR: JAIME ANDRÉS ARANDA CUBILLO
FECHA: ENERO 2019
PROF. GUÍA: DR. CESAR AUGUSTO AZURDIA MEZA

ANALYSIS AND EVALUATION OF NYQUIST-I PULSES IMPAIRED BY INTER-SYMBOL AND CO-CHANNEL INTERFERENCE

Las actuales tendencias en los sistemas de comunicaciones inalámbricas, nos llevan a diseñar sistemas con un eficiente uso del espectro, ya que los requisitos de tasas de transmisión, de manera conservadora, se duplican cada año. La transmisión de señales a altas tasas genera interferencia inter-simbólica (ISI), efecto que degrada el rendimiento de los sistemas de comunicaciones. El diseño de señales libres de ISI en canales limitados en banda fue un problema abordado por Nyquist. El primer criterio de Nyquist (Nyquist-I), garantiza que una secuencia de pulsos será libre de ISI siempre y cuando sea muestreada en múltiplos del tiempo de símbolo. De la misma forma, el desarrollo de nuevas tecnologías, como *Machine to Machine Communication* (M2MC), *Internet of Things* (IoT) o redes móviles 5G, han introducido una gran cantidad de dispositivos demandando también un uso eficiente del espectro. En estos ambientes, la detección de datos de un usuario a menudo se corrompe por señales de otros usuarios ubicados en distancias cercanas o moderadas que usan la misma banda de frecuencia. El objetivo del re-uso de frecuencias es incrementar la eficiencia espectral. Este tipo de interferencia es llamada interferencia co-canal (CCI) y afecta negativamente el desempeño de los sistemas de comunicaciones. Así, la evaluación de diferentes pulsos de Nyquist-I, que mitigan los efectos de interferencias, es de considerable interés.

En el presente trabajo se realiza la evaluación, comparación y análisis de distintos pulsos de Nyquist-I, considerando los efectos de la ISI, CCI y simultáneamente, ISI y CCI en sistemas banda-base y pasa-banda. Se considera la respuesta completa y truncada de los pulsos. Además se consideran 2 modelos para representar los efectos del CCI, el modelo sinusoidal y Preciso. Este análisis se realiza debido a que el tópico es escasamente tratado en la literatura. Luego, para realizar una comparación justa, los parámetros de los pulsos son optimizados considerando restricciones en el dominio de la frecuencia para condiciones particulares de los sistemas de comunicaciones. Los pulsos se evaluan principalmente en términos de la probabilidad de error de bit (BER) y, en todos los casos se presenta su comportamiento en el dominio de la frecuencia. Lo resultados indican que existen diferencias significativas en cuanto al desempeño de los pulsos, considerando distintos tipos de interferencias y tipos de respuesta. Los resultados anteriores pueden ser utilizados para hacer un diseño más eficiente de los sistemas de comunicaciones o también crear filtros adaptativos que modifiquen sus parámetros considerando las condiciones particulares de propagación.

Summary

The current trends in wireless communications systems, lead us to design better spectral efficient digital communication systems, as data rate requirements are conservatively doubling each year. Transmitting signals at high transmission rates introduce inter-symbol interference (ISI), degrading the performance of communication systems. The design of ISI free signals in band-limited channels was a problem considered by Nyquist. Nyquist first criterion (Nyquist-I) guarantees that a sequence of pulses will be ISI-free by sampling signals in multiples of the symbol time. In the same way, the introduction of new technologies, like Machine to Machine Communication (M2MC), Internet of Things (IoT) and 5G mobile networks have introduced large amount of devices, demanding an efficient use of the spectrum. In such crowded environments, the detection of one user's data is often corrupted by signals from users located in near or moderate distances using the same frequency band. The aim of the frequency reuse is to increase the spectrum efficiency. This interference is called co-channel interference (CCI) and affects negatively the performance of digital communication systems. Therefore, evaluate different Nyquist-I pulses, which mitigate the interference effects, is of considerable interest.

In the present work, the evaluation, comparison and, analysis of different Nyquist-I pulses is performed, considering the effects of ISI, CCI and simultaneously ISI and CCI in base-band and pass-band systems. The complete and truncated response of the pulses is considered. Also, 2 models to represent the effects of CCI are taking into account, the sinusoidal and Precise models. This analysis is performed because the topic is barely treated in the literature. Then, to make a fair comparison, the pulses parameters are optimized considering restrictions in the frequency domain for particular conditions of the communication systems. All the pulses are evaluated mainly in terms of the bit error probability (BER), and in all the cases the behavior in the frequency domain is presented. The results indicate that exists significant differences respect to the performance of the pulses, considering different kinds of interference and response types. The prior results can be used to make a more efficient design of communication systems or also create adaptive filters that modify their parameters considering the particular propagation conditions.

A mi familia,

Acknowledgements

Este trabajo resume largo años de estancia en la universidad, largos años de lucha, de esfuerzo, de ponerle ganas, de noches sin dormir, sufrimientos, impotencias, des-encuentros, pero también, porque no todo es de extremos, de alegrías, cambios, evoluciones, sorpresas, amores y esperanza. Han sido 8 años desde que inicié el camino de formación profesional, sin saber realmente lo que significaba, ni las tremendas responsabilidades que esto conlleva.

Agradezco enormemente a mi mamá y mi papá, quienes toda su vida han luchado para darme la oportunidad de educarme, agradezco todos las comiditas ricas, los paseos, vacaciones, toda la entrega que tienen cuando se trata de sus hijos. A mis hermanos, el Mati y la Andreita, por su paciencia para soportarme todos estos años, también por su compañía y su hermandad. A mi familia Materna y Paterna por siempre estar dispuestos a juntarnos, conversar, tomar oncecita, por ser parte de mi vida.

Agradezco, al profesor Cesar Azurdia, quien me ha apoyado incondicionalmente durante mi instancia en Ing. Eléctrica, por ser comprensivo y apañador, por todas las pichangas que nos jugamos, espero que sean muchas más y espero haber estado a la altura del desafío. A los profesores que tuve durante mi formación, a mis compañeros de laboratorio, Alexis, Tomás, Pablo, Adriana, Lerko, Sebi, Sandy por siempre estar dispuestos a resolver alguna duda, apoyar con ideas o simplemente procastinar. A Samuel por su ayuda, siempre aportando a todos con ideas locas.

Agradezco a mis amigxs de la vida, a Paino, Avito, Paipin, por darme su amistad, compartir distintas cosas, lo bueno, lo malo, espero que sigamos siendo familia. También agradezco a mis amigos de la Universidad, a Solsticio, al Chela, Matus, Estebin, al Isma, Guaja, Dress por su apañe, su compañía, buena onda y acudir al llamado. También agradezco a la FAE, grande cabros!. A mis amigxs de la comparsa, sin ustedes este último año hubiese sido imposible.

Finalmente quiero dedicarme un par de palabras; este proceso que culminará pronto abrirá las puertas a un sin fin de oportunidades, cuando estés confundido pregúntate, ¿Cuál es el camino con corazón?, lucha incesantemente por lo que te parece justo, no hagas vista gorda a las injusticia y nunca pare de soñar, que una idea puede más que cien misiles, siempre firme hacia adelante, a no rendirse jamás!.

Contents

List of Tables

List of Figures

Acronyms

BER Bit Error Rate

SNR Signal to Noise Ratio

TO Timing Offset

UE User Equipment

BS Base Station

OFDM Orthogonal Frequency-Division Multiplexing

ICI Inter Carrier Interference

SC-FDMA Single-Carrier Frequency-Division Multiple Access

PAPR Peak-to-Average Power Ratio

ISI Inter-Symbol Interference

CCI Co-Channel Interference

ACI Adjacent Channel Interference

PSF Pulse Shaping Filter

ADR Asymptotic Decay Rate

PSD Power Spectral Density

FIR Finite Impulse Response

AWGN Additive White Gaussian Noise

RC Raised Cosine

RRC Root Raised Cosine

PLCP Parametric Linear Combination Pulse

LCP Linear Combination Pulse

ELP Exponential Linear Pulse

SPLCP Sinc Parametric Linear Combination Pulse

IPLCP Improved Parametric Linear Combination Pulse

MKEF Modified K-Exponential Filter

PFE Piecewise Flipped-Exponential

RV Random Variable

Chapter 1

Introduction

1.1 Motivation

The current trends in wireless communications systems lead us to design better spectral efficient systems as data rate requirements are conservatively doubling each year [1]. Transmitting signals at higher transmission rates introduces ISI, which impacts negatively the communication performance. The design of ISI free signals in band-limited channels was a problem considered by Nyquist [2], [3]. Nyquist first criterion (Nyquist-I) guarantees that a sequence of pulses will be ISI-free by sampling signals at the optimum and uniformly spaced instants. Additionally to the ISI-free prerequisite, pulse shaping filters have to show low sensitivity to timing errors. To meet the prior constraints, several pulses that comply with the first Nyquist criterion (Nyquist-I pulses) have been reported, being the most popular ISI-free Nyquist pulse for distortionless transmissions the traditional raised cosine (RC) pulse. The RC pulse has been proposed by the 3rd Generation Partnership Project (3GPP) as the pulse shaping filter to be implemented at the user equipment (UE) and at the base station (BS) [4, 5].

In [6], an efficient series used to compute the bit error probability (BER) in a binary symmetric channel subject to additive noise and affected by ISI is derived. This series is extensively used in the literature to study the effects of ISI in base-band systems for various Nyquist-I pulses, reporting better results in terms of BER [2, 7, 8, 9, 3] than the RC pulse in the presence of symbol timing errors and for different roll-off factors. Besides the effects caused by ISI, other types of interference could affect more severely the performance of the communication system.

On the other hand, the emergence of new technologies such as Machine to Machine Communication (M2MC), Internet of Things (IoT), and 5G mobile networks have introduced a large amount of devices connected to the network, demanding an efficient use of the spectrum. In such crowded environments, the detection of one user's data is often corrupted by signals from users located in near or moderate distances using the same frequency band. The aim of the frequency reuse is to increase the spectrum efficiency. This type of interference is knows as CCI and generates adverse effects on the digital communication systems. The limitations

in the performance of the digital communication systems are ruled by different sources of interference. Therefore, analyzing the performances of these systems in the presence of CCI is of considerable interest.

Different approaches for representing the effects of CCI have been investigated. In [10], the sinusoidal model (sum of sinusoids) is presented and evaluated in a pass-band system. Unfortunately, the sinusoidal interference model always underestimates the effects of interference on the BER for large values of SNR. Research has been ongoing over the last decades trying to develop more accurate models to represent the CCI effects. In [11], the resultant interference contribution is modeled by an additive Gaussian noise with mean and variance equal to the mean and variance of the sum of the interfering signals. However, the Gaussian model overestimates the effects of the CCI. For this reason, in [12], the Precise interference model for representing the CCI is used. In this model, the interfering signals are assumed to have the same modulation and nature as the desired signal.

Studies regarding the performance of Nyquist-I pulses considering the effects of ISI and CCI simultaneously is very scarce in the literature. In fact, the only existing model, proposed in [6], which considers the sinusoidal model to represent the CCI effect, has not been used to evaluate the performance of novel Nyquist-I pulses. Further, exact models have not been developed considering both interference, giving a great research opportunity.

Finally, the optimization of Nyquist-I pulses is an open research topic which has attracted attention recently. The optimization of Nyquist-I pulses consists in finding the parameters that minimize one or more objective functions. Usually, the BER is minimized considering base-band, orthogonal frequency-division multiplexing (OFDM) or single carrier orthogonal frequency division multiple access (SC-FDMA) systems, impaired by different sources of interference. In several works [13, 14], the parameters of Nyquist-I pulses are optimized without taking into account frequency domain restrictions, resulting in excellent BER performance but at expenses of poor frequency characteristics. In addition, and to our best knowledge, there are no studies related to the optimization of Nyquist-I pulses considering frequency domain restrictions or multiple sources of interference.

1.2 Hyphothesis

- The evaluation and fair comparison of recently proposed Nyquist-I pulses, considering the effects of ISI, CCI, and both interference simultaneously, can be performed in base-band and pass-band communication systems.

1.3 Objectives

1.3.1 General Objective

To evaluate Nyquist-I pulses with optimal parameters in base-band and pass-band systems impaired by ISI, CCI, and the combination of ISI and CCI, for the sinusoidal and Precise interference models, considering different scenarios in terms of BER.

1.3.2 Specific Objectives

- To evaluate the performance of recently proposed Nyquist-I pulses, including the exponential linear pulse (ELP), in base-band system impaired by ISI, CCI, ISI and CCI simultaneously considering the BER and eye diagram opening for the ideal and time-limited version of its impulse responses.
- To integrate the Precise interference model for representing the CCI effect along with the ISI model, develop an expression to compute the BER in presence of time symbol errors, and evaluate different Nyquist-I pulses in terms of BER for several evaluation scenarios for pass-band systems.
- To optimize Nyquist-I pulses in terms of BER considering different interference models by imposing restrictions on the frequency response of the pulses to be optimized.

1.4 Thesis Structure

The present work is organized as follows:

- Chapter 2 presents the general background of the work, describing the basic blocks of a digital communication systems. Nyquist's first criterion for distortion-less transmission and its use in the matched filter scheme are presented. Then, different approaches to formulate Nyquist-I pulses are described, and for every pulse, its time and frequency behavior is shown.
- Chapter 3 evaluates the Nyquist-I pulse known as ELP in the time and frequency domain using different evaluation tools, and compares its performance with other existing pulses.
- Chapter 4 evaluates recently proposed Nyquist-I pulses in terms of bit error rate (BER) considering first, the effect of CCI and later, the ISI and CCI simultaneously, under the effects of time jitter.
- Chapter 5 introduces the Precise model to represent the CCI effects more accurately. Then, a pass-band system is evaluated under ISI and CCI simultaneously, using the new model, for various Nyquist-I pulses in several scenarios under the effect of time jitter.
- Chapter 6 formalizes the optimization problem to minimize the BER in a system impaired by ISI and later by ISI and CCI, using the Precise model, and considering

Nyquist-I pulses obtained by a linear combination. Then, optimized pulses are evaluated under both interference scenarios.

- Chapter 7 summarizes the conclusions in this work, and presents future work.

Chapter 2

Background

2.1 Digital Communication Systems

The objective of a digital communication system is to send data efficiently from a transmitter to a receiver through a channel, subject to noise and multiple interference. A general digital communication system is shown in Fig. 2.1. The data is provided by the **Source**, and passed to the **Source Coding** block, which usually chooses and represents the data in digital form. Then, the information is treated by the **Channel Coding** block, which is responsible for adding bits of redundancy to the sequence. These bits would allow detecting and correct errors generated in the transmission. The **Digital Modulation** block performs the conversion of digital data to an analog signal in base-band, and limits the bandwidth of the transmitted signal, according to the channel requirements, by applying a filter. Finally, the **Pass-Band Modulation** block positions the analog signal in the frequency band chosen for the subsequent transmission.

The signal travels through a communications channel, namely the physical medium that can be wired, optical fiber, or wireless. The information is corrupted in a randomly by a variety of possible mechanisms, such as additive thermal noise, ISI, multi-path, shadowing, CCI or adjacent channel interference (ACI).

When the signal arrives at the Receiver, the **Pass-Band Demodulation** process is performed, shifting the central frequency to the base-band spectrum and filtering the base-band signal, usually with a matching filter, improving the signal-to-noise ratio. Then, the signal is **Sampled** at uniform spaced instants, using at least the Nyquist rate for a successful reconstruction of the signal. The **Detection** process is then performed by estimating the transmitted symbol based on the received samples. The **Channel De-coding** block is responsible for detecting and correcting errors by reviewing the redundant bits, and finally the **Source De-codification** recovers the original data.

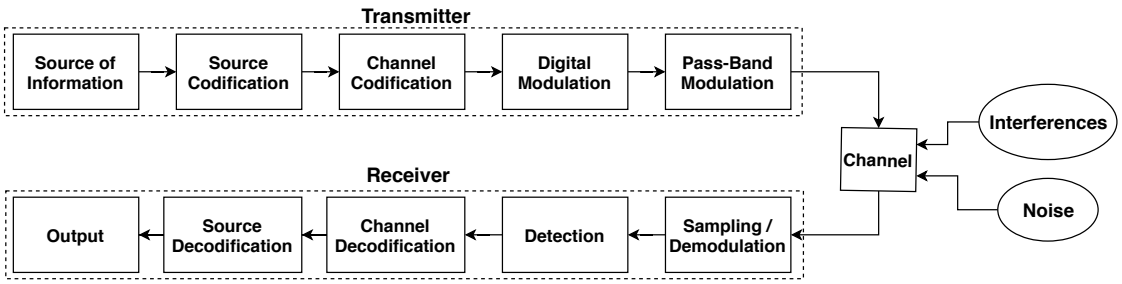

Figure 2.1: Standard digital communication system.

2.1.1 Matched Filter

In the Digital Modulation and Demodulation blocks, there exists a filtering process which converts the digital data into an analog signal, and then after the signal travels through a communication channel affected by Additive White Gaussian Noise (AWGN), transforms back the signal from analog to digital. If both filters in cascade form a matched filter, then the Signal to Noise (SNR) ratio is maximized at the output of the receiver. If we group all the filtering effects into one equivalent system its transfer function $H(f)$, considering $H_T(f)$, $H_R(f)$, $H_C(f)$ the response filter in the transmitter, receiver, and channel, respectively, is given by

$$H(f) = H_T(f)H_C(f)H_R(f). \tag{2.1}$$

To prove that the matched filter maximizes the SNR at the output of the receiver consider that a known signal $s(t)$ plus AWGN $n(t)$ is the input to a linear time-invariant filter followed by a sampler. At time $t = T$, the sampler output consists of a signal component a_i and a noise component σ_0^2, therefore the instantaneous signal power to average noise power at time $t = T$, $(S/N)_T$ at the output of the sampler is

$$\left(\frac{S}{N}\right)_T = \frac{a_i^2}{\sigma_0^2}. \tag{2.2}$$

We wish to find the filter transfer function ($H_0(f)$) that maximizes (2.2). If we denote $S(f)$ the Fourier transform of the input signal, we can express the signal a_i at the filter output before the optimization as

$$a_i(t) = \int_{-\infty}^{\infty} H(f)S(f)e^{j2\pi ft}df, \tag{2.3}$$

if the two-sided power spectral density of the input noise is $N_0/2$ watts/hertz, then we can express the output noise power as

$$\sigma_0^2 = \frac{N_0}{2}\int_{-\infty}^{\infty} |H(f)|^2 df, \tag{2.4}$$

combining (2.3) and (2.4) to express $(S/N)_T$

$$\Big(\frac{S}{N}\Big)_T = \frac{\Big|\int_{-\infty}^{\infty} H(f)S(f)e^{j2\pi ft}df\Big|^2}{\frac{N_0}{2}\int_{-\infty}^{\infty}|H(f)|^2df}. \tag{2.5}$$

Next, we find the value of $H(f) = H_0(f)$ for which the maximum $(S/N)_T$ is achieved, using the *Schwarz's* inequality, we can write the upper bound of (2.3) as

$$\Big|\int_{-\infty}^{\infty} H(f)S(f)e^{j2\pi ft}df\Big|^2 \leq \int_{-\infty}^{\infty}|H(f)|^2df\int_{-\infty}^{\infty}|S(f)|^2df. \tag{2.6}$$

Substituting into (2.5), yields

$$\Big(\frac{S}{N}\Big)_T \leq \frac{2}{N_0}\int_{-\infty}^{\infty}|S(f)|^2df, \tag{2.7}$$

or

$$max\Big(\frac{S}{N}\Big)_T = \frac{2E}{N_0}, \tag{2.8}$$

where the energy of the input signal, $s(t)$ is

$$E = \int_{-\infty}^{\infty}|S(f)|^2df. \tag{2.9}$$

The equality in (2.8) holds only if the optimum filter transfer function $H_0(f)$ is employed, such that

$$H_0(f) = kS^*(f)e^{-j2\pi fT}, \tag{2.10}$$

since $s(t)$ is a real-valued signal, we can write

$$f(x) = \begin{cases} ks(T-t), & 0 \leq t \leq T, \\ 0, & \text{elsewhere.} \end{cases} \tag{2.11}$$

Therefore, the impulse response of a filter that produces the maximum output SNR is the mirror image of the message signal, $s(t)$ delayed by the symbol time duration. So, the matched filter condition expressed in (2.11), can be composed of the convolution of 2 separated filters, as is showed in Fig. 2.2.

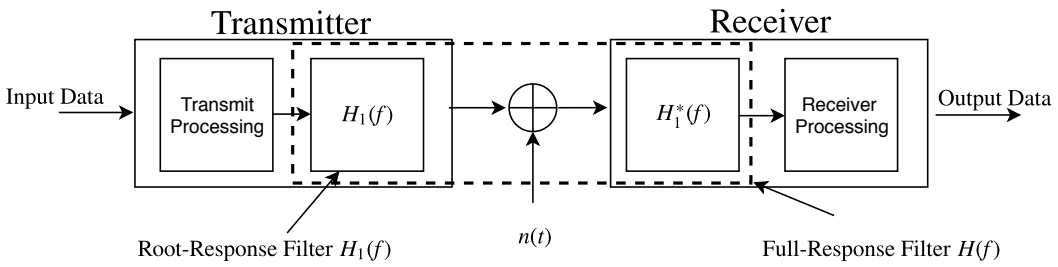

Figure 2.2: Matched Filter.

2.2 Nyquist Criterion in the time and frequency domain

When signals are transmitted over a communication channel, there exist various types of interference which distort the desired signal making the communication less reliable. The ISI is the effect of one symbol interferes with subsequent symbols. The spreading of the pulse beyond its allotted time interval causes interference to neighbor pulses degrading the performance of the overall system. In [15], Harry Nyquist established three criteria, related to the signal waveform, that result in distortion-less transmission considering an AWGN channel. The first and more used criterion is defined as

$$h\left(kT\right) = \begin{cases} 1, \ k = 0 \\ 0, \ k = \pm 1, \pm 2, \pm 3 \pm 4, \ldots, \end{cases} \tag{2.12}$$

where $h(t)$ is the impulse response of the filter, and T is the symbol period. In the frequency domain, the Fourier transform of 2.12 is given as follows

$$\frac{1}{T} \sum_{m=-\infty}^{\infty} H(f + \frac{m}{T}) = 1, \tag{2.13}$$

where H(f) is the Fourier transform of h(t). The first Nyquist criteria [16] is exemplified in Fig. 2.3, where the desired signal located at $t = 0$ reaches its maximum amplitude at $h(0) = 1$, meanwhile, its lateral side lobes evaluated at $t = kT$ for $k = \{\pm 1, \pm 2, \pm 3 \pm 4, \ldots, \}$ are equal to $h(kT) = 0$. When the resultant filter, built by the transmitter and receiver filters in cascade, comply with the first Nyquist criterion the transmission is not affected by ISI. But, if exists deviation from the optimum sampling instants, the system will be impaired by ISI, degrading its performance. In practical receivers, the presence of timing jitter causes the actual sampling points to diverge from the optimal ones; hence, symbol timing errors are produced. So, in addition to the ISI-free prerequisite, pulse shaping filters have to exhibit low sensitivity to timing errors.

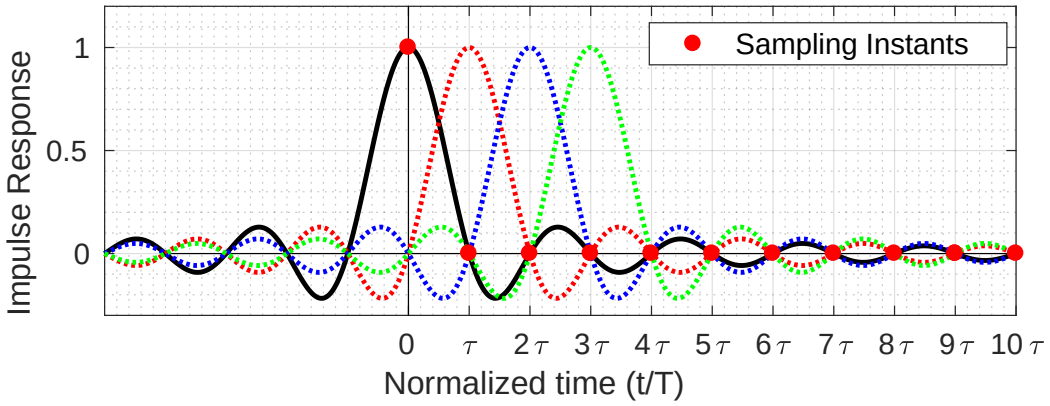

Figure 2.3: Train of Sinc pulses.

2.2.1 Nyquist-I pulses

There exists theoretically an infinite number of filters that comply with the first Nyquist criteria, namely Nyquist-I pulses, with multiple shapes and frequency characteristic. In this section, various classical and recently proposed Nyquist-I pulsed are detailed, including their impulse and frequency responses.

Rect Filter

The *Rectangular* filter or zero-order hold filter, is the simplest filter which complies with the first Nyquist criteria. In Fig. 2.4, the impulse response and the frequency characteristic of the pulse are shown. It can be seen from the Impulse response that the filter would exhibit no ISI at all even considering time jitter, but in exchange for having an infinite stop-band value in its spectral characteristic, not fulfilling the bandwidth (B) restriction imposed by the channel. Further, this pulse cannot be implemented due to the sharp edges of its impulse response and the non-causal response.

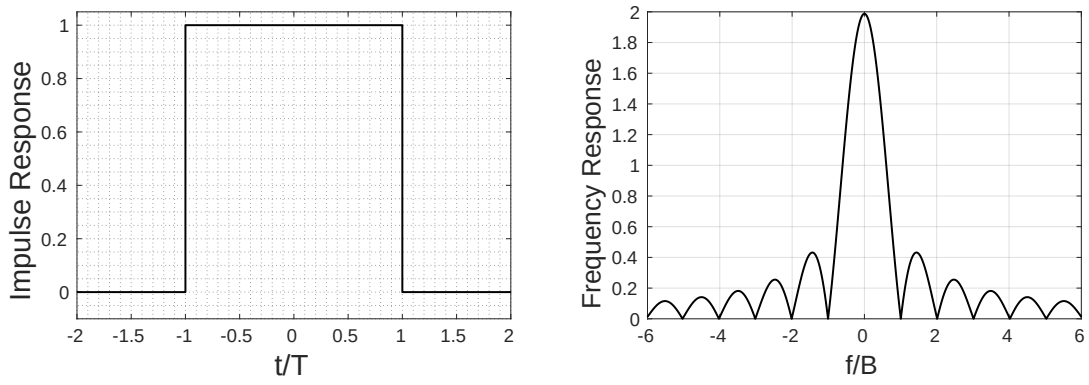

Figure 2.4: Impulse Response and Frequency characteristic of the Rect Filter.

Sinc Filter

The *Sinc* pulse, which also complies with the first Nyquist criteria, is the most bandwidth efficient pulse because its frequency characteristic is a rectangular shape ($-1/2T < f/B < 1/2T$). This pulse, derived by Nyquist [15], is defined in the time and frequency domain respectively as:

$$h_{sinc}(t) = \frac{\sin(\pi t/T)}{\pi t/T}, \tag{2.14}$$

$$H_{sinc}(f) = \begin{cases} 1, & 0 \leq |f| \leq \dfrac{1}{2T} \\ 0, & |f| \geq \dfrac{1}{2T}. \end{cases} \tag{2.15}$$

In Fig. 2.5, its impulse response and frequency characteristic is shown

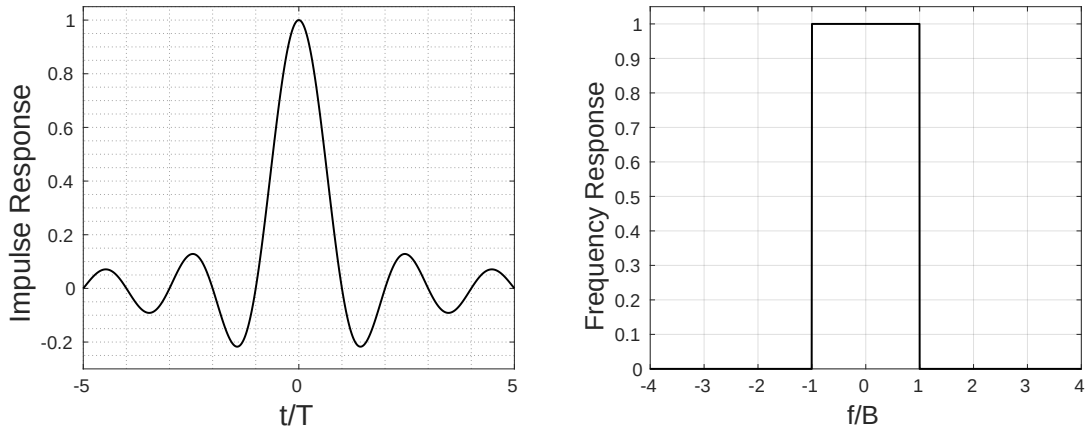

Figure 2.5: Impulse Response and Frequency characteristic of the Sinc Filter.

Besides its optimal frequency characteristic response, the slow extinction of the lateral

side lobes causes severe ISI when the system is not sampled at optimal instants, degrading the Bit Error Rate (BER), the main performance of communication systems. It is for this reason that any pulse that complies with the first Nyquist criteria, have to exhibit a fast decay of its lateral side lobes to exhibit low sensitivity to time jitter effects. As drawback of having fast decay of the lateral side lobes, the stop band value of the filter's frequency characteristic would increase beyond the most bandwidth efficient value, $\pm 1/2T$.

2.2.2 Raised Cosine Filter

Nyquist demonstrated that pulses satisfying a vestigial side band criterion, namely, that the pulse has an excess bandwidth with odd-symmetry around Nyquist frequency ($B = 1/2T$), will comply with the first Nyquist criteria. A family of such pulses, known as *Raised Cosine pulse* (RC), produces a signal with bandwidth $(1/2T)(1+\alpha)$, where $\alpha \in [0,1]$ namely the roll-off factor, the parameter that controls the amount of excess of bandwidth. The RC pulse is defined in the time and frequency domain as

$$h(t)_{RC} = \frac{\sin(\pi t/T)}{\pi t/T}\frac{\cos(\pi\alpha t/T)}{1-(2\alpha t/T)^2}, \tag{2.16}$$

$$H_{RC}(f) = \begin{cases} T, & 0 \le |f| \le \dfrac{1-\alpha}{2T} \\ \dfrac{T}{2}\left[1+\cos\left(\dfrac{\pi T}{\alpha}\right)\left(|f|-\dfrac{1-\alpha}{2T}\right)\right], & \dfrac{1-\alpha}{2T} \ge |f| \ge \dfrac{1+\alpha}{2T} \\ 0, & |f| \ge \dfrac{1+\alpha}{2T}. \end{cases} \tag{2.17}$$

Figure 2.6 depicts the impulse and frequency response of the RC pulse.

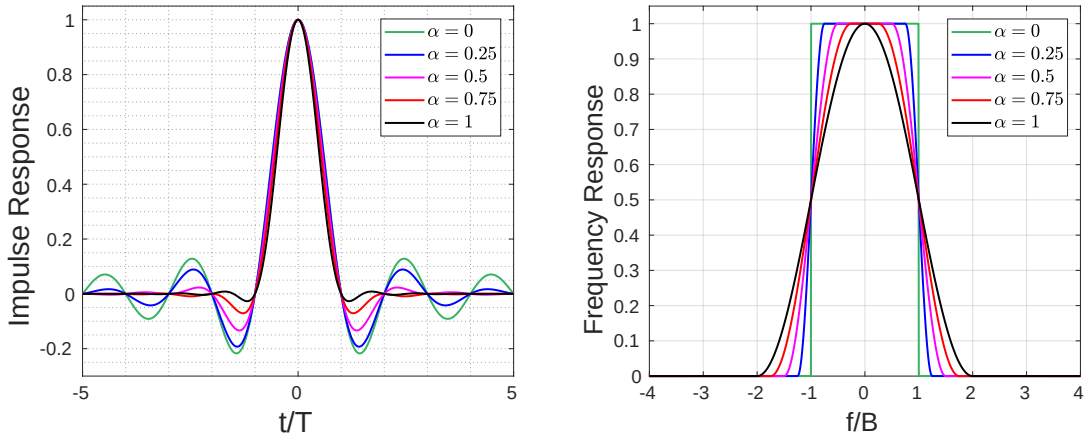

Figure 2.6: Impulse Response and Frequency characteristics of the RC Filter.

The root version of the RC filter, the *root-raised cosine* (RRC) filter, with roll-off factor of $\alpha = 0.22$ is the transmitting pulse-shaping filter used by the 3rd Generation Partnership

Project (3GPP) as the pulse shaping filter to be implemented at the user equipment (UE) and at the base station (BS), for transmission and reception, forming in cascade a RC filter. The frequency spectrum and the impulse response of the RRC are given by

$$H_{RRC}(f) = \sqrt{H_{RC}}, \tag{2.18}$$

$$h_{RRC}(t) = \frac{4\alpha}{\pi\sqrt{T}} \frac{\cos\left(\frac{(1+\alpha)\pi t}{T}\right) + \frac{T}{4\alpha t}\sin\left(\frac{(1-\alpha)\pi t}{T}\right)}{1-\left(\frac{4\alpha t}{T}\right)^2}. \tag{2.19}$$

2.2.3 Parametric Approach

There is an infinite number of pulses that comply with the first Nyquist criteria having different vestigial side-bands. In [2], the author proposed a parametric approach for constructing families of ISI-free pulses with the same excess bandwidth. The pulses that comply with the parametric approach are specified by the frequency spectra given in (2.20)

$$S(f) = \begin{cases} T, & 0 \le f < 0 \\ T\mathcal{G}(\gamma_n[f - B(1-\alpha)]^n), & B(1-\alpha) \le f \le B \\ T\{1 - \mathcal{G}(\gamma_n[B(1+\alpha) - f]^n), & B < f \le B(1+\alpha) \\ 0, & B(1+\alpha) < f, \end{cases} \tag{2.20a}$$

$$\gamma_n = \frac{\gamma_0}{\alpha^n B^n}, \tag{2.20b}$$

$$\gamma_0 = \mathcal{G}^{-1}\left(\frac{1}{2}\right). \tag{2.20c}$$

In (2.20), $\mathcal{G}(f)$ is a function satisfying $\mathcal{G}(0) = 1$ and $n \ge 0$ is a parameter that defines different pulses. The author, in the same work, proposed several $\mathcal{G}$ functions, which results in different Nyquist-I family of pulses.

The time domain properties of the pulses specified by the frequency spectra of (2.20) are analyzed to establish how rapidly the tails of the pulses decay in time, namely the Asymptotic Decay Rate (ADR). The ADR is computed from the spectrum of the pulse by means of Theorem 1,

Theorem 1 If the first $m-1$ derivatives of $S(f)$ are continuous and the m^{th} derivative of $S(f)$ has one or more finite amplitude discontinuities, then $|p(t)|$ decays as $1/|t|^{m+1}$ when $|t|$ is large.

Considering the RC pulse, its impulse response ADR is $1/|t|^3$ when $|t|$ is sufficiently large.

2.2.4 Linear combination approach

Further, in [17] a new approach for finding families of Nyquist-I pulses is derived. The linear combination of two or more Nyquist-I pulses ensures that the resulting pulse will also be ISI-free keeping the same stop-band value ($(1+\alpha)(1/2T)$). The linear combination is described by the equation (2.21),

$$h(t) = a_1 h_1(t) + a_2 h_2(t) + ... + a_n h_n(t), \tag{2.21}$$

The linear constants have to follow the following relation $\sum_{n=1}^{N} a_n = 1$.

PLCP

In [18], the author proposed a linear combination of 2 pulses used to reduce peak-to-average power ratio (PAPR) in SC-FDMA systems. The Parametric Linear Combination Pulse (PLCP) is composed of 2 previously proposed pulses [2], the parametric linear pulse for n=1 and n=2 with $\mathcal{G}(f) = 1 - f$, keeping the same stop-band value. The new pulse contains one degree of freedom and is described by the equation (2.22)

$$\begin{aligned} h_{PLCP}(t) &= \mu h(t)_{PLP_{n=1}} + (1-\mu) h(t)_{PLP_{n=2}} \\ &= \frac{sin(\pi\tau)}{\pi\tau} \times \frac{4(1-\mu)\sin(\pi\alpha\tau/2)^2 + \pi\alpha\mu\tau\sin(\pi\alpha\tau)}{\pi^2\alpha^2\tau^2}, \end{aligned} \tag{2.22}$$

where τ is the normalized time ($\tau = t/T$), μ is the constant that correspond to the linear combination and defined for all real numbers. The impulses responses of $PLP_{n=1}$ and $PLP_{n=2}$ are given in [2], and decay as $1/t^2$ and $1/t^3$ respectively meanwhile the PLCP decays as $1/t^2$. The impulse response of the pulse is shown in Fig. 2.7

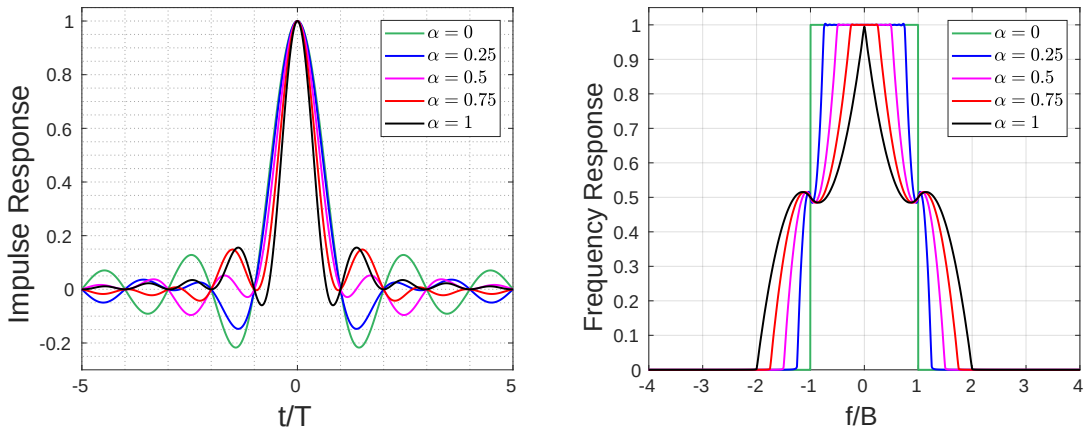

Figure 2.7: Impulse Response and Frequency characteristic of the PLCP Filter for $\mu = 2.418$.

LCP

In [3], the author proposed another combination of 2 pulses, the parametric linear pulse for $n = 1$ and RC pulse. The Linear Combination Pulse (LCP) contains a new design parameter

β, giving an additional degree of freedom to minimize the bit error probability performance in the presence of symbol-timing errors, for a given roll-off factor (α). The impulse response of the pulse is given by

$$\begin{aligned} h(t)_{LCP} &= \beta h(t)_{PLP_{n=1}} + (1-\beta)h(t)_{RC} \\ &= \frac{sin(\pi\tau)}{\pi\tau} \times \Big(\frac{\beta \sin(\pi\alpha\tau)}{\pi\alpha\tau} + \frac{(1-\beta)\cos(\pi\alpha\tau)}{1-4\alpha^2\tau^2}\Big). \end{aligned} \tag{2.23}$$

The characteristic function, $\mathcal{G}$, corresponds to $\mathcal{G}(f)_{PLP_{n=1}} = 1 - f$ and $\mathcal{G}(f)_{RC} = \cos(f)^2$ with decay rate equal to $1/t^2$ and $1/|t|^3$, respectively. Thus, the decay rate of the LCP pulse is $1/t^2$

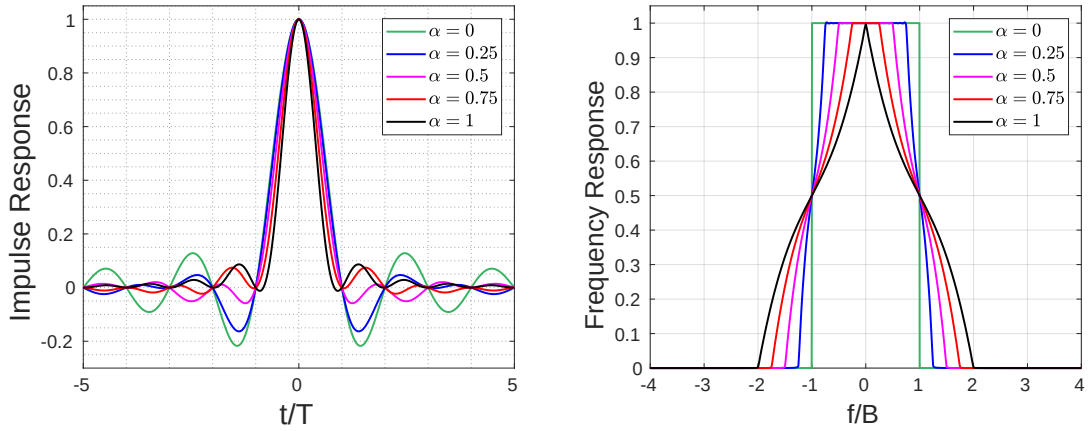

Figure 2.8: Impulse Response and Frequency characteristic of the LCP Filter for $\beta = 1.7$.

r Filter

In [19], pulses with an asymptotic decay rate of t^{-k} for any integer value of k are proposed. The $\mathcal{G}(f)$ function used is a polynomial function given by $\mathcal{G}(f) = \sum_{i=0}^{n} a_i f^i$ with n being the polynomial degree. Later, in [9], this method is used to construct families of pulses based on the linear combination of several pulses.

In the first case, the linear combination technique for a pair of pulses is applied, one has an ADR of t^{-2} ($s_2(t)$) and the other with an ADR of t^{-3} ($s_3(t)$), resulting in ADR of t^{-2} (r(t)),

$$r(t) = as_2(t) + (1-a)s3(t). \tag{2.24}$$

The impulse and frequency response of the constituent pulse of the linear combination is illustrated in Fig. 2.9

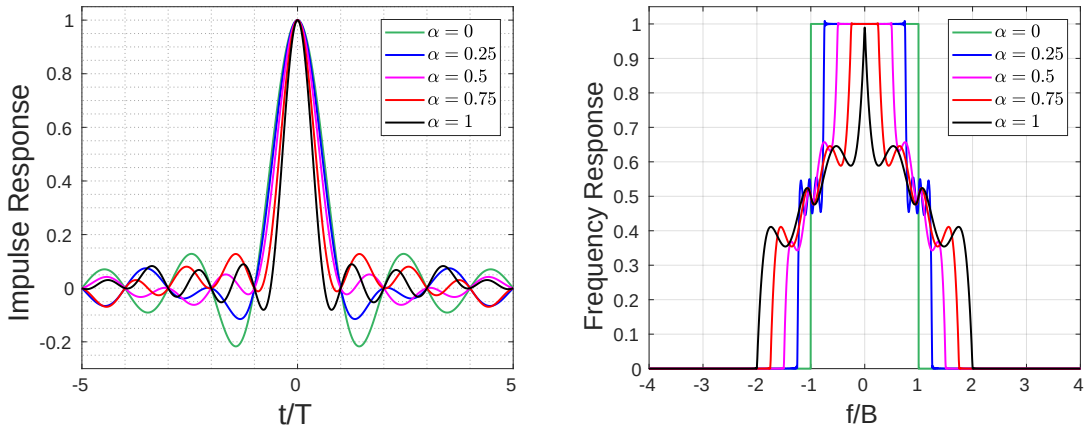

Figure 2.9: Impulse Response and Frequency characteristic of the r Filter for $a = 1.618$.

q Filter

The same approach is followed using a linear combination of the CC3 pulse ($p(t)$) and the $s_3(t)$ pulse. The CC3 pulse, proposed in [7], is based on a piece-wise parabolic frequency characteristic. The linear combination ($q(t)$) is described by the equation (2.25),

$$q(t) = ap(t) + (1 - a)s_3(t). \tag{2.25}$$

The impulse and frequency responses of the $q(t)$ pulse defined in equation (2.25), is shown in the Fig. 2.10. The ADR of $q(t)$ is t^{-2}

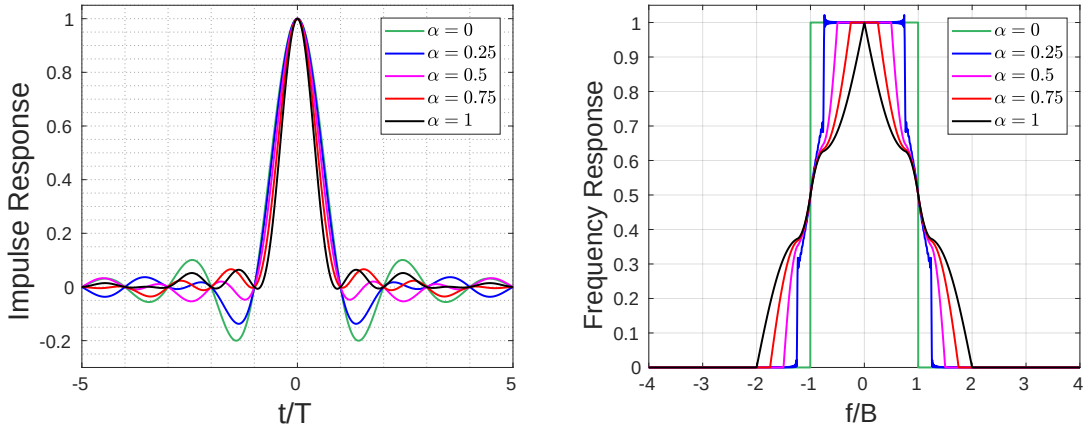

Figure 2.10: Impulse Response and Frequency characteristic of the q Filter, for $a = 0.797$.

v Filter

In [20], 2 pulses were proposed based on a piece-wise rectangular-polynomial frequency characteristic, p_{x2} and p_{x3}, using second and third-degree polynomials respectively. In [9] the

proposed pulse is obtained as a result of the linear combination,

$$v(t) = ap_{x2}(t) + (1-a)p_{x3}(t). \tag{2.26}$$

The impulse and frequency response of (2.26) are shown in Fig.(2.11), the ADR of the $v(t)$ is t^{-2}

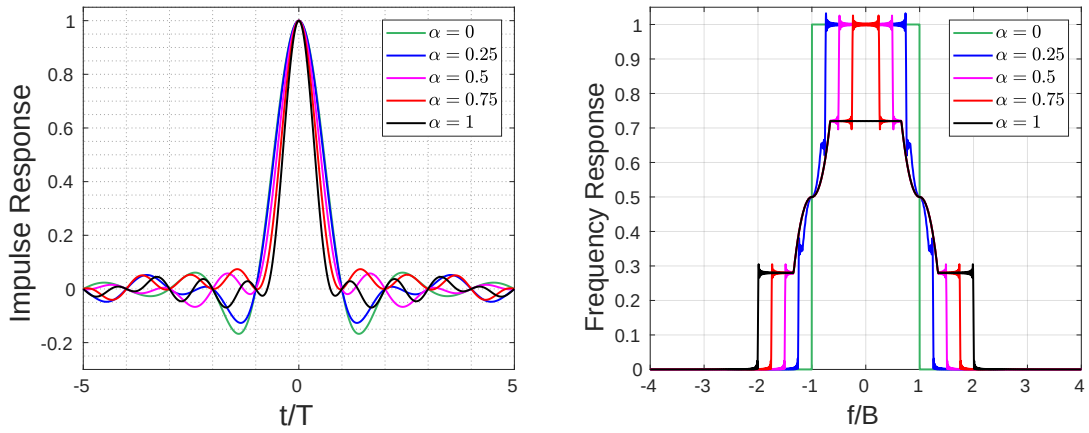

Figure 2.11: Impulse Response and Frequency characteristic of the v Filter for $a = 0.788$.

2.2.5 Time Approach Domain

Another methodology to construct Nyquist families of pulses is to formulate them in the time domain, namely, propose its impulse response. This methodology results in pulses with more degrees of freedom than the previous pulses, and in this way, these families are more general and can represent a variety of pulses. As a counterpart, the analytical Fourier transform cannot be found, thus, for every parameter, the filter's stop-band needs to be computed applying the discrete Fourier transform of the impulse response. Usually, the filter's stop-band of the pulses formulated in the time domain is greater than the formulated in the frequency domain, increasing the bandwidth used for the pulses.

ELP

First, the *exponential linear filter* (ELP) [21], is a hybrid filter composed of two main elements, a finite impulse response (FIR) filter, and a Nyquist-I pulse,

$$h(t)_{\mathrm{ELP}} = e^{-\pi(\beta/2)(t/T)^2} \times \frac{\sin(\pi t/T)}{(\pi t/T)} \times \frac{\sin(\pi \alpha t/T)}{(\pi \alpha t/T)}. \tag{2.27}$$

The impulse response and frequency characteristic can be seen in Fig. 2.12

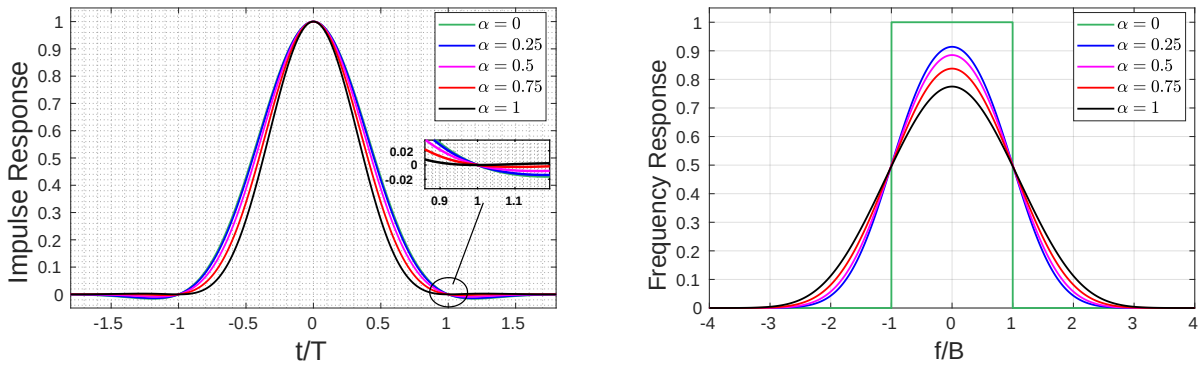

Figure 2.12: Impulse Response and Frequency characteristic of the ELP Filter.

SPLCP

The *sinc parametric linear combination pulse* (SPLCP), proposed in [22], is the product of a modified *sinc* function and the PLCP, previously defined in 2.7. The modified *sinc* function adds two additional degrees of freedom, b, and γ, which controls the amplitude of the main and lateral side lobes of the filter. The explicit time-domain expression is given by the equation (2.28),

$$\begin{aligned} h(t)_{SPLCP} &= \left(\frac{\sin(b\tau)}{b\tau}\right)^{\gamma} \times h(t)_{PLCP} \\ &= \left(\frac{\sin(b\tau)}{b\tau}\right)^{\gamma} \times \frac{\sin(\pi\tau)}{\pi\tau} \times \frac{4(1-\mu)\sin(\pi\alpha\tau/2)^2 + \pi\alpha\mu\tau\sin(\pi\alpha\tau)}{\pi^2\alpha^2\tau^2}. \end{aligned} \tag{2.28}$$

The impulse response and frequency characteristic can be seen in Fig. 2.13

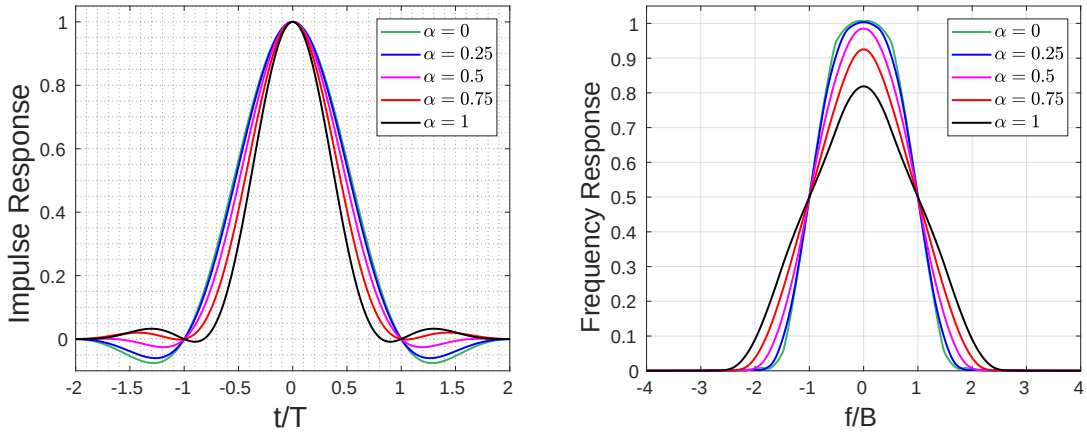

Figure 2.13: Impulse Response and Frequency characteristic of the SPLCP Filter.

IPLCP

The *improved parametric linear combination pulse* (IPLCP) proposed in [23], is equivalent to the γ-th power of a PLCP multiplied by the exponential factor $\exp(-\epsilon\pi^2(\tau)^2)$. These last two operations add two extra degrees of freedom to the pulse-shaping function: γ and ϵ.

$$h(t)_{IPLCP} = \exp(-\epsilon\pi^2(\tau)^2) \times \left(\frac{\sin(\pi\tau)}{\pi\tau} \times \frac{4(1-\mu)\sin(\pi\alpha\tau/2)^2 + \pi\alpha\mu\tau\sin(\pi\alpha\tau)}{\pi^2\alpha^2\tau^2}\right)^{\gamma}. \quad (2.29)$$

The impulse response and frequency characteristic can be seen in Fig. 2.14

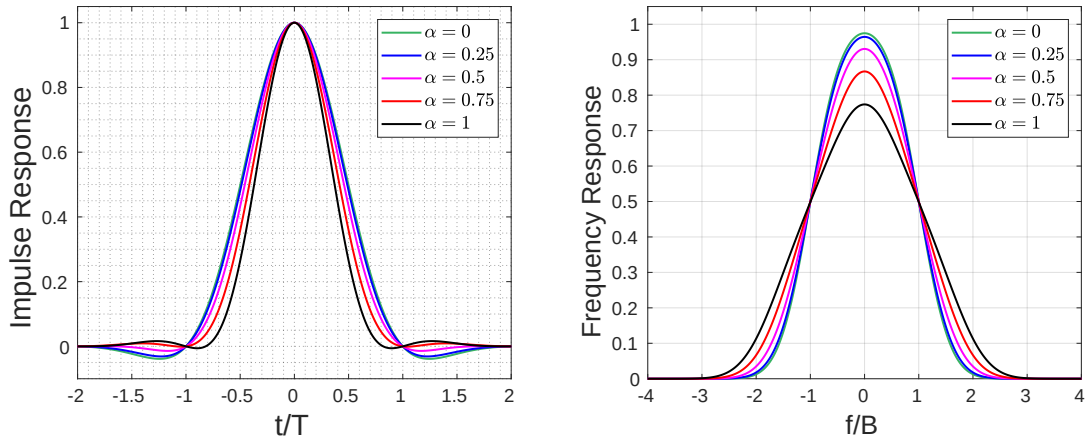

Figure 2.14: Impulse Response and Frequency characteristic of the IPLCP Filter.

Chapter 3

Analysis of the Exponential Linear Pulse in base-band system impaired by ISI

3.1 Introduction - ISI

In practical receivers, it has been verified that the presence of errors in the sampling period may cause deviation respect to sampling points; hence, symbol timing errors are produced and due to this effect the bit error rate (BER) increases. Therefore, it is expected that the tails of the filter must decay rapidly outside the pulse interval in order to eliminate the undesired effects of timing errors [8], [23]. Further, the implementation of the filter in practical systems has to consider a finite or limited version of its impulse response which is carried out through a truncation process, adding new challenges to the design of Nyquist-I filters because its frequency spectrum would be affected [24].

To overcome the prior concerns, several Nyquist-I pulses have been proposed. The most popular ISI-free Nyquist-I pulse for distortion-less transmissions is the traditional raised cosine (RC) pulse. Besides the RC pulse, other Nyquist-I pulses with lower BER and wider eye openings have been proposed. The authors in [19] presented a family of ISI-free polynomial pulses that can have an asymptotic decay rate of t^{-k} for any integer value of k, whereas in [3], [18], [9] a new ISI-free linear combination of pulses with different decay rates has been proposed. Authors in [25] proposed a family of ISI-free pulses with senary piece-wise polynomial frequency characteristic. Other ISI-free pulses denoted as piece-wise flipped-exponential (PFE) have also been proposed in [7]. In [2], the authors presented several families of Nyquist-I pulses by using a parametric approach, adding more degrees of freedom in the design of ISI-free pulses. Furthermore, the proposed pulses in [2] incorporate reviewed pulses as special cases. To the authors best knowledge, the analysis of time-limited pulses in literature is very scarce, for example in [7], the practical implementation details of the truncated realization of the PFE is discussed and compared. Meanwhile, in [24] the design and implementation of the truncated version of the improved Nyquist filters are studied.

In [26] the exponential linear pulse (ELP) was derived and optimized for peak-to-average power ratio (PAPR) reduction in single carrier orthogonal frequency division multiple access

(SC-FDMA). The proposed filter outperforms other existing filters in terms of PAPR and symbol error rate. Later, in [27], the ELP was used to mitigate the inter-carrier interference (ICI) in orthogonal frequency-division multiplexing (OFDM) systems, giving excellent results. Therefore, in this chapter, the performance of the ELP is studied considering a base-band digital communication system impaired by ISI. The optimum ELP derived in [26] is evaluated and the results are compared with other recently proposed pulses in terms of the average BER, distribution of spectral energy and spectral regrowth, for various roll-off factors and symbol timing errors. Further, the eye diagram opening of the ELP is evaluated and compared with the traditional RC pulse. Finally, the effects of the impulse response truncation, which leads to the implementation in practical systems of the pulses, are investigated.

The remainder of the chapter is organized as follows: in Section 3.2, the ELP, and its impulse response are presented. Section 3.3 describes the tools used to evaluate the pulses, and the results are presented for the complete and time-limited version. Section 3.4 shows the frequency characteristic and presents the spectral energy distribution for the ELP and the other evaluated pulses. Finally, partial conclusions are reported in Section 3.5.

3.2 Exponential Linear Pulse

The ELP is a hybrid filter, composed of two main elements: a finite impulse response (FIR) filter and a Nyquist-I pulse [26]. The explicit time-domain expression of the ELP is given by

$$h(t)_{\mathrm{ELP}} = e^{-\pi(\beta/2)(t/T)^2} \times \frac{\sin\left(\pi t/T\right)}{(\pi t/T)} \times \frac{\sin(\pi\alpha t/T)}{(\pi\alpha t/T)}. \tag{3.1}$$

The term α is the roll-off factor defined for $0 \leq \alpha \leq 1$, and t/T is the normalized time. The coefficient β is defined for $0 \leq \beta \leq 1$, and it is used to control the amplitude of the central lobe and the side-lobes of the pulse. It can be seen that the hybrid ELP is the product of an exponential expression and the linear pulse (LP) for $n = 1$. The parameter n defines a family of pulses in the frequency domain, and for each value, a new pulse is generated with an arbitrary excess of bandwidth α [2]. The $sinc(t/T)$ function in (3.1) is considered as a FIR filter. The family of pulses defined in (3.1), evaluated for $\lim_{t\to 0}(\cdot)$, and for any value of α, and β is always equal to one. Additionally, the ELP, evaluated for $k = \pm 1, \pm 2, \pm 3, \pm 4, \ldots$, and for any value of α and β is always equal to zero. Therefore, the family of pulses described in (3.1) fulfills Nyquist's ISI-free criterion, previously described in (2.12). In the Fig. 3.1 the Impulse and Frequency response of the ELP filter for various values of β is shown. It can be seen how the lateral side-lobes are reduced for values of β close to 1 but, at expenses of having a narrower central lobe and a poor spectral behavior.

Throughout this manuscript, $\beta = \{0.5, 1\}$ will be used, as observed in [26]. The ELP with $\beta = 0.5$ is considered as a pulse with a balance between the amplitude of the side lobes and the central lobe and the ELP with $\beta = 1$ as the pulse with the faster extinction and smaller side lobes.

Figs. 3.2a and 3.2b present the impulse response of the $\mathrm{ELP}_{\beta=1}$, $\mathrm{ELP}_{\beta=0.5}$, the SPLCP,

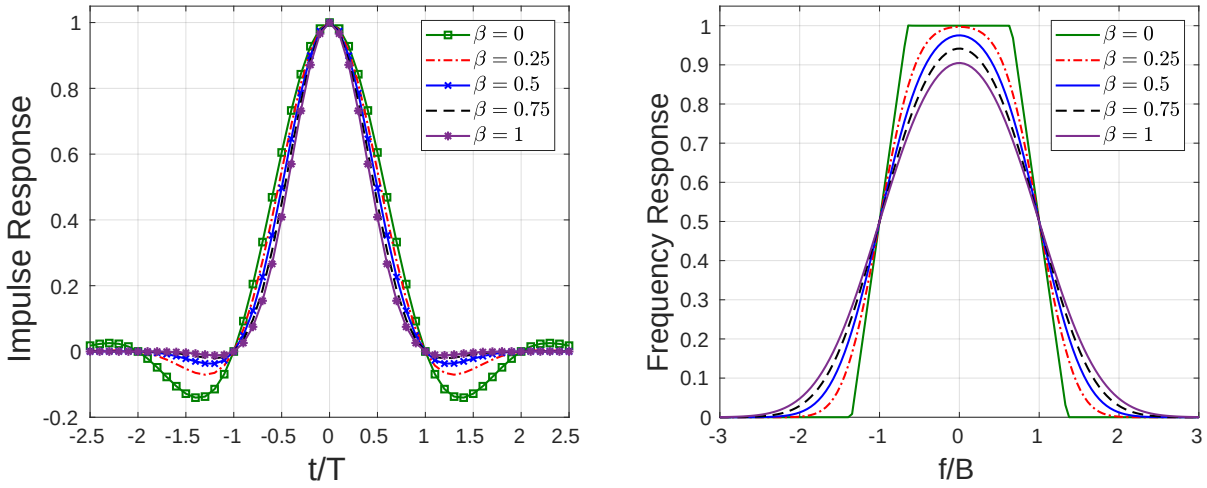

Figure 3.1: Impulse and Frequency response of the Exponential Linear Pulse for $\beta = \{0, 0.25, 0.5, 0.75, 1\}$ and $\alpha = 0.35$

proposed in [8], and the traditional RC pulse with a roll-off factor equal to 0.35 and 0.50, respectively for comparison purposes. It can be seen that the impulse response of ELP pulse, in both cases, decay rapidly having amplitude values close to zero from $t/T = 2$ and beyond. The behavior of the SPLCP pulse is similar to the $\text{ELP}_{\beta=1}$ for both values of α. The impulse response of the $\text{ELP}_{\beta=1}$ has smaller relative magnitudes in its side-lobes compared to the $\text{ELP}_{\beta=0.5}$ and the traditional RC pulse, but at expenses of having a narrower central lobe compared with both, $\text{ELP}_{\beta=0.5}$ and RC. Consequently, robustness against ISI and a larger eye-opening are expected for the $\text{ELP}_{\beta=1}$. Through the experiments realized it could be noticed that the trend is the same for other roll-off factors and values of β. Because the side-lobes of the ELP are rapidly diminished the undesired effects of jitter should decrease, and the pulse would be less sensitive to timing errors, resulting in a lower BER [2, 19, 3, 9],

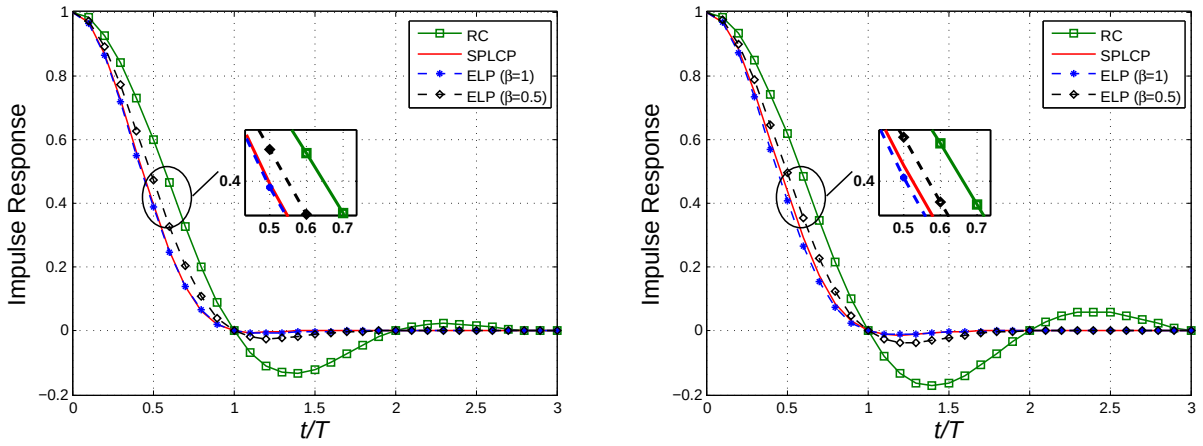

(a) (b)

Figure 3.2: Impulse response of the $\text{ELP}_{\beta=1}$, $\text{ELP}_{\beta=0.5}$, SPLCP and the RC pulse for an excess bandwidth of $\alpha = 0.35$ (a) and $\alpha = 0.5$ (b).

3.3 Performance Evaluation

In this section, the performance of the ELP is evaluated by using two main practical tools. One of the tools used to analyze the performance of the ELP is the eye diagram. The eye diagram is a useful tool to visually evaluate the susceptibility of the transmission systems due to ISI [28, 29]. The eye diagrams were generated by superimposing 10^5 individual binary antipodal signaling sequences, and by inserting two consecutive symbol periods as was reported in the literature [9, 7]. Binary phase shift keying (BPSK) was the binary antipodal digital modulation used. In Figs 3.3a and 3.3b the eye diagrams of the ELP$_{\beta=1}$ and RC pulse with α equal to 0.35 and 0.5 are plotted respectively. The results show that ELP exhibits a much wider eye-opening than the RC pulse for both values of α; therefore, a lower BER is expected because the ELP diminishes the undesired effects of jitter.

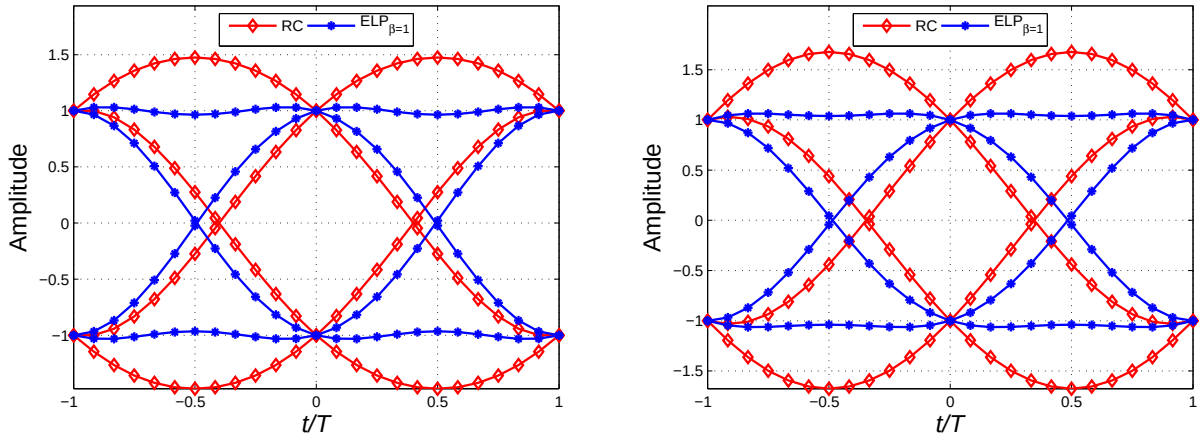

Figure 3.3: Average envelopes of the eye diagram of the ELP$_{\beta=1}$ and RC pulses for an excess bandwidth of $\alpha = 0.35$ (a) and $\alpha = 0.5$ (b).

The next step of the evaluation process involves the calculation of the BER in the presence of different time sampling errors, roll-off factors for the ideal and truncated response of the pulses. The BER is certainly the most important metric of performance in digital communication systems because it considers the effects of additive Gaussian white noise (AWGN), distortion, synchronization, among other physical phenomena. To determine the BER of the ELP in the presence of time-sampling errors, the truncated Fourier series proposed in [6] is used as follows,

$$\mathbb{P}_e = \frac{1}{2} - \frac{2}{\pi} \sum_{\substack{m=1 \\ m\ odd}}^{M} \frac{exp(-m^2w^2/2)sin(mwg_o)}{m} \prod_{\substack{k=N_1 \\ k\neq 0}}^{N_2} cos(mwg_k) \tag{3.2}$$

The latter truncated Fourier series is the de facto evaluation metric used in the literature to determine BER in the presence of symbol timing errors [2, 7, 8, 9]. The expression given in (3.2) assumes AWGN in the channel and BPSK binary antipodal signaling. In

(3.2), $w = 2\pi/T_f$ is the period used in the series, M represents the number of coefficients used to converge the truncated Fourier series, whereas N_1 and N_2 indicate the number of interfering symbols before and after the transmitted symbol, respectively. For the expression $g_k = p\,(kT + \eta)$, $p(t)$ is the ISI-free pulse evaluated at the receiver at time kT plus symbol timing error η. Thus, the term g_0 represent the amplitude of the impulse response of the ISI-free pulse under evaluation at time $t = \eta$. The parameters used to make the truncated Fourier series converge are consistent with the parameters used in [7, 8, 23, 3], and are depicted in Table 4.1. The BER for the complete impulse response in the presence of time-sampling errors was determined for the ELP, the RC pulse, the recently proposed PFE [7], as well as the recently evaluated SPLCP [8] and the improved parametric linear combination pulse (IPLCP) [23]. To the authors best knowledge, the PFE, SPLCP, and IPLCP are the pulses with the best BER performance found in the literature. A signal-to-noise ratio (SNR) of 15 dB has been assumed, while 2^{10} interfering symbols were generated.

Table 3.1: System simulation parameters of base-band system impaired by ISI.

Parameter	Value
M	100
T_f	60
Interfering Symbols	2^{10}
Channel	AWGN
Digital Modulation	BPSK
Signal-to-noise ratio	15 dB
Symbol timing errors, t/T	$\pm 0.05, \pm 0.10, \pm 0.20$
Roll-off factor, α	$0.25, 0.35, 0.5$

Complete Impulse Response

Table 3.2 presents the obtained results for the different pulses and scenarios. In general, the ELP for $\beta = 0.5$ and $\beta = 1$ performed well for different roll-off factors and timing offsets compared to the other pulses. Further, the $\text{ELP}_{\beta=1}$ has the smallest error rates for $\alpha = 0.25$ and $\alpha = 0.35$, among all of the evaluated timing offsets compared to the RC and the pulses proposed in [7, 8, 23]. This behavior is consistent with the wider eye opening of the ELP and because its side-lobes vanish rapidly compared to the other pulses. For the case of α equal to 0.50, SPCLP has the best performance for all timing offsets, even though the $\text{ELP}_{\beta=1}$ was very close. To clarify this point, it can be seen from Fig 3.2b that the SPLCP, beside having a wider central lobe, its tails have smaller amplitude than the $\text{ELP}_{\beta=1}$. So the contributions of the adjacent pulses in the compute of BER would be smaller. In general, it can be seen that increasing the value of the time-sampling error, for a fixed excess bandwidth α, the BER increases for all pulses. Further, for a fixed sampling time error, a larger BER is obtained with a smaller roll-off factor due to the increase of the tails of the impulse response.

Table 3.2: Bit Error Probability for 2^{10} Interfering Symbols and SNR= $15dB$

α	Pulse	$t/T = 0.05$	$t/T = 0.10$	$t/T = 0.20$
	RC	8.2189e-08	2.8184e-06	9.7472e-04
	PFE	4.5110-e08	7.9603e-07	1.9140e-04
0.25	SPLCP	1.3870e-08	4.4260e-08	2.4530e-06
	IPLCP	1.5232e-08	5.8295e-08	3.7486e-06
	ELP ($\beta = 1$)	**1.3444e-08**	**3.9914e-08**	**2.1059e-06**
	ELP ($\beta = 0.5$)	1.7221e-08	8.0914e-08	6.0494 e-06
	RC	3.9253e-08	5.4021e-07	1.0129e-04
	PFE	3.0130e-08	3.3720e-08	5.6450e-05
0.35	SPLCP	1.3380e-08	3.9432e-07	2.0438e-06
	IPLCP	1.4476e-08	5.0372e-08	3.0138e-06
	ELP ($\beta = 1$)	**1.3323e-08**	**3.8656e-08**	**1.9911e-06**
	ELP ($\beta = 0.5$)	1.6175e-08	6.8666e-08	4.7534e-6
	RC	2.4134e-08	1.8580e-07	2.0878e-05
	PFE	1.8921e-08	1.1615e-07	1.3072e-05
0.50	SPLCP	**1.2867e-08**	**3.4079e-08**	**1.5437e-06**
	IPLCP	1.3437e-08	3.9955e-08	2.0958e-06
	ELP ($\beta = 1$)	1.3174e-08	3.6974e-08	1.8220e-06
	ELP ($\beta = 0.5$)	1.4595e-08	5.1589e-08	3.1092e-06

Time-limited impulse response

The Nyquist pulses are digitally implemented in practical systems using a truncated version of the impulse response that results in the same or lower BER performance because amplitude values beyond the truncation are not considered [30]. Due to the truncation process, the pulse does not fulfill the first Nyquist criterion anymore and as a consequence even if the transmitter and receiver are perfectly synchronized errors due to ISI will arise. Table 3.3 shows the obtained results for different Nyquist pulses truncated at [-5.5 t/T, 5.5 t/T] and for different roll-off factors following the procedure detailed in [7]. The performance of all pulses improves compared to the pulses with the ideal impulse response, but except for those with side-lobes that rapidly become extinguished and the truncation operation does not affect them. It is desirable that the tails of the pulse decay rapidly in order to allow quick truncation and decrease the number of coefficients that represent the digital filter.

3.4 Frequency Characteristic

To design a modulation filter, the designer needs to consider carefully both representations of the signal, in the time and frequency domain. Thus, in the designing process, time or frequency representation has to be compromised at the expenses of the other, and it is a particular application that defines the final compromise [30]. .

Table 3.3: Bit error probability for the truncated pulse version in [-5.5 t/T; 5.5 t/T] for 2^{10} Interfering Symbols and SNR= $15dB$

α	Pulse	$t/T = 0.05$	$t/T = 0.10$	$t/T = 0.20$
0.25	RC	8.2158e-08	2.8157e-06	9.7340e-04
	PFE	4.2680e-08	6.8789e-07	1.5600e-04
	SPLCP	1.3867e-08	4.4257e-08	2.4534e-06
	IPLCP	1.5232e-08	5.8295e-08	3.7486e-06
	ELP ($\beta = 1$)	**1.3444e-08**	**3.9914e-08**	**2.1059e-06**
	ELP ($\beta = 0.5$)	1.7222e-08	8.0914e-08	6.0494e-06
0.35	RC	5.9982e-08	1.3886e-06	3.9043e-04
	PFE	2.8305e-08	2.9460e-07	4.6706e-05
	SPLCP	1.3380e-08	3.9428e-08	2.0426e-06
	IPLCP	1.4476e-08	5.0372e-08	3.0138e-06
	ELP ($\beta = 1$)	**1.3323e-08**	**3.8656e-08**	**1.9911e-06**
	ELP ($\beta = 0.5$)	1.6175e-08	6.8666e-08	4.7534e-06
0.50	RC	3.9721e-08	5.4880e-07	1.0213e-04
	PFE	1.8071e-08	1.0345e-07	1.1500e-05
	SPLCP	**1.2864e-08**	**3.4066e-08**	**1.5397e-06**
	IPLCP	1.3436e-08	3.9954e-08	2.0958e-06
	ELP ($\beta = 1$)	1.3174e-08	3.6974e-08	1.8220e-06
	ELP ($\beta = 0.5$)	1.4595e-08	5.1589e-08	3.1092e-06

Complete Frequency Response

Figs. 3.4a and 3.4b show the frequency response of the $\text{ELP}_{\beta=0.5}$, $\text{ELP}_{\beta=1}$, SPLCP, and the traditional RC pulse for roll-off factors 0.35 and 0.5 respectively considering the complete impulse response. It can be seen from the frequency characteristic that both ELP pulses will introduce additional out-of-band radiation compared to the RC pulse, which has a stop band value of $f/B = 1 + \alpha$. This out-of-band radiation can be interpreted as a transfer of energy from the low spectral region ($f/B \leq 1 - \alpha$) to the high spectral region ($f/B \geq 1 + \alpha$) resulting in a more open receiver eye in the eye diagram and a faster extinction of the tails in the impulse response, giving better results in therm of BER [31]. Therefore, there is a trade-off between out-of-band radiation and lower BER due to ISI.

Table 3.4 presents the energy contained in different intervals for the normalized frequency considering the pulses with the best BER performance and the RC for comparison purposes for different roll-off factors. The energy of the RC pulse is allocated completely in the low spectral zone, having the highest energy for the main lobe ($0 \leq f/B < 1 - \alpha$) compared to the other pulses for all the roll-off factors. Considering the $\text{ELP}_{\beta=1}$, and the SPLCP, its energy distribution is almost the same, but the ELP concentrates a bit more energy (less than 2 %) in the high spectral zone, ($f/B > 1 + \alpha$) than the SPLCP. Comparing the distribution of energy of the $\text{ELP}_{\beta=0.5}$ and the $\text{ELP}_{\beta=1}$ it can be seen that the out-of-band radiation can be controlled by modifying β, and for lower values, the out-of-band radiation decreases.

The frequency response of the ELP pulse is not explicit known, because the filter was formulated in the time domain. So, for the calculation of the spectrum shape starting from the impulse response, numerical methods like fast Fourier transform (FFT) need to be used. Thus, the relation between the filter stop-band and parameters of the pulse is not explicit,

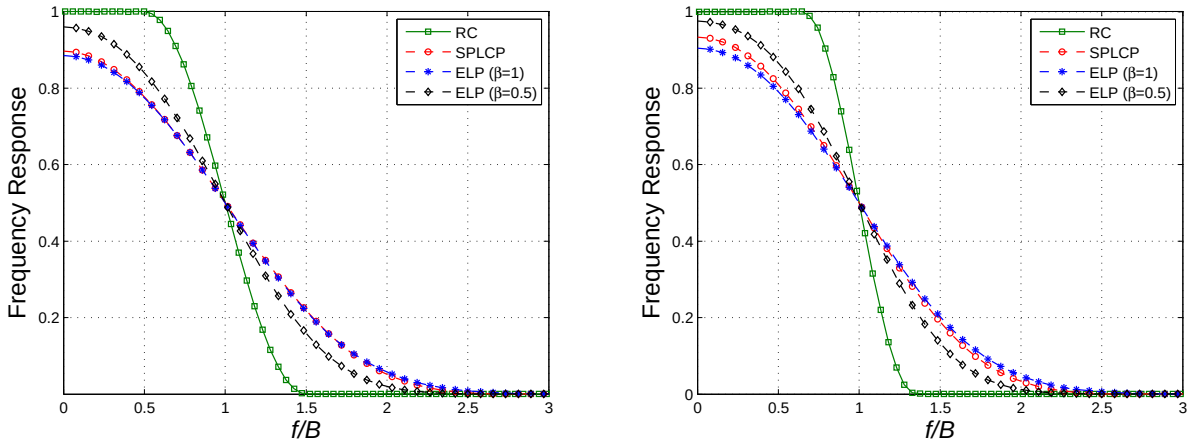

(a) (b)

Figure 3.4: Frequency response of $ELP_{\beta=1}$, $ELP_{\beta=0.5}$ and RC pulses for $\alpha = 0.35$ (a) and $\alpha = 0.5$ (b), considering the complete impulse response.

Table 3.4: Distribution of the spectral energy in percentage for the $\text{ELP}_{\beta=1}$, $\text{ELP}_{\beta=0.5}$, SPLCP, and RC for $\alpha = \{0.25, 0.35, 0.5\}$ considering the ideal impulse response.

α	Pulse	$0 \leq f/B < 1-\alpha$	$1-\alpha \leq f/B < 1+\alpha$	$f/B \geq 1+\alpha$
0.25	RC	74.81	25.16	0.03
	SPLCP	64.37	24.93	10.71
	ELP (β=1)	62.15	24.90	12.95
	ELP (β=0.5)	67.66	24.96	7.39
0.35	RC	65.10	34.88	0.02
	SPLCP	56.34	34.95	8.71
	ELP (β=1)	54.83	34.91	10.27
	ELP (β=0.5)	59.60	34.93	5.47
0.5	RC	50.53	49.46	0.02
	SPLCP	43.27	49.50	7.22
	ELP (β=1)	42.87	49.36	7.77
	ELP (β=0.5)	46.54	49.50	3.97

so for every α and β parameter selection, the stop-band value needs to be found.

Spectral Regrowth

When the complete impulse response of the pulses is truncated at a certain value, its representation in the frequency domain changes (this phenomenon is called spectral regrowth) introducing harmonics that can spread frequency components over the stop-band value. In Figs. 3.5a and 3.5b the spectral regrowth is presented for the $\text{ELP}_{\beta=1}$, $\text{ELP}_{\beta=0.5}$, SPLCP and RC for roll-off factor 0.35, 0.5 and truncation at [-3.5 t/T, 3.5 t/T] for demonstration purposes. It can be seen that the spectral-regrowth affects only the RC pulse, because its tails decay at a lower rate than the ELP, increasing the stop-band value beyond $f/B = 1+\alpha$. For higher values of α, the spectral regrowth decreases. An increase in the truncation length (i.e. the use of more taps for representing the digital filter) is necessary in order to have both, low spectral re-growth and reliable error probability performance. Moreover, the increase of

the truncation length determines bigger latency and at the same time the increase of hardware complexity, so a trade-off exists and is a task for the designer to choose the optimal combination for the concrete application.

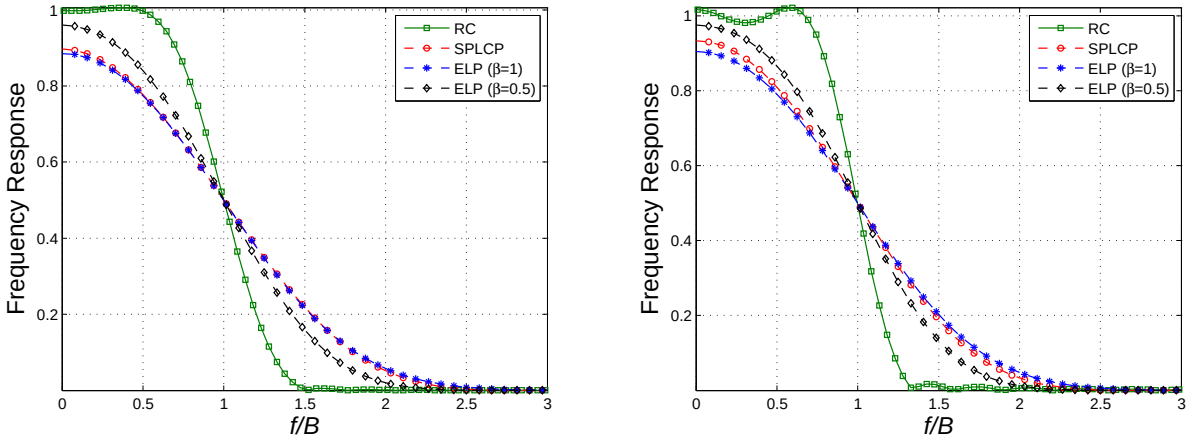

(a) (b)

Figure 3.5: Frequency response of $ELP_{\beta=1}$, $ELP_{\beta=0.5}$, SPLCP and RC pulses for $\alpha = 0.35$ (a) and $\alpha = 0.5$ (b) considering the time-limited impulse response.

.

3.5 Conclusions - ISI

In this work, the ELP pulse was numerically analyzed and compared with respect to the latest pulses given in the literature, like the SPLCP, IPLCP, PFE and the traditional RC pulse for reference, in the time and frequency domains. The eye diagram of each impulse response in the transmitter side and the BER in the receiver side were used as evaluation tools. For the complete impulse response, the ELP for $\beta = 1$ generates the smaller BER compared to the other evaluated pulses for $\alpha = \{0.25, 0.35\}$. For $\alpha = 0.5$ only the Sinc Parametric Linear Combination Pulse (SPLCP) outperform the $\text{ELP}_{\beta=1}$. For the time-limited version of the pulses, the behavior improves in terms of BER for the pulses with tails that decays slowly. These results allow communications systems to use lower power levels to achieve the same BER value, making more efficient use of energy resources.

Considering the Frequency response, the ELP introduces additional out-of-band radiation compared to the RC pulse. The excess of bandwidth introduced by the family of pulses analyzed in this chapter explains the good performance in the time domain, in terms of BER and wider eye opening. Finally, for the truncated frequency response, the ELP does not present additional spectral regrowth. The performance of the ELP could potentially be improved by using optimization techniques, specifically designed for BER reduction in presence of time sampling errors.

Chapter 4

Error Probability Analysis Considering ISI and CCI

4.1 Introduction - ISI + CCI

The use of the pulse-shaping technique, along with the design and optimization of different Nyquist-I pulses, is a widely researched topic [2, 7, 8, 9, 3]. For example, in orthogonal frequency-division multiplexing (OFDM) systems, Nyquist pulses are used for ICI reduction and BER improvement in the presence of carrier frequency offset [32, 27, 33]. In single-carrier frequency division multiple access (SC-FDMA) systems, Nyquist pulses are used to reduce the peak-to-average power ratio (PAPR) [34, 26], whereas for next-generation wireless communication systems, 5G, Nyquist pulses are used to reduce the out-of-band radiation [35].

In the literature, the effects of ISI have been studied for various Nyquist-I pulses [2, 7, 8, 9, 3], considering the average BER in the presence of symbol timing errors and different roll-off factors [6]. By contrast, the study of the effects of CCI considering Nyquist-I pulses is very scarce, although different models for CCI were developed. In [36], the authors studied the effects of CCI and fading in terms of BER for band-limited binary phase shift keying (BPSK) environments. The authors assume different Nakagami-m distributions for the fading of the desired and interfering signals. The authors also assumed that the interfering signals have the same modulation format as the desired user signal. In [37], an equation to compute the BER was developed for BPSK modulation, considering fast fading channels subject to timing errors and asynchronous co-channel interferer signals. In the prior works, the equations to compute the error are too complex and computationally expensive, mainly because they do not have a closed-form equation.

In this chapter, the closed-form equations given in [6] are used to compute the BER under CCI and both, ISI and CCI effects simultaneously using BPSK modulation, additive white Gaussian noise (AWGN) channel, and considering the effects of time jitter in the receiver. Also, the effects of the number of interfering signals are studied for a fixed interference power. The remainder of this chapter is organized as follows: in Section 4.2, the sinusoidal interference model and its expressions to compute the BER under CCI and CCI+ISI simultaneously

are described. In Section 4.3 the performance of the evaluated Nyquist-I pulses is presented and discussed. Finally, partial conclusions are reported in Section 4.4.

4.2 System Model - ISI + CCI

Consider a binary symmetric channel with additive noise, the output at the receiver has the form

$$y(t) = s(t) + n(t), \tag{4.1}$$

where $s(t)$ is the received signal and $n(t)$ is the noise signal. It is assumed that the noise follows a zero-mean normal distribution with variance $\sigma^2 = 1$. Consider the suppression on t for compactness sake. The signal s, which includes the desired signal and the contribution due to co-channel, inter-symbol or both types of interferences is expressed as

$$s = \sum_{k=N_1}^{N_2} b_k g_k + \sum_{i=1}^{L} r_i \cos(\phi_i), \tag{4.2}$$

where b_k is a random variable that assumes the values $\{-1, 1\}$ with equal probability and is assumed to be independent. The term $g_k = p(t - kT - \eta)$ represents the ISI-free pulse shaping filter evaluated at the receiver time kT plus a normalized symbol time error η. The desired signal corresponds to $b_0 g_0$ and the ISI contribution (z) due to N_1 and N_2 predecessors and successive symbols, respectively is expressed as

$$z = \sum_{\substack{k=N_1 \\ k\neq 0}}^{N_2} b_k g_k = \sum_{\substack{k=N_1 \\ k\neq 0}}^{N_2} z_k, \tag{4.3}$$

additionally, the co-channel interference (ν) modeled as the addition of L fixed amplitude signals (r_i) with random phase (ϕ_i) to the received signal, is expressed as

$$\nu = \sum_{i=1}^{L} r_i \cos(\phi_i) = \sum_{i=1}^{L} \nu_i, \tag{4.4}$$

being the amplitudes and the random phases independent of each other, and the phases are assumed to be uniformly distributed on the interval $[0, 2\pi)$. The effect from ν in the desired signal is a bias whose nature will depend on the number of interfering signals L.

Following the steps detailed in [6], where the characteristic function method is used, the average bit error probability assuming AWGN in the channel, BPSK binary antipodal signaling for CCI ($s = b_0 g_0 + \nu$) and time sampling errors is

$$\mathbb{P}_{\substack{e \\ \text{CCI}}} = \frac{1}{2} - \frac{2}{\pi} \sum_{\substack{m=1 \\ m\ odd}}^{M} \frac{\exp(-m^2 w^2/2)\sin(m w g_o)}{m} \prod_{i=1}^{L} J_0(m w r_i), \tag{4.5}$$

being M a positive integer that controls the truncation of the Fourier series, $w = 2\pi/T$ the period in the series, and $J_0(\cdot)$ the zeroth-order Bessel function of the first kind. For the case

where ISI ($s = b_o g_0 + z$) and symbol time error are present, the average BER is given by [6]

$$\mathbb{P}_{\substack{e \\ \text{ISI}}} = \frac{1}{2} - \frac{2}{\pi} \sum_{\substack{m=1 \\ m\ odd}}^{M} \frac{\exp(-m^2 w^2/2)\sin(mwg_o)}{m} \times \prod_{\substack{k=N1 \\ k\neq 0}}^{N2} \cos(mwg_k). \tag{4.6}$$

Finally, and considering the CCI and ISI ($s = b_0 g_0 + z + \nu$) simultaneously, the average probability of error is [6]

$$\mathbb{P}_{\substack{e \\ \text{CCI+ISI}}} = \frac{1}{2} - \frac{2}{\pi} \sum_{\substack{m=1 \\ m\ odd}}^{M} \frac{\exp(-m^2 w^2/2)\sin(mwg_o)}{m} \times \prod_{\substack{k=N1 \\ k\neq 0}}^{N2} \cos(mwg_k) \prod_{i=1}^{L} J_0(mwr_i). \tag{4.7}$$

The signal-to-noise power ratio (SNR) and the signal-to-interference power ratio (SIR) are defined as

$$SNR = g_0^2, \quad SIR = g_0^2 \Big/ \sum_{i=1}^{L} r_i^2 = g_0^2/(Lr_i^2), \tag{4.8}$$

the last expression indicates that the total amount of power is distributed among L interfering signals [10]. The products of the two inferences, CCI in (4.5), $\prod_{i=1}^{L} J_0(mwr_i)$, and ISI in (4.6) $\prod_{\substack{k=N1 \\ k\neq 0}}^{N2} \cos(mwg_k)$, are multiplied in (4.7). This is because both interferences are statistically independent; hence, their characteristic function can be separated.

Other models exist in the literature for determining the interference more precisely, for example, the exact or Gaussian interference models [10]. But in this work, and as an initial approach and for sake of simplicity, the sinusoidal interference model is used.

4.3 Numerical Results and Discussion

In this section, we evaluate several Nyquist-1 pulses described in Section 3.2 considering different types of interferences. First of all, we consider the effects of CCI and time sampling errors simultaneously because this type of analysis is very scarce in the literature and it will be used later to clarify the effects of both interferences. Later, we consider the effects of CCI and ISI simultaneously to compute the BER. The parameters used to make the truncated Fourier series converge in (4.6) comply with the parameters used in [7, 8, 38, 39], and are depicted in Table 4.1 along with L. The same parameters are used to make the truncated Fourier series given in (4.5) and (4.7) converge, as previously shown in [6].

4.3.1 BER considering CCI

Tables 4.2 and 4.3 present the average BER only for CCI using different pulses, roll-off factors, and time sampling errors for $L = 2$ and $L = 6$ interfering signals, respectively. The RC pulse has the smallest error rate for all the evaluated scenarios, even though the BTRC was very close. This behavior is consistent with Fig. 3.2a and 3.2b, where the impulse response

Table 4.1: System parameters of base-band system impaired by ISI and CCI, considering the sinusoidal model.

Parameter	Value
M	100
T_f	60
Interfering Symbols	2^{10}
Channel	AWGN
Digital Modulation	BPSK
Signal-to-noise ratio	15 dB
Signal-to-interference ratio	10 dB
Symbol timing errors, t/T	$\pm 0.05, \pm 0.10, \pm 0.20$
Roll-off factor, α	$0.25, 0.35, 0.5$
Number of interferers, L	$1, 2, 6, 15$

of the RC has the greatest main-lobe and intuitively is the most robust under amplitude interferences or noise considering or not timing offset. The performance of the other recent pulses (SPLCP, ELP, and IPLCP) is in the same order of magnitude as the RC pulse.

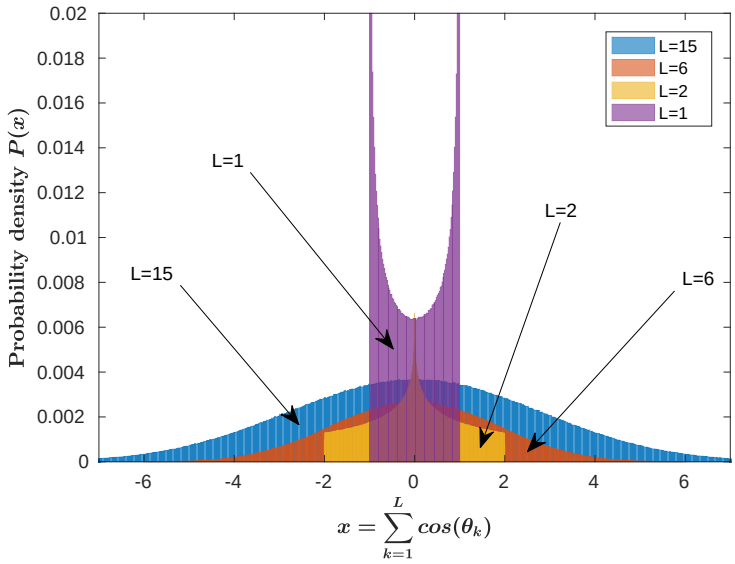

Figure 4.1: Approximate pdf for ν using $L = \{1, 2, 6, 15\}$ as the number of interferer signals. The x axis is truncated originally from $[-15t/T,\ 15t/T]$ because the contribution of the tails for the pdf $(L = 15)$ is marginal.

It is noted from Tables 4.2 and 4.3 that for a fixed interference power, the BER is smaller when the total interference power is concentrated in two interferer signals than when it is distributed among six interfering signals. This can be explained by looking at Fig. 4.1, where the probability density function (pdf) of ν, expression (4.4), is shown for $L = \{1, 2, 6, 15\}$. When the number of interfering signals increases for a fixed interference power, the range of the pdf also increases, and ν can take larger values. This means that having multiple interferer signals instead of a few, affects severely the performance of the system, even if each of the interferer signals has a fraction of the total power.

Table 4.2: Bit Error Probability with CCI only using $SNR = 15dB$, $SIR = 10dB$ AND $L = 2$ Interfering Singals

α	Pulse	$t/T = 0.05$	$t/T = 0.10$	$t/T = 0.20$
0.25	RC	**3.7910E-05**	**4.8981E-05**	**1.2815E-04**
	BTRC	3.8030E-05	4.9586E-05	1.3384E-04
	SPLCP	4.0374E-05	6.2383E-05	2.9129E-04
	IPLPC	4.0000E-05	6.0209E-05	2.5904E-04
	ELP (β=1)	4.1129E-05	6.6903E-05	3.6369E-04
	ELP (β=0.5)	3.9534E-05	5.7576E-05	2.2339E-04
0.35	RC	**3.8018E-05**	**4.9524E-05**	**1.3324E-04**
	BTRC	3.8254E-05	5.0729E-05	1.4501E-04
	SPLCP	4.0726E-05	6.4475E-05	3.2408E-04
	IPLPC	4.0260E-05	6.1709E-05	2.8080E-04
	ELP (β=1)	4.1333E-05	6.8165E-05	3.8575E-04
	ELP (β=0.5)	3.9732E-05	5.8682E-05	2.3801E-04
0.5	RC	**3.8248E-05**	**5.0696E-05**	**1.4466E-04**
	BTRC	3.8735E-05	5.3237E-05	1.7153E-04
	SPLCP	4,1485E-05	6.9133E-05	4.0483E-04
	IPLPC	4.0816E-05	6.5009E-05	3.3244E-04
	ELP (β=1)	4.1770E-05	7.0917E-05	4.3650E-04
	ELP (β=0.5)	4.0154E-05	6.1097E-05	2.7190E-04

4.3.2 BER considering CCI+ISI

Second, we evaluate the probability of error of the Nyquist-I pulses under CCI and ISI simultaneously. Table 4.4 presents the obtained results for the pulses considering $L = 2$. The $\text{ELP}_{\beta=1}$ has the smallest error rate for $\alpha = 0.25$, whereas for $\alpha = \{0.35, 0.5\}$ SPLCP presents the best performance among all timing offsets. These results are consistent with those presented in [21], where $\text{ELP}_{\beta=1}$ presents the best performance for $\alpha = \{0.25, 0.35\}$ considering only the ISI effect. For $\alpha = 0.35$ our results differ from the ones in [21]. This is due to the fact that when considering the simultaneous effect of ICI and ISI, in addition to the reduction of the lateral side-lobes of the pulses, the magnitude of the main lobe must be considered as well for decrease the BER.

The results for the case of $L = 6$ interfering signals are presented in Table 4.5. It can be noticed that the CCI effect is stronger than the case of a single interfering signal, following the same behavior of the case when only CCI was considered. For $\alpha = 0.25$ and timing offset $t/T = \{0.1, 0.2\}$, $\text{ELP}_{\beta=1}$ has the smallest BER. Meanwhile, for the same value of α, but for $t/T = \{0.05\}$, SPLCP achieved the best performance. Further, for the remaining values of α, SPLCP outperformed the other pulses. These results indicate that the SPLCP is the pulse with the best compromise between the magnitude of its central and lateral side-lobes in terms of BER.

Generally, in the literature the main focus is to optimize Nyquist-I pulses, considering only the ISI effects, by reducing the magnitude of the lateral side-lobes of the impulse response. But when the effects of CCI and ISI are considered, besides the reduction of the lateral side lobes, the magnitude of the main lobe should be considered as well. Further, when the number of interfering signals is large, the effects of the CCI are stronger than those of the

Table 4.3: Bit Error Probability with CCI only using $SNR = 15dB$, $SIR = 10dB$ AND $L = 6$ interfering signals

α	Pulse	$t/T = 0.05$	$t/T = 0.10$	$t/T = 0.20$
0.25	RC	**1.4194E-04**	**1.7284E-04**	**3.6293E-04**
	BTRC	1.4228E-04	1.7448E-04	3.7534E-04
	SPLCP	1.4897E-04	2.0821E-04	6.8672E-04
	IPLPC	1.4791E-04	2.0260E-04	6.2672E-04
	ELP (β=1)	1.4659E-04	1.9574E-04	5.5851E-04
	ELP (β=0.5)	1.5111E-04	2.1974E-04	8.1670E-04
0.35	RC	**1.4225E-04**	**1.7431E-04**	**3.7405E-04**
	BTRC	1,4293E-04	1.7757E-04	3.9938E-04
	SPLCP	1.4997E-04	2.1357E-04	7.4634E-04
	IPLPC	1.4865E-04	2.0647E-04	6.6737E-04
	ELP (β=1)	1.5169E-04	2.2292E-04	8.5519E-04
	ELP (β=0.5)	1.4715E-04	1.9863E-04	5.8675E-04
0.5	RC	**1.4291E-04**	**1.7748E-04**	**3.9864E-04**
	BTRC	1.4430E-04	1.8429E-04	4.5492E-04
	SPLCP	1.5211E-04	2.2536E-04	8.8812E-04
	IPLPC	1.5023E-04	2.1493E-04	7.6133E-04
	ELP (β=1)	1.5292E-04	2.2983E-04	9.4210E-04
	ELP (β=0.5)	1.4835E-04	2.0489E-04	6.5083E-04

ISI; therefore, the optimization of the Nyquist-I pulses in terms of the main lobe should be an important issue when the sinusoidal interference model is considered.

4.4 Conclusion - ISI + CCI

In this chapter, recent proposed Nyquist-I pulses, as well as some traditional pulses, were evaluated under different kinds of interference. First, the CCI, different symbol timing errors, and roll-off factors were considered in the average BER computation. The results indicate that the RC pulse achieved the best performance. This is because the RC pulse possesses the greatest central lobe magnitude compared to the other evaluated pulses. Second, considering the combined effects of CCI and ISI with symbol timing errors, in general, the SPLCP outperform the other pulses by presenting the smallest average BER for roll-off factors $\alpha = \{0.35, 0.5\}$. For $\alpha = 0.25$, the $\text{ELP}_{\beta=1}$ presents the best performance.

These results indicate that when ISI and CCI are both taken into consideration, the magnitude of the main lobe is preponderant and is even more important than the magnitude of the side-lobes as the number of interferer signals increases for a fixed interference power. In this chapter, we used the sinusoidal interference model to represent the CCI as well as non-fading environment as an initial approach, but as future work, we will use more precise models and consider fading for the desired and interfering signals.

Table 4.4: Bit Error Probability considering ISI+CCI for 2^{10} interfering symbols using $SNR = 15dB$, $SIR = 10dB$, and $L = 2$ interfering signals

α	Pulse	$t/T = 0.05$	$t/T = 0.10$	$t/T = 0.20$
0.25	RC	8.9927E-05	5.0896E-04	8.8845E-03
	BTRC	7.7705E-05	3.6833E-04	6.1701E-03
	SPLCP	4.2845E-05	8.0001E-05	7.4930E-04
	IPLPC	4.4315E-05	8.9277E-05	9.0274E-04
	ELP (β=1)	**4.2630E-05**	**7.8291E-05**	**7.1323E-04**
	ELP (β=0.5)	4.6384E-05	1.0251E-04	1.1156E-03
0.35	RC	7.8791E-05	3.7992E-04	6.4028E-03
	BTRC	6.5551E-05	2.4883E-04	3.7782E-03
	SPLCP	**4.2391E-05**	**7.6987E-05**	**6.9414E-04**
	IPLPC	4.3529E-05	8.4287E-05	8.2098E-04
	ELP (β=1)	4.2563E-05	7.7765E-05	7.0095E-04
	ELP (β=0.5)	4.5292E-05	9.5496E-05	1.0025E-03
0.5	RC	6.5953E-05	2.5205E-04	3.8416E-03
	BTRC	5.3046E-05	1.4841E-04	1.8823E-03
	SPLCP	**4.2055E-05**	**7.4338E-05**	**6.2860E-04**
	IPLPC	4.2497E-05	7.7612E-05	7.0470E-04
	ELP (β=1)	4.2552E-05	7.7465E-05	6.8779E-04
	ELP (β=0.5)	4.3629E-05	8.4947E-05	8.3184E-04

Table 4.5: Bit Error Probability considering ISI+CCI for 2^{10} interfering symbols using $SNR = 15dB$, $SIR = 10dB$, and $L = 6$ interfering signals

α	Pulse	$t/T = 0.05$	$t/T = 0.10$	$t/T = 0.20$
0.25	RC	2.4214E-04	8.3629E-04	9.2600E-03
	BTRC	2.2074E-04	6.6405E-04	6.6832E-03
	SPLCP	**1.5424E-04**	2.4182E-04	1.2973E-03
	IPLPC	1.5709E-04	2.5757E-04	1.4752E-03
	ELP (β=1)	1.5431E-04	**2.4132E-04**	**1.2736E-03**
	ELP (β=0.5)	1.6109E-04	2.7968E-04	1.7152E-03
0.35	RC	2.2269E-04	6.7888E-04	6.9026E-03
	BTRC	1.9837E-04	5.0430E-04	4.4144E-03
	SPLCP	**1.5352E-04**	**2.3744E-04**	**1.2377E-03**
	IPLPC	1.5561E-04	2.4934E-04	1.3824E-03
	ELP (β=1)	1.5430E-04	2.4109E-04	1.2651E-03
	ELP (β=0.5)	1.5895E-04	2.6789E-04	1.5880E-03
0.5	RC	1.9915E-04	5.0917E-04	4.4767E-03
	BTRC	1.7416E-04	3.5387E-04	2.5332E-03
	SPLCP	**1.5333E-04**	**2.3523E-04**	**1.1798E-03**
	IPLPC	1,5381E-04	2.3893E-04	1.2536E-03
	ELP (β=1)	1.5458E-04	2.4216E-04	1.2647E-03
	ELP (β=0.5)	1.5575E-04	2.5020E-04	1.3934E-03

Chapter 5

Precise model for Co-channel Interference

5.1 Introduction - Precise CCI

The introduction of new technologies, like Machine to Machine Communication (M2MC), Internet of Things (IoT) and 5G mobile networks have introduced large amount of devices, demanding an efficient use of the spectrum. The limitations in the performance of the digital communication systems are ruled by different sources of interference. In such crowded environments, the detection of one user's data is often corrupted by signals from users located in near or moderate distances using the same frequency band. The aim of the frequency reuse is to increase the spectrum efficiency. This interference is called CCI and affects negatively the performance of the communication systems. Therefore, analyzing the performances of digital communications in the presence of CCI is of considerable interest.

In [6] the author presents closed expressions to evaluate Nyquist-I pulses in terms of the bit error rate (BER) considering a base-band system impaired by CCI, ISI, or ISI and CCI simultaneously. The approach used to analyze the CCI interference was the sinusoidal model (sum of sinusoids) considering multiple interferer signals. Later in [10] is mentioned that the sinusoidal interference model for representing the CCI impacts always underestimates the effects of interference on the BER and conclude that the sinusoidal model may not be a good approximation for moderate to strong cases of Signal to Interference Ratio (SIR). In the literature other more accurate models to represent the CCI effects have been used. In [11] the resultant interference contribution is modeled by an additive Gaussian noise with mean and variance equal to the mean and variance of the sum of the interfering signals. This model is based on a central limit theorem which states that under certain conditions the distribution of a sum of many independent RV's approaches to a Gaussian distribution. However, the Gaussian model always overestimates the effect of CCI. For this reason, in [12], the Precise interference model for representing the CCI is used. In this model, the interfering signals are assumed to have the same modulation and nature as the desired signal, that is, the interferer signals are quadrature phase-shift keying (QPSK) modulated with the same symbol

rate, but with random carrier phase shifts and random symbol timing offsets relative to the desired signal. In the present chapter, an expression to compute the BER in presence of ISI and CCI simultaneously is proposed, using QPSK modulation for the Precise interference model. Later, the performance of recently proposed Nyquist-I pulses is evaluated for various parameters and scenarios.

The rest of the chapter is organized as follows, the system model including the transmitted signal, the received signal and the detection process is described in Section 5.2. In Section 5.3 the expression to compute the BER considering the ISI and CCI (Precise model) simultaneously is presented. In Section 5.4 the results are presented and analyzed. Finally, conclusions are shown in Section 5.5.

5.2 System Model - Precise CCI

Transmitted Signal

Considering the transmission of a signal modulated with QPSK, namely the desired signal,

$$S(t) = S_a \sin(2\pi f_c t) + S_b \cos(2\pi f_c t), \tag{5.1}$$

where $S_a(t)$ and $S_b(t)$ are the baseband signals on the in- phase and quadrature paths respectively, and f_c is the carrier frequency. The base band signals ($S_a(t)$ and $S_b(t)$) are given by

$$\begin{aligned} S_a(t) &= \sum_{k=-\infty}^{\infty} a_k g^d(t - kT), \\ S_b(t) &= \sum_{k=-\infty}^{\infty} b_k g^d(t - kT), \end{aligned} \tag{5.2}$$

where T is the symbol interval, and $g^d(t)$ is the impulse response of the transmitter filter, where the upper index d represent the desired signal. Usually, the transmitted filter in cascade with the Received filter forms a matched filter, so the root response needs to be used on each side. But sometimes is more convenient to use the complete response in the transmitter or receiver side. Is assumed that the complete response of the filters complies with the Nyquist criterion. The sequence a_k and b_k represents the binary data transmitted in-phase and quadrature respectively and is assumed that a_k and a_j ($-\infty \leq k \leq \infty$, $-\infty \leq j \leq \infty$, $a_k \neq a_j$), b_k and b_j ($-\infty \leq k \leq \infty$, $-\infty \leq j \leq \infty$, $b_k \neq b_j$) are independent. The data bits are random variables (RVs) that assume the values $\{-1, -1\}$ with equal probability, therefore it follows a Rademacher distribution.

Received Signal

If we assume that L co-channel interferer signals are present, the total received signal can be written as

$$r(t) = R_s S(t) + \sum_{l=1}^{L} R_l S_l(t) + n(t), \tag{5.3}$$

where $S(t)$ and $S_l(t)$ represent the contributions from the desired signal and the lth interfering signal, respectively, and $n(t)$ is the AWGN noise. The terms R_s and R_l represent the channel gain amplitude affecting the desired and the lth interfering signal respectively. In this work, flat fading channel is considered. If we use the Precise interference model to represent the contribution of the CCI, the signal S_l is given by

$$S_l(t) = S_{c_l}(t)\sin(2\pi f_c t + \theta_l) + S_{d_l}(t)\cos(2\pi f_c t + \theta_l), \tag{5.4}$$

The variables S_{c_l} and S_{d_l} represent the base-band in-phase and quadrature components of the lth interfering signal, respectively. They are given by,

$$\begin{aligned} S_{c_l}(t) &= \sum_{j=-\infty}^{\infty} c_{k_l} g^i(t - jT), \\ S_{d_l}(t) &= \sum_{j=-\infty}^{\infty} d_{k_l} g^i(t - jT), \end{aligned} \tag{5.5}$$

where c_k, and d_k, can take values of $\{-1, +1\}$ with equal probabilities and they represent the in-phase and the quadrature data bits of the lth interfering signal, respectively. The data bits of the interfering signals c_{k_l}, c_{j_l}, d_{k_l} and d_{j_l} ($-\infty \leq k \leq \infty$, $-\infty \leq j \leq \infty$, $0 \leq l \leq L$) are assumed to be mutually independent. The term g^i represents the transmitter filter from the interferer signals. The phase θ_l, is a RV uniformly distributed in $[0, 2\pi]$ and it represents the random phase of the lth interfering signal carrier.

Detection process

At the receiver, the total received signal is split into an in- phase component and a quadrature component, filtered by a low-pass filter, usually a matched filter and the detection is then performed. Perfect carrier phase and frequency tracking are assumed for the desired signal, in general, difficult to achieve, thus the results present a best case situation. The signal at the output of the receiver filter ($y_a(t)$) can be written as

$$y_a(t) = R_s V_a(t) + \sum_{l=1}^{L} R_l[V_{c_l}\cos(\theta_l) - V_{d_l}\sin(\theta_l)] + n_w(t), \tag{5.6}$$

with $n_w(t)$ the filtered Gaussian noise with mean zero and variance σ_n^2, V_{c_l} and V_{d_l} are the base-band in-phase and in quadrature components of the l interfering signal respectively.

$$\begin{aligned} V_{c_l} &= \sum_{k=-\infty}^{\infty} c_{k_l} g^i(t - kT - \upsilon_l), \\ V_{d_l} &= \sum_{k=-\infty}^{\infty} d_{k_l} g^i(t - kT - \upsilon_l). \end{aligned} \tag{5.7}$$

is assumed that the filter g^i comply with the first Nyquist criteria, with the complete impulse response. The RV υ_l is uniformly distributed in $[0, T]$ and it represents a possible offset between the symbol timing epochs of the desired and the lth interfering signals, namely, the effect of the ISI produced by the CCI.

5.3 Error rate on AWGN channel

Consider the diagram presented in Fig. 5.1, which represents a pass-band system impaired by 2 kinds of interferences, ISI and CCI (modeled as Precise model) in an AWGN channel.

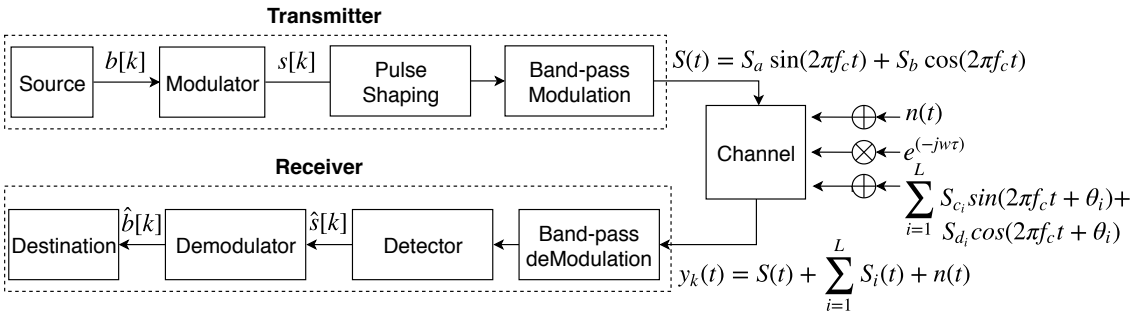

Figure 5.1: System impaired by ISI+CCI for the Precise model of interference.

The expression to compute the BER in this system is given by

$$\underset{\text{ISI+CCI}}{\mathbb{P}_e} = \frac{1}{2} - \frac{2}{\pi} \sum_{\substack{m=1 \\ m\ odd}}^{M} \frac{\exp(-m^2 w^2/2) \sin(mwg_o^i)}{m} \prod_{\substack{n=N_1 \\ n\neq 0}}^{N_2} \cos(mwg_n) \prod_{l=1}^{L} A_{(l,m)}, \tag{5.8}$$

where

$$A_{(l,m)} = \frac{1}{2\pi T} \int_0^{2\pi} \int_0^{T} \Big(\prod_{k=-P}^{P} [\cos(mwR_l g_{k_l}^d \cos(\theta_l)) \cos(mwR_l g_{k_l}^d \sin(\theta_l))] \Big)\, d\theta_l\, d\upsilon_l. \tag{5.9}$$

The double integral given in (6.6) seems not to be reduced to a closed form expression. However, it can be computed numerically using one of the broad family of algorithms used

to solve definite integrals by numerical integration. The derivation of the expression given in (5.8) is detailed in Chapter 8, Section 8.1.

From the equation (5.5) and (5.2) can be seen that the desired and interfering signals are filtered by a pulse g^d and g^i respectively. Thereby, we can evaluate the performance of the system considering different Nyquist-I pulses in the desired and interfering signals.

5.4 Numerical Results and Discussion

In this section, the BER considering ISI and CCI using the Precise model presented in section 5.3 is computed for various scenarios and multiple Nyquist-I pulses. The Nyquist-I pulses evaluated are the RC, BtRC, SPLCP, IPLCP and ELP for $\beta = \{0.5, 1\}$ described in Chapter 4, Section 4.3.2. Additionally, 2 other recently proposed pulses, called, Improved Double Jump 1 (**IDJ1**) and Improved Double Jump Linear Combination (**IDJLC**) are added to the analysis.

The IDJ1 pulse proposed in [13] results from the combination of a Gaussian function and the Double Jump 1 (DJ1) pulse, characterized by an extra design parameter $\beta \in \mathbb{R}^+$ for a certain roll-off factor α

$$\begin{aligned} h(t)_{IDJ1}(t) &= P_{Gauss}(t) \times P_{DJ1}(t) \\ h(t)_{IDJ1}(t) &= \exp[-\beta(t/T)^2] sinc(t/T)[(1-\alpha)\cos(\pi\alpha t/T) + \alpha sinc(\alpha t/T)]. \end{aligned} \tag{5.10}$$

In [40], the IDJ1 pulse is optimized for reduce the ICI and the BER in an Orthogonal Frequency Division Multiplexing (OFDM) system. The optimization was done for the DVB-C2 standard which uses $\alpha = 0.15$, resulting in $\beta_{opt} = 1.9951$. The filter outperforms various pulse shaping filters in terms of the SNR and frequency offset times OFDM symbol period requirements at the FEC limit, namely, the BER.

Alike, the IDJLC pulse which results from the exponential function times a linear combination of double jump functions, is characterized by two degrees of freedom, called as β and γ, for a certain roll-off factor. In [5] the IDJLC pulse is optimized considering a OFDM system in terms of BER and ICI for $\alpha = 0.22$.

$$h(t)_{IDJLC} = sinc(t/T)[(1-\alpha\beta)\cos(\pi\alpha t/T) + \alpha\beta sinc(\alpha t/T)] \exp(-\gamma(t/T)^2), \tag{5.11}$$

the optimum values obtained in the document are $\beta_{opt} = -31.7507$ and $\gamma_{opt} = 1.1242$ are used in the evaluation of the system.

The parameters used in the computation of the BER are presented in the Table 5.1. We evaluate different scenarios, from low (10 dB) to moderate (15, 20 dB) values of SIR, low (5 dB) to strong (15 dB) values of SNR and few ($L = 2$) to moderate ($L = 6, 15$) number of interfering signals.

Table 5.1: System parameters of pass-band system impaired by ISI and CCI, considering the Precise model.

Parameter	Value
M	99
T_f	60
Interfering Symbols	2^{10}
Channel	AWGN
Digital Modulation	QPSK
Signal-to-noise ratio	5, 15 dB
Signal-to-interference ratio	10,15,20 dB
Symbol timing errors, t/T	$\pm 0.05, \pm 0.10, \pm 0.20$
Roll-off factor, α	$0.25, 0.35, 0.5$
Number of interferers, L	$2, 6, 15$

For the reader's convenience all the results are presented in the Chapter 8, Section 8.2. In the Tables 5.2 and 5.3 we present a summary of the results, showing the pulse with the best performance in each case.

The results for SNR=15 dB, SIR=10 dB and L=$\{2, 6\}$ presented in the Table 8.10 and Table 8.13 respectively, are up to one order of magnitude lower than the computed in the Section 4.3.2 for the same parameters but using the sinusoidal model for representing the CCI effects. This confirms the fact that the sinusoidal model underestimates the effects of interference on the BER [10].

For the results given in Tables 5.2 and 5.3, it can be seen that the performance of all pulses in term of BER is worse when low regimes of SNR are analyzed compared to high regimes. Considering the number of interfering signals, when the BER is evaluated at a moderate number, it is slightly worse than the case when the evaluation is performed with a low number of interfering signals. Considering low regimes of SNR (5 dB) in Table 5.2, the 3 pulses with the best performance are the IDJ1 and the SPLCP followed closely for the IPLCP. The IDJ1 performs well for low values of SIR, and the SPLCP and IPLCP for high values of SIR. Considering high regimes of SNR (15 dB), Table 5.3, the IDJ1 pulse outperform other pulses in term of BER for all the SIR regimes, and the number of interfering signals followed closed by the IDJLC pulse.

The results indicate that the pulse with the best performance, in terms of BER, is the IDJ1, which outperforms other evaluated pulses for all the scenarios, namely different regimes of SNR, SIR, and number of interfering signals.

Moreover, in Fig. 5.2, the spectral behavior of the pulses for roll-off factors $\alpha = \{0.25, 0.35, 0.5\}$ are presented. It can be seen that the pulses with the biggest out-of-band radiation (OBR) are the IDJLC and IDJ1 increasing the bandwidth used. In many standards used in communication systems, the pulses used in the transmitter side needs to comply with a spectrum mask. The increase of bandwidth used would introduce adjacent channel interference (ACI) decreasing the performance of the communication system and not complying with the technical requirements. The excess of OBR is related to the optimization of the parameters, of both pulses, where the optimization process did not consider restrictions on the frequency

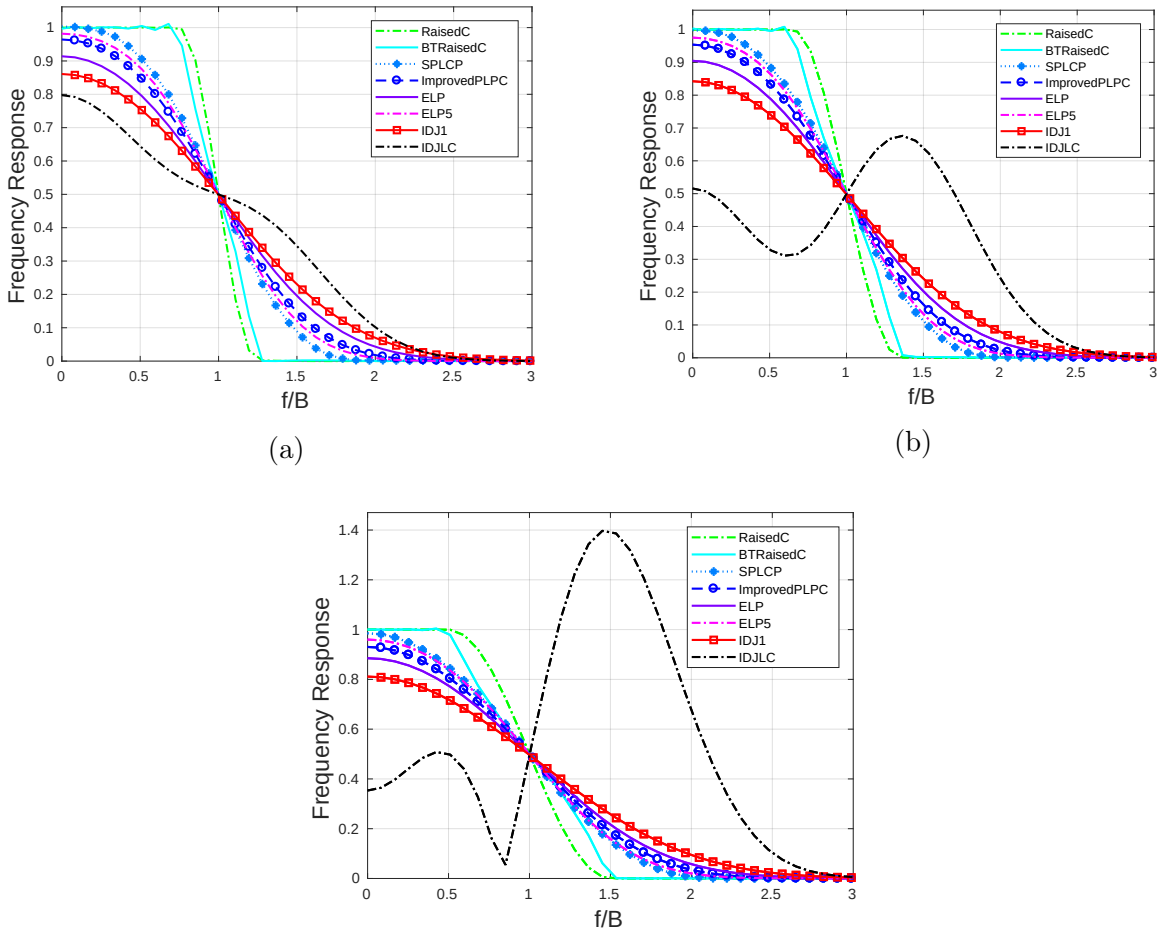

Figure 5.2: Spectral characteristic of RC, BtRC, SPLCP, IPLCP, ELP$_\beta$ = 1, ELP$_\beta$ = 0.5, IDJ1 and IDLC pulses.

characteristic. Therefore, the great performance of both pulses can be explained looking the Section 3.4 from Chapter 3, where it was mentioned that there exists a trade-off between out-of-band radiation and lower BER due to ISI effects.

	SNR=5	SIR=10	L=2
α	$\tau = 0.05$	$\tau = 0.1$	$\tau = 0.2$
0.25	IDJLC	IDJ1	IPLCP
	5.2658E-02	**5.9198E-02**	**7.9691E-02**
0.35	IDJ1	IDJ1	$\text{ELP}_{\beta=0.5}$
	5.3563E-02	**5.9169E-02**	**7.9727E-02**
0.5	$\text{ELP}_{\beta=1}$	IDJ1	SPLCP
	5.4224E-02	**5.9185E-02**	**7.9139E-02**

	SNR=5	SIR=10	L=6
α	$\tau = 0.05$	$\tau = 0.1$	$\tau = 0.2$
0.25	IDJLC	IDJ1	IPLCP
	5.2641E-02	**5.9157E-02**	**7.9570E-02**
0.35	IDJ1	IDJ1	$\text{ELP}_{\beta=0.5}$
	5.3539E-02	**5.9131E-02**	**7.9602E-02**
0.5	IDJ1	IDJ1	SPLCP
	5.3108E-02	**5.9150E-02**	**7.9017E-02**

	SNR=5	SIR=10	L=15
α	$\tau = 0.05$	$\tau = 0.1$	$\tau = 0.2$
0.25	IDJLC	IDJ1	IPLCP
	5.2635E-02	**5.9144E-02**	**7.9533E-02**
0.35	IDJ1	IDJ1	$\text{ELP}_{\beta=0.5}$
	5.3531E-02	**5.9119E-02**	**7.9565E-02**
0.5	IDJ1	IDJ1	SPLCP
	5.3101E-02	**5.9139E-02**	**7.8979E-02**

	SNR=5	SIR=15	L=2
α	$\tau = 0.05$	$\tau = 0.1$	$\tau = 0.2$
0.25	IDJLC	IPLCP	$\text{ELP}_{\beta=0.5}$
	4.3671E-02	**4.8091E-02**	**6.6160E-02**
0.35	IDJ1	IPLCP	$\text{ELP}_{\beta=0.5}$
	4.3751E-02	**4.8054E-02**	**6.6084E-02**
0.5	IDJ1	SPLCP	SPLCP
	4.3701E-02	**4.7969E-02**	**6.5567E-02**

	SNR=5	SIR=15	L=6
α	$\tau = 0.05$	$\tau = 0.1$	$\tau = 0.2$
0.25	IDJLC	IPLCP	$\text{ELP}_{\beta=0.5}$
	4.3670E-02	**4.8089E-02**	**6.6149E-02**
0.35	IDJ1	IPLCP	$\text{ELP}_{\beta=0.5}$
	4.3750E-02	**4.8052E-02**	**6.6073E-02**
0.5	IDJ1	SPLCP	SPLCP
	4.3701E-02	**4.7966E-02**	**6.5557E-02**

	SNR=5	SIR=15	L=15
α	$\tau = 0.05$	$\tau = 0.1$	$\tau = 0.2$
0.25	IDJLC	IPLCP	$\text{ELP}_{\beta=0.5}$
	4.3670E-02	**4.8088E-02**	**6.6145E-02**
0.35	IDJ1	IPLCP	SPLCP
	4.3750E-02	**4.8051E-02**	**6.5955E-02**
0.5	IDJ1	SPLCP	SPLCP
	4.3701E-02	**4.7965E-02**	**6.5553E-02**

	SNR=5	SIR=20	L=2
α	$\tau = 0.05$	$\tau = 0.1$	$\tau = 0.2$
0.25	$\text{ELP}_{\beta=1}$	IPLCP	$\text{ELP}_{\beta=0.5}$
	4.0528E-02	**4.4232E-02**	**6.1684E-02**
0.35	IPLCP	SPLCP	SPLCP
	4.0521E-02	**4.4215E-02**	**6.1440E-02**
0.5	IPLCP	SPLCP	SPLCP
	4.0507E-02	**4.4072E-02**	**6.1159E-02**

	SNR=5	SIR=20	L=6
α	$\tau = 0.05$	$\tau = 0.1$	$\tau = 0.2$
0.25	$\text{ELP}_{\beta=1}$	IPLCP	$\text{ELP}_{\beta=0.5}$
	4.0528E-02	**4.4231E-02**	**6.1683E-02**
0.35	IPLCP	SPLCP	SPLCP
	4.0521E-02	**4.4215E-02**	**6.1439E-02**
0.5	IPLCP	SPLCP	SPLCP
	4.0507E-02	**4.4072E-02**	**6.1158E-02**

	SNR=5	SIR=20	L=15
α	$\tau = 0.05$	$\tau = 0.1$	$\tau = 0.2$
0.25	$\text{ELP}_{\beta=1}$	IPLCP	$\text{ELP}_{\beta=0.5}$
	4.0529E-02	**4.4231E-02**	**6.1682E-02**
0.35	IPLCP	SPLCP	SPLCP
	4.0521E-02	**4.4215E-02**	**6.1438E-02**
0.5	IPLCP	SPLCP	SPLCP
	4.0507E-02	**4.4072E-02**	**6.1158E-02**

Table 5.2: Summary of results for a pass-band system impaired by ISI+CCI for the Precise model, considering SNR=5 dB, SIR=$\{10, 15, 20\}$ dB, L=$\{2, 6, 15\}$.

	SNR=15	SIR=10	L=2
α	$\tau = 0.05$	$\tau = 0.1$	$\tau = 0.2$
0.25	IDJLC	IDJLC	IDJ1
	1.4255E-04	**2.7787E-04**	**1.7287E-03**
0.35	IDJ1	IDJ1	IDJ1
	1.6231E-04	**2.7328E-04**	**1.6889E-03**
0.5	IDJ1	IDJ1	IDJ1
	1.4762E-04	**2.5639E-04**	**1.6789E-03**

	SNR=15	SIR=10	L=6
α	$\tau = 0.05$	$\tau = 0.1$	$\tau = 0.2$
0.25	IDJLC	IDJLC	IDJ1
	3.0792E-04	**5.2243E-04**	**2.6252E-03**
0.35	IDJLC	IDJ1	IDJ1
	3.6072E-04	**6.0442E-04**	**2.5445E-03**
0.5	IDJ1	IDJ1	IDJ1
	3.5039E-04	**5.4246E-04**	**2.4697E-03**

	SNR=15	SIR=10	L=15
α	$\tau = 0.05$	$\tau = 0.1$	$\tau = 0.2$
0.25	IDJLC	IDJLC	IDJLC
	3.7430E-04	**6.1156E-04**	**2.8747E-03**
0.35	IDJLC	IDJ1	IDJ1
	3.8943E-04	**7.2933E-04**	**2.7868E-03**
0.5	IDJ1	IDJ1	IDJ1
	4.3401E-04	**6.5049E-04**	**2.6953E-03**

	SNR=15	SIR=15	L=2
α	$\tau = 0.05$	$\tau = 0.1$	$\tau = 0.2$
0.25	IDJLC	IDJ1	IDJ1
	1.9704E-06	**4.6168E-06**	**7.2404E-05**
0.35	IDJ1	IDJ1	IDJ1
	2.0795E-06	**4.4406E-06**	**7.0463E-05**
0.5	IDJ1	IDJ1	IDJ1
	1.9269E-06	**4.2646E-06**	**7.0848E-05**

	SNR=15	SIR=15	L=6
α	$\tau = 0.05$	$\tau = 0.1$	$\tau = 0.2$
0.25	IDJLC	IDJ1	IDJ1
	3.3392E-06	**8.3781E-06**	**1.0087E-04**
0.35	IDJ1	IDJ1	IDJ1
	3.9715E-06	**7.8873E-06**	**9.7281E-05**
0.5	IDJ1	IDJ1	IDJ1
	3.5228E-06	**7.2758E-06**	**9.5804E-05**

	SNR=15	SIR=15	L=15
α	$\tau = 0.05$	$\tau = 0.1$	$\tau = 0.2$
0.25	IDJLC	IDJLC	IDJ1
	3.9967E-06	**9.7815E-06**	**1.1179E-04**
0.35	IDJ1	IDJ1	IDJ1
	4.9649E-06	**9.5771E-06**	**1.0755E-04**
0.5	IDJ1	IDJ1	IDJ1
	4.3369E-06	**8.7134E-06**	**1.0526E-04**

	SNR=15	SIR=20	L=2
α	$\tau = 0.05$	$\tau = 0.1$	$\tau = 0.2$
0.25	IDJ1	IDJ1	IDJ1
	1.3059E-07	**3.1920E-07**	**9.1021E-06**
0.35	IDJ1	IDJ1	IDJ1
	1.2645E-07	**3.1228E-07**	**8.9244E-06**
0.5	IDJ1	IDJ1	IDJ1
	1.2098E-07	**3.0976E-07**	**9.1556E-06**

	SNR=15	SIR=20	L=6
α	$\tau = 0.05$	$\tau = 0.1$	$\tau = 0.2$
0.25	IDJ1	IDJ1	IDJ1
	1.5380E-07	**3.8536E-07**	**1.0081E-05**
0.35	IDJ1	IDJ1	IDJ1
	1.5500E-07	**3.7369E-07**	**9.8446E-06**
0.5	IDJ1	IDJ1	IDJ1
	1.4566E-07	**3.6480E-07**	**1.0020E-05**

	SNR=15	SIR=20	L=15
α	$\tau = 0.05$	$\tau = 0.1$	$\tau = 0.2$
0.25	IDJLC	IDJ1	IDJ1
	1.6234E-07	**4.1150E-07**	**1.0424E-05**
0.35	IDJ1	IDJ1	IDJ1
	4.0521E-02	**3.9774E-07**	**1.0167E-05**
0.5	IDJ1	IDJ1	IDJ1
	1.5544E-07	**3.8599E-07**	**1.0320E-05**

Table 5.3: Summary of results for a pass-band system impaired by ISI+CCI for the Precise model, considering SNR=15 dB, SIR=$\{10, 15, 20\}$ dB, L=$\{2, 6, 15\}$.

5.5 Conclusion - Precise CCI

In this Chapter, an expression for computing the BER considering ISI and CCI, for the Precise model, in a pass-band system was presented and evaluated for recently proposed Nyquist-I pulses. Considering low regimes of SNR (5 dB), the 3 pulses with the best performance are the IDJ1 and the SPLCP followed closely for the IPLCP. The IDJ1 performs well for low values of SIR, and the SPLCP and IPLCP for high values of SIR. Considering high regimes of SNR (15 dB), the ID1 pulse outperforms the other pulses in term of BER, followed by the IDJLC.

The results indicate that the pulse with the best performance, in terms of BER, is the IDJ1, which outperforms other evaluated pulses for all the scenarios, namely different regimes of SNR, SIR, and number of interfering signals.

Moreover, the pulses with the biggest out-of-band (OBR) radiation are the IDJLC and IDJ1. This phenomenon would introduce adjacent channel interference (ACI), decreasing the performance of the communication system. The excess OBR is related to the optimization of the parameters, of both pulses, where the optimization process did not consider restrictions on the frequency characteristic.

For these reasons, in future work, we will consider restrictions in the frequency characteristic of the pulses to optimize their parameters in terms of BER while considering the ISI and CCI for the Precise model.

Chapter 6

Optimization

6.1 Introduction - Optimization

The most popular ISI-free Nyquist pulse for distortionless transmissions is the traditional raised cosine (RC) pulse, which depends on just one parameter, the roll-off factor (α). In general, the value of the roll-off factor is fixed by the particular standard used, and therefore this pulse cannot be adjusted to different channel conditions. Nyquist-I pulses with several numbers of parameters have been proposed in the literature [18, 4, 8, 26]. If we consider the BER as the main metric to compare different Nyquist-I pulses, for every system parameters, there exists an optimum value of the pulses parameters that minimizes that metric.

The optimization of Nyquist-I pulses is a topic that has attracted a lot of attention recently. In [41] the Piecewise Flipped-Exponential (PFE) pulse, which possesses 1 extra design parameter (b), is proposed and optimized to obtain a minimum value of symbol error rate taking into account fixed values of the excess bandwidth α, and timing offsets, η. The technique used to optimize the pulse was the Nelder-Mead method. In the optimization procedure, was found that the parameter b and the timing offset follows a cubic relationship. The same relation was found between the parameter and the excess bandwidth. In this way, the choice of the optimum parameters can be performed simply considering the relations with α and τ. Later, in [42] the Modified K-Exponential Filter (MKEF), which present 2 extra degrees of freedom, the parameters β and k, was presented and optimized. The main advantage of the pulse is its capacity of becoming different pulses, like the double jump filter [43], triple jump filter, or the K-exponential filter [44] depending on the choice of parameters. The optimization of the pulse was achieve also by means of the Nelder-Mead optimization technique, for fixed values of excess bandwidth and timing offsets. This optimization technique used for the optimization of the pulses parameters, its a heuristic technique that treats non-linear optimization problems and can converge to non-stationary points [45].

In many recent works, pulses formulated in time domain [5, 40, 26] with many extra parameters have been proposed and optimized in function of the Peak-to-Average Power Ratio (PAPR) and BER in SC-FDMA systems [46, 47], ICI and BER in OFDM systems [48, 49, 50, 51], or the BER in base-band systems [52] giving promising results. However,

in all the cases, the spectral behavior of the pulses is not taken in consideration for the optimization process giving as result larger stop-band values, increasing the bandwidth and in many cases not fulfilling the bandwidth restriction imposed by the channel, although many authors evaluate the out-of-band power [53]. For this reason, in this chapter, the linear combination of 2 Nyquist-I pulses, formulated in the frequency domain, are optimized in terms of average bit error rate for a fixed excess bandwidth and timing offset values. The bandwidth used for the linear combination of Nyquist-I pulses does not change when the linear constant is modified. Thus, the bandwidth restriction is implicit in the formulation of the new pulses.

The rest of the work is organized as follows, first in section 6.2 the optimization problem is formalized for a system impaired by ISI and then affected by ISI and CCI, using the Precise model. It is showed that the problem turns in to a minimization of a convex function over convex sets for both cases. In section 6.3, the system is evaluated for different Nyquist-I pulses, with their parameters optimized. Finally, the final remarks are given in section 6.4

6.2 Formalization of the problem

6.2.1 Optimization considering ISI

Consider a band-base system impaired by ISI and additive white gaussian noise, detailed in the Fig. 6.1

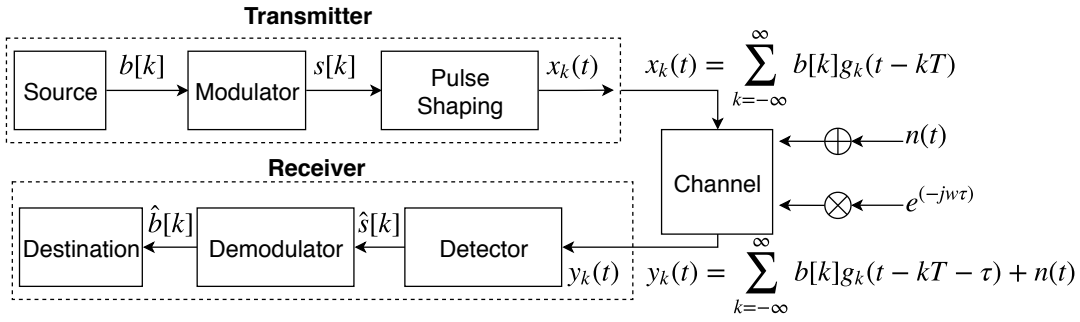

Figure 6.1: System impaired by ISI.

We assume that the pulse shaping filter used in the transmitter and receiver sides, comply with the first Nyquist criteria. We optimize different linear combination of pulses being formulated in the frequency domain under the parametric approach presented in 2.2.3. In this way, the filter stop-band of the pulses keeps at the $(1+\alpha)(1/2T)$ value.

The optimization problem to minimize the average probability of error is given by

$$\begin{aligned} \underset{a}{\text{minimize}} \quad & \mathbb{P}_{\substack{e \\ \text{ISI}}} = \frac{1}{2} - \frac{2}{\pi} \sum_{\substack{m=1 \\ m\ odd}}^{M} \frac{\exp(-m^2 w^2/2)\sin(mwg_o)}{m} \times \prod_{\substack{k=N1 \\ k\neq 0}}^{N2} \cos(mwg_k) \\ \text{subject to} \quad & g(t) = ah_1(t) + (1-a)h_2(t) \end{aligned} \tag{6.1}$$

where $g_k = p\left(kT + \eta\right)$, $p(t)$ is the ISI-free pulse evaluated at the receiver at time kT plus symbol timing error η. The details of the expression given in (6.1) can be found in Section 3.3.

Convexity of $\mathbb{P}_e$ due to ISI

To solve the optimization problem, we need to investigate if the function $\mathbb{P}_{\substack{e \\ \text{ISI}}}$ is or not convex. The convexity makes optimization easier than the general case since a local minimum must be a global minimum. First of all, we need to prove that we are working with a convex set.

A subset of C of $\mathbb{R}^n$ is called convex if any linear combination of 2 elements of the set is also contained in C

$$k_l h_1(t) + (1-k_l)h_2(t) \in C, \ \ \forall h_1, h_2 \in C, \ \forall k_l \in [0,1] \tag{6.2}$$

Here, the set C its the set of all the pulses that comply with the first Nyquist criterion. We need to prove that a linear combination of Nyquist pulses it is also a Nyquist Pulse. Fortunately, in [17] it is probed that the combination of 2 or more Nyquist-I pulses results in an ISI-free pulse as well.

Second, we need to prove that the function $(\mathbb{P}_{\substack{e \\ \text{ISI}}})$ is convex. Let C be a convex subset of $\mathbb{R}^n$. The function $\mathbb{P}_{\substack{e \\ \text{ISI}}} : C \to \mathbb{R}$ is called convex if for $\forall\ \theta \in [0,1]$,

$$\mathbb{P}_{\substack{e \\ \text{ISI}}}(\theta h_1 + (1-\theta)h_2) \leq \theta \mathbb{P}_{\substack{e \\ \text{ISI}}}(h_1) + (1-\theta)\mathbb{P}_{\substack{e \\ \text{ISI}}}(h_2) \ \forall h_1, h_2 \in C \tag{6.3}$$

If we consider the PLCP pulse as a particular case, described in Section 2.2.3, which is composed from the linear combination of the $\text{PLP}_{n=1}$ and $\text{PLP}_{n=2}$, the following inequality need to be proved,

$$\mathbb{P}_{\substack{e \\ \text{ISI}}}(h_{PLCP}) = \mathbb{P}_{\substack{e \\ \text{ISI}}}(ah_{PLP_{n=1}} + (1-a)h_{PLP_{n=2}}) \leq a\mathbb{P}_{\substack{e \\ \text{ISI}}}(h_{PLP_{n=1}}) + (1-a)\mathbb{P}_{\substack{e \\ \text{ISI}}}(h_{PLP_{n=2}}) \ \forall a \in [0,1]. \tag{6.4}$$

To explore if the $\mathbb{P}_{\substack{e \\ \text{ISI}}}$ function is convex, first we show graphically if the inequality given in (6.4) is fulfilled. The parameters used are $\alpha = \{0.25, 0.35, 0.5\}$, SNR=15 dB, $\eta = \{0.05, 0.1, 0.2\}$ considering the complete impulse response. From the results shown in the Fig. 6.2, it can be seen that for all cases and for $a \in [0,1]$ the left side of the inequality holds below the right side. This would indicate us that the expression given in (6.3) would be convex.

To perform the optimization of the nonlinear convex problem, we use the interior point method and implemented it using the MATLAB software.

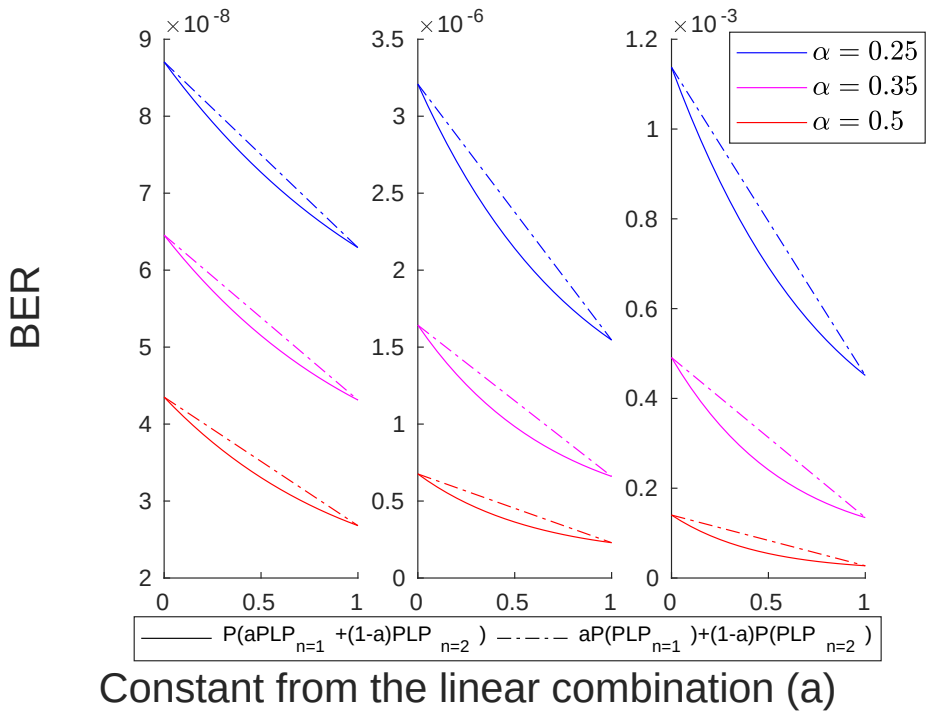

Figure 6.2: Convexity of the BER expression considering the ISI effect for different timing offset values. The PLCP, $\text{PLP}_{n=1}$, $\text{PLP}_{n=2}$ pulse with parameters $\alpha = \{0.25, 0.35, 0.5\}$ SNR=15 dB, and the complete response are considered. Each plot shows the inequality expression, in solid line the left side and dashed line the right side for $\eta = t/T = \{0.05, 0.1, 0.2\}$.

6.2.2 Optimization considering ISI + CCI

Consider a band-base system impaired by ISI, CCI and white noise, detailed in the Figure 5.1. Taking into account the same assumptions given in 6.2.1, the optimization problem to minimize the average probability of error is given by

$$\begin{aligned} \underset{a}{\text{minimize}} \quad & \mathbb{P}_{\substack{e \\ \text{ISI+CCI}}} = \frac{1}{2} - \frac{2}{\pi} \sum_{\substack{m=1 \\ m \text{ odd}}}^{M} \frac{\exp(-m^2 w^2/2)\sin(mwg_o)}{m} \times \prod_{\substack{k=N1 \\ k\neq 0}}^{N2} \cos(mwg_k) \times \prod_{l=1}^{L} A_{(l,m)} \\ \text{subject to} \quad & g(t) = ah_1(t) + (1-a)h_2(t) \end{aligned} \tag{6.5}$$

with

$$A_{(l,m)} = \frac{1}{2\pi T} \int_0^{2\pi} \int_0^{T} \Big(\prod_{k=-P}^{P} [\cos(mwR_l g_{k_l}^d \cos(\theta_l)) \cos(mwR_l g_{k_l}^d \sin(\theta_l))] \Big)\, d\theta_l \, d\upsilon_l. \tag{6.6}$$

Convexity of $\mathbb{P}_e$ due to ISI+CCI

As in 6.2.1, we need to investigate if the function $\underset{\text{ISI+CCI}}{\mathbb{P}_e}$ is or not convex.

$$\underset{\text{ISI+CCI}}{\mathbb{P}_e}(\theta h_1 + (1-\theta)h_2) \leq \theta \underset{\text{ISI+CCI}}{\mathbb{P}_e}(h_1) + (1-\theta)\underset{\text{ISI}}{\mathbb{P}_e}(h_2)\ \forall h_1, h_2 \in C \tag{6.7}$$

We explore if the inequality given in (6.7) is fulfilled. For this, we consider the PLCP as well. The parameters used are $\alpha = \{0.25, 0.35, 0.5\}$ SNR=15 dB, SIR=10 dB, L=2 and the complete response of the filter is considered for $\eta = \{0.05, 0.1, 0.2\}$. From the results depicted in the Fig. 6.3, it can be seen that for all cases and for $\alpha \in [0, 1]$ the left side of the inequality holds below the right side. This would indicate us that the expression given in (6.7) is convex

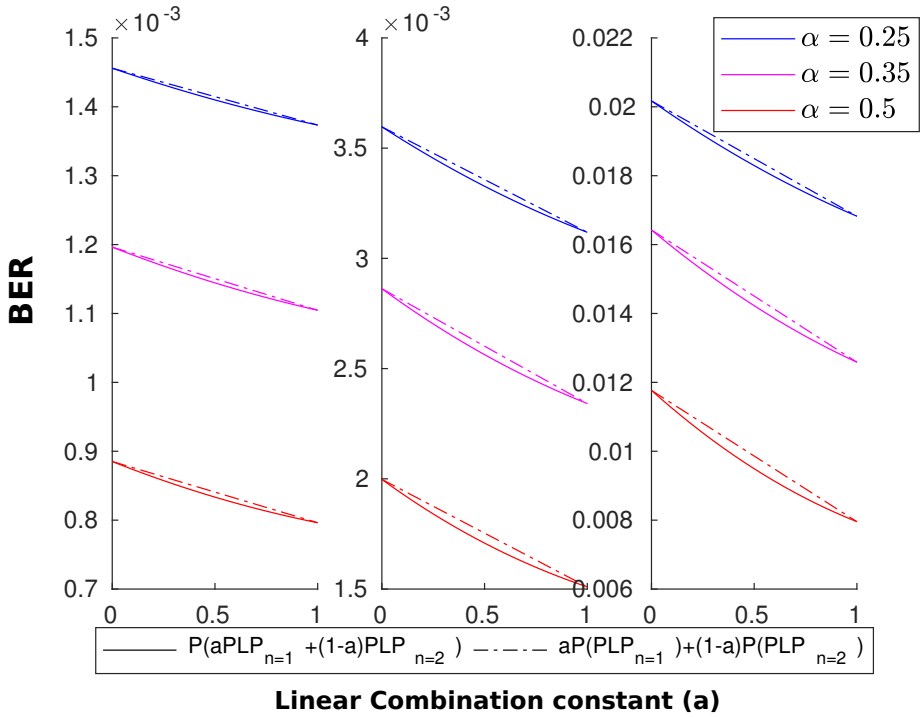

Figure 6.3: Convexity of the BER expression considering the ISI and CCI effects for different timing offset values. The PLCP, $\text{PLP}_{n=1}$, $\text{PLP}_{n=2}$ pulse with parameters $\alpha = \{0.25, 0.35, 0.5\}$ SNR=15 dB, SIR=10 dB, L=2 and the complete response are considered. Each plot shows the inequality expression, in solid line the left side and dashed line the right side for $\eta = t/T = \{0.05, 0.1, 0.2\}$.

6.3 Experiments

6.3.1 Performance evaluation in systems impaired by ISI

In this section, several pulses formulated as a linear combination of different Nyquist-I pulses, are optimized in term of the BER considering a base-band system impaired by ISI, for different values of roll-off factors (α), time offsets (η) and truncation values. The pulses optimized and evaluated are, the RC, in first instance used as a reference, and the following Linear Combination Pulses, PLCP, LCP, v, r and q, described in Section 2.2.4. The pulses formulated in the time domain like the ELP, SPLCP or IDJLC are not evaluated in this section because they would not meet the frequency constraints of the channel or communication standard, as described in Section 2.2.5.

First, in Fig. 6.4 we illustrate the effectiveness of the optimization algorithm for the complete impulse response of the PLCP, using $\alpha = 0.25$, $\tau = 0.05$, SNR=15 dB. The result is compared with the numerical solution method, which performs an exhaustive search of the optimal point exploring a limited region of the search space [18, 3, 7]. It can be seen that the results are very close, if we consider the numerical solution as the true optimal value, the relative error in terms of the BER is only of 0.14%. The difference of results is due to the choice of parameters which controls the accuracy of the optimization results. The termination tolerance on the first-order optimality, which is related to the gradient of the function, is set to 1×10^{-10} being a fair choice between the accuracy and computation time of the solution.

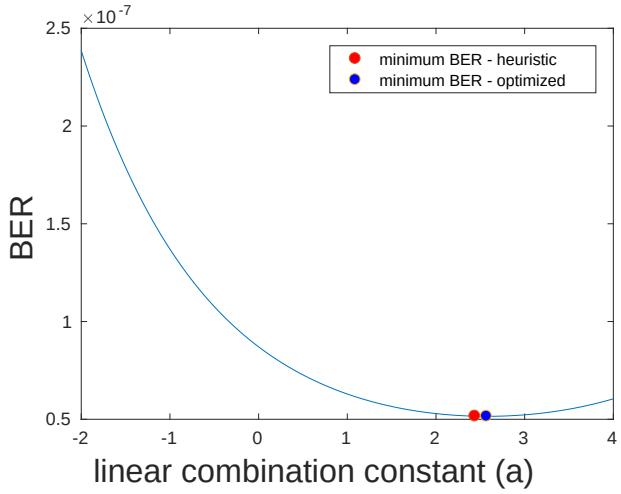

Figure 6.4: Comparison of results for the PLCP pulse, considering the optimization process and the exhaustive method for a base-band system impaired by ISI.

The results of the optimization problem are presented in Tables 6.1 for the complete impulse response and in 6.2 for the truncated version $[-5.5t/T,\ 5.5t/T]$. For the ideal case, considering $\alpha = 0.25$, and timing offset equals to $t/T = \{0.05, 0.1\}$ the pulse with the

best performance is the v pulse, and for $t/T = \{0.2\}$ is the q pulse. For $\alpha = 0.35$ and $t/T = \{0.1, 0.2\}$ the pulse with the best performance is the v pulse and for $t/T = \{0.05\}$ the r pulse. Finally, for $\alpha = 0.5$, the pulse with the best performance is the v pulse for all timing offsets. Considering the truncated version of the pulses, the performance follows the same structure than the case where the complete versions of the pulses are considered. For $\alpha = 0.25$ and $t/T = \{0.1, 0.2\}$ the pulse with the best performance is the v pulse, and for $t/T = \{0.05\}$ is the q pulse. For $\alpha = 0.35$ and $t/T = \{0.05\}$ the pulse with the best performance is the r pulse. For all the remain cases, the v pulse outperforms the other evaluated Nyquist-I pulses. Considering the optimization results for the truncated and complete version of the pulses, it can be seen that the optimization converges to a different value of linear constant depending on the pulse, roll-off factor and timing offset. Also, the BER is significantly lower for all the truncated version of the pulses compared with the complete version, except for the RC pulse, which does not possess any extra degree of freedom. The major performance variation correspond to the v pulse, with a maximum percentage variation of -44% for $\alpha = 0.5$ and $t/T = 0.2$ considering the truncated impulse response.

α	Pulse	$t/T = 0.05$	$t/T = 0.1$	$t/T = 0.2$
	RC	8.219E-08	2.818E-06	9.746E-04
	μ	(2.499)	(2.325)	(2.203)
	PLCP	5.154E-08	1.058E-06	2.807E-04
	β	(4.062)	(2.686)	(2.535)
	LCP	5.371E-08	1.016E-06	2.662E-04
0.25	a	(3.361)	(2.582)	(3.258)
	V	**4.527E-08**	**8.105E-07**	2.022E-04
	a	(0.595)	(0.968)	(0.877)
	R	5.048E-08	8.825E-07	2.207E-04
	a	(0.970)	(0.838)	(0.766)
	Q	4.548E-08	8.138E-07	**1.969E-04**
	RC	6.000E-08	1.390E-06	3.908E-04
	μ	(1.549)	(2.071)	(1.902)
	PLCP	3.772E-08	4.585E-07	8.598E-05
	β	(2.294)	(2.407)	(2.162)
	LCP	3.478E-08	4.396E-07	8.129E-05
0.35	a	(7.092)	(0.681)	(1.342)
	V	3.788E-08	**3.569E-07**	**6.101E-05**
	a	(1.242)	(1.168)	(1.024)
	R	**3.208E-08**	3.776E-07	6.560E-05
	a	(1.120)	(0.936)	(0.783)
	Q	3.210E-08	3.866E-07	6.855E-05
	RC	3.972E-08	5.489E-07	1.022E-04
	μ	(2.057)	(1.898)	(1.615)
	PLCP	2.202E-08	1.656E-07	1.992E-05
	β	(2.433)	(2.121)	(1.813)
	LCP	2.153E-08	1.582E-07	1.892E-05
0.5	a	(1.744)	(2.118)	(2.844)
	V	**1.911E-08**	**1.207E-07**	**1.609E-05**
	a	(1.333)	(1.229)	(0.927)
	R	2.000E-08	1.324E-07	1.613E-05
	a	(1.312)	(1.098)	(0.802)
	Q	2.065E-08	1.451E-07	1.765E-05

Table 6.1: BER considering ISI for linear combination of pulse with optimized parameters. The parameters used are, 2^{10} Interfering Symbols and SNR=15 dB for the complete pulse version.

6.3.2 Performance evaluation in systems impaired by ISI+CCI

In this section, the same linear combination of pulses that were evaluated in subsection 6.3.1 are optimized in terms of the BER considering a pass-band system impaired by ISI and CCI, for the Precise model, different values of roll-off factors (α), time offsets (τ), and truncation values. First, we illustrate the effectiveness of the optimization results for the PLCP filter. In Fig. 6.4 the result of the optimization is compared with the extensive computer simulations for $\alpha = 0.25$, $\tau = 0.05$, considering the complete impulse response and SNR=15 dB. It can be seen that the results are very close, begin the relative error only of 0.001%.

α	Pulse	$t/T = 0.05$	$t/T = 0.1$	$t/T = 0.2$
	RC	8.2158E-08	2.8157E-06	9.7340E-04
	μ	(2.229)	(2.539)	(2.406)
	PLCP	5.0527E-08	9.5682E-07	2.4322E-04
	β	(3.335)	(2.923)	(2.758)
	LCP	4.8480E-08	9.2292E-07	2.3178E-04
0.25	a	(-0.130)	(5.834)	(6.730)
	V	4.2298E-08	**6.2580E-07**	**1.2675E-04**
	a	(1.322)	(1.244)	(1.139)
	R	4.3459E-08	7.3610E-07	1.7143E-04
	a	(1.324)	(1.178)	(1.075)
	Q	**4.0383E-08**	6.3236E-07	1.3866E-04
	RC	5.9982E-08	1.3886E-06	3.9043E-04
	μ	(2.527)	(2.113)	(1.927)
	PLCP	3.4841E-08	4.5042E-07	8.3577E-04
	β	(2.692)	(2.435)	(2.223)
	LCP	3.3828E-08	4.2586E-07	7.7455E-05
0.35	a	(0.917)	(-0.350)	(1.371)
	V	2.9458E-08	**2.9410E-07**	**4.0723E-05**
	a	(1.825)	(1.691)	(1.444)
	R	**2.8468E-08**	2.9668E-07	4.6798E-05
	a	(1.416)	(1.205)	(1.002)
	Q	2.9387E-08	3.2082E-07	5.2633E-05
	RC	3.9721E-08	5.4880E-07	1.0213E-04
	μ	(2.542)	(1.884)	(1.627)
	PLCP	2.2517E-08	1.6416E-07	1.9632E-05
	β	(2.392)	(2.272)	(1.829)
	LCP	2.1448E-08	1.5667E-07	1.8596E-05
0.5	a	(1.986)	(1.683)	(3.263)
	V	**1.7654E-08**	**9.3881E-08**	**9.0108E-06**
	a	(1.026)	(1.552)	(1.186)
	R	2.0025E-08	1.1312E-07	1.2705E-05
	a	(1.601)	(1.157)	(0.838)
	Q	2.0683E-08	1.4156E-07	1.7121E-05

Table 6.2: BER considering ISI for linear combination of pulse with optimized parameters. The parameters used are, 2^{10} Interfering Symbols and SNR=15 dB for the truncated pulse version ($[-5.5t/T; 5.5t/T]$).

The results of the optimization process considering the system impaired by ISI and CCI for the Precise model, are presented in Tables 6.3 and 6.4 for the complete and truncated version of the pulses. It can be seen that the results in terms of BER for the truncated version are slightly better than for the complete version of the pulses. Comparing the results with the presented in Table 8.10, where different recently proposed pulses formulated in the time domain were evaluated for the BER expression which considers ISI + CCI interference, considering the Precise model, it can be seen that the present results are bigger up to one order of magnitude, which can be explained considering the large out-of-band radiation of the pulses presented in Chapter 5. Also, comparing the results with the given in Section 4.3.2, where the performance of pulses being formulated in the time domain are evaluated in a base-band system considering ISI and CCI using the sinusoidal model are shown, it can be seen that in this case, the BER is smaller for all the conditions. The prior met the fact that the sinusoidal always underestimates the effects of interference on the BER.

Considering the complete impulse response of the pulses, the v pulse outperforms other pulses for all timing offsets and roll-off factors, following the same behavior of the case where only the ISI effect is considered. For the truncated version, the pulse with the best performance for $\alpha = 0.25$ and all timing offsets is the q pulse, for $\alpha = 0.35$ and all timing offsets is the r pulse and for $\alpha = 0.5$ and all timing offsets is the v pulse. These varieties of results are explained due to the optimization of the BER considering the truncation version of the pulses, so, for every truncation value, a new optimum constant value needs to be found. Also, as in the case of the system impaired by ISI, the constant of the linear combination converge to different values depending on the pulse, roll-off factor and timing offset.

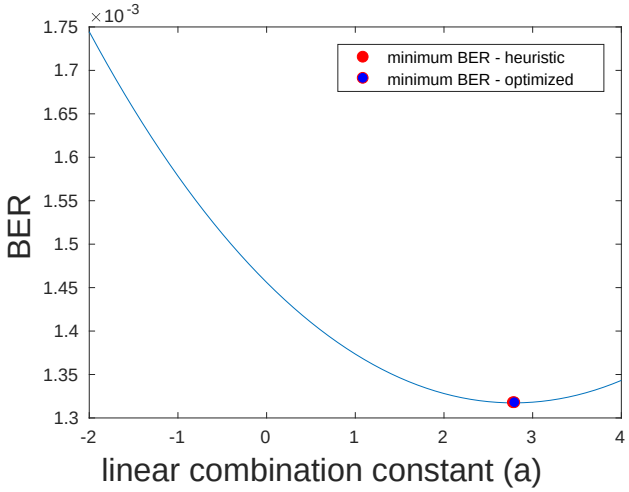

Figure 6.5: Comparison of results for the PLCP pulse, considering the optimization process and the exhaustive method for a pass-band system impaired by ISI+CCI.

6.4 Conclusions - Optimization

In this chapter, the optimization of linear combination of Nyquist-I pulses considering first a base-band system impaired by ISI and later a pass-band system impaired by ISI+CCI, for the Precise model, were performed. The complete and truncated version of the Nyquist-I pulses were considered. The optimal parameters resultant from the optimization process were compared with the optimal parameters found exhaustively, finding minimal differences between their values. For the base-band system impaired by ISI, the BER is significantly lower for the truncated version of the pulses compared with the complete version. The pulse with the best performance in terms of BER was the v pulse, considering its complete and truncated version.

Considering the pass-band system impaired by ISI + CCI for the Precise model, the results show that the BER for the truncated version of the pulse is slightly lower than for the complete impulse response. Considering the complete impulse response, the pulse with the best performance was the v pulse for all the roll-off factors and timing offsets. Moreover, for the truncated version, the pulse with the best performance for $\alpha = 0.25$ and all timing

offsets is the q pulse, for $\alpha = 0.35$ and all timing offsets is the r pulse and for $\alpha = 0.5$ and all timing offsets is the v pulse. In general, for every system parameter, α, η and truncation value, the optimal parameter of the Nyquist-I pulse need to be found. As future work, the convexity of the optimization problem will be prove and other optimization algorithms will be used.

α	Pulse	$t/T = 0.05$	$t/T = 0.1$	$t/T = 0.2$
	RC	1.4413e-03	3.5098e-03	1.9568e-02
	μ	(2.784)	(2.721)	(2.661)
	PLCP	1.3173e-03	2.8148e-03	1.4734e-02
	β	(3.257)	(3.179)	(3.102)
	LCP	1.3122e-03	2.7871e-03	1.4542e-02
0.25	a	(8.866)	(1.165)	(1.468)
	V	**1.2848e-03**	**2.6381e-03**	**1.3494e-02**
	a	(1.247)	(1.208)	(1.165)
	R	1.2950e-03	2.6948e-03	1.3901e-02
	a	(1.079)	(1.046)	(1.009)
	Q	1.2862e-03	2.6474e-03	1.3568e-02
	RC	1.1794e-03	2.7638e-03	1.5701e-02
	μ	(2.521)	(2.457)	(2.360)
	PLCP	1.0537e-03	2.0783e-03	1.0757e-02
	β	(2.926)	(2.847)	(2.724)
	LCP	1.0490e-03	2.0539e-03	1.0586e-02
0.35	a	(-0.072)	(0.100)	(0.332)
	V	**1.0336e-03**	**1.9678e-03**	**9.9194e-03**
	a	(1.586)	(1.531)	(1.444)
	R	1.0341E-03	1.9755E-03	1.0027E-02
	a	(1.222)	(1.179)	(1.105)
	Q	1.0353E-03	1.9825E-03	1.0085E-02
	RC	8.6775e-04	1.8985e-03	1.0983e-02
	μ	(2.139)	(2.100)	(1.976)
	PLCP	7.6220e-04	1.3412e-03	6.8245e-03
	β	(2.443)	(2.397)	(2.246)
	LCP	7.5903e-04	1.3250e-03	6.7098e-03
0.5	a	(1.891)	(1.966)	(2.279)
	V	**7.4279e-04**	**1.2417e-03**	**6.1183e-03**
	a	(1.415)	(1.382)	(1.263)
	R	7.4864e-04	1.2713e-03	6.3084e-03
	a	(1.275)	(1.243)	(1.126)
	Q	7.5311e-04	1.2950E-03	6.5020E-03

Table 6.3: BER considering ISI+CCI for linear combination of pulse with optimized parameters. The parameters used are, 2^{10} Interfering Symbols, SNR=15dB, SIR=10dB, number of interfering signals $L = 2$, for the complete impulse response. In all the cases the interfering pulse used was the RC pulse.

α	Pulse	$t/T = 0.05$	$t/T = 0.1$	$t/T = 0.2$
	RC	1.4410e-03	3.5091e-03	1.9564e-02
	μ	(3.016)	(2.950)	(2.886)
	PLCP	1.3068e-03	2.7575e-03	1.4324e-02
	β	(3.508)	(3.427)	(3.347)
	LCP	1.3023e-03	2.7334e-03	1.4157e-02
0.25	a	(2.479)	(2.936)	(3.380)
	V	1.2701e-03	2.5539e-03	1.2844e-02
	a	(1.582)	(1.535)	(1.478)
	R	1.2743e-03	2.5848e-03	1.3131e-02
	a	(1.472)	(1.431)	(1.375)
	Q	**1.2575e-03**	**2.4959e-03**	**1.2516e-02**
	RC	1.1793e-03	2.7634e-03	1.5698e-02
	μ	(2.547)	(2.483)	(2.384)
	PLCP	1.0522e-03	2.0702e-03	1.0698e-02
	β	(2.994)	(2.915)	(2.788)
	LCP	1.0462e-03	2.0390e-03	1.0479e-02
0.35	a	(-0.631)	(-0.405)	(-0.064)
	V	1.0218e-03	1.9037e-03	9.4091e-03
	a	(2.104)	(2.045)	(1.917)
	R	**1.0114e-03**	**1.8585e-03**	**9.2050e-03**
	a	(1.511)	(1.465)	(1.371)
	Q	1.0179e-03	1.8927e-03	9.4540e-03
	RC	8.6773e-04	1.8984e-03	1.0982e-02
	μ	(2.149)	(2.110)	(1.986)
	PLCP	7.6167e-04	1.3385e-03	6.8030e-03
	β	(2.457)	(2.412)	(2.261)
	LCP	7.5842e-04	1.3218e-03	6.6844e-03
0.5	a	(2.111)	(2.195)	(2.551)
	V	**7.32156e-04**	**1.1852e-03**	**5.6205e-03**
	a	(1.683)	(1.655)	(1.519)
	R	7.4026e-04	1.2286e-03	6.0065e-03
	a	(1.317)	(1.286)	(1.167)
	Q	7.5169e-04	1.2877e-03	6.4473e-03

Table 6.4: BER considering ISI+CCI for linear combination of pulse with optimized parameters. The parameters used are, 2^{10} Interfering Symbols, SNR=15dB, SIR=10dB, number of interfering signals $L = 2$, for the truncated pulse version ($[-5.5t/T; 5.5t/T]$). In all the cases the interfering pulse used was the RC pulse.

Chapter 7

Conclusions and Future Work

In this work, the ELP pulse was numerically analyzed and compared with respect to recently proposed pulses given in the literature and the traditional RC pulse in the time and frequency domains. Considering a base-band system impaired by ISI and additive white noise, the ELP obtains the smallest BER for the ideal impulse response and $\beta = 1$ compared to the other evaluated pulses considering $\alpha = \{0.25, 0.35\}$. For $\alpha = 0.5$ only the Sinc Parametric Linear Combination Pulse (SPLCP) outperforms the $\text{ELP}_{\beta=1}$. For the time-limited version of the pulses, its behavior is improved in terms of BER for the pulses with tails that decay more slowly than those of the ELP. Considering the frequency response, the ELP introduces additional out-of-band radiation compared to the RC pulse. The excess of bandwidth introduced by the family of pulses analyzed in this manuscript explains the good performance in the time domain, in terms of BER and a wider eye opening. Finally, for the truncated frequency response, the ELP did not present additional spectral regrowth. The performance of the ELP could potentially be improved by using optimization techniques, specifically designed for BER reduction in presence of time sampling errors.

Further, the same Nyquist pulses were evaluated considering a base-band system impaired first by CCI and later by CCI+ISI, using the sinusoidal model of interference. For both cases, the average BER was computed for different symbol timing errors and roll-off factors. The results indicate that the RC pulse achieved the best performance considering only CCI. This is because the RC pulse possesses the greatest central lobe magnitude compared to the other evaluated pulses. Second, considering the combined effects of CCI and ISI, in general, the SPLCP outperformed the other pulses by presenting the smallest average BER for roll-off factors $\alpha = \{0.35, 0.5\}$ and L=$\{2, 6\}$ number of interfering signals. For $\alpha = 0.25$, the $\text{ELP}_{\beta=1}$ obtains the best performance for all number of interfering signals. These results indicate that when ISI and CCI are both taken into consideration, the magnitude of the main lobe is preponderant and is even more important than the magnitude of the side-lobes as the number of interferer signals increases for a fixed interference power.

Because the sinusoidal interference model for representing the CCI always underestimates the effects of interference on the BER, we developed an expression to compute the BER in a pass-band system impaired by ISI and CCI simultaneously, for the Precise interference model. This interference model is assumed to have the same modulation and nature as the desired

signal, that is, the interfering signals are quadrature phase-shift keying (QPSK) modulated with the same symbol rate, but with random carrier phase shifts and random symbol timing offsets relative to the desired signal. Then, using this new expression we evaluated different recently proposed Nyquist-I pulses, for various scenarios. The results indicated that the pulse with the best performance, in terms of BER, is the IDJ1, which outperforms other evaluated pulses for all the scenarios, namely different regimes of SNR, SIR, and number of interfering signals. Moreover, the pulses with the biggest out-of-band (OBR) radiation are the IDJLC and IDJ1. This phenomenon would introduce adjacent channel interference (ACI) decreasing the performance of the communication system. The excess of OBR is related to the optimization of the parameters, of both pulses, where the optimization process did not consider restrictions on the frequency characteristic.

Later, considering linear combination of Nyquist-I pulses, we performed the optimization in terms of BER first for a base-band system impaired by ISI and later a pass-band system impaired by ISI+CCI, for the Precise model. The ideal and truncated version of the Nyquist-I pulses were considered for each case. The use of linear combination Nyquist-I pulses ensured that the stop-band frequency remains at $(1+\alpha)(1/2T)$. Considering the pass-band system impaired by ISI + CCI for the Precise model, the results showed that the BER for the truncated version of the pulse is slightly lower than for the ideal impulse response. Considering the ideal impulse response, the pulse with the best performance was the v pulse. Moreover, for the truncated version, the pulse with the best performance for $\alpha = 0.25$ and all timing offsets was the q pulse, for $\alpha = 0.35$ and all timing offsets was the r pulse and for $\alpha = 0.5$ and all timing offsets was the v pulse.

Within this work, we have successfully evaluated recently proposed and standard Nyquist-I pulses in base-band and pass-band systems impaired by different kinds of interferences, ISI, CCI, and the combination of ISI and CCI, for the sinusoidal and Precise interference models. Also, the bases of the optimization of linear combination of Nyquist-I pulses have been settled, and as future work, we hope to demonstrate good properties of the optimization problems.

As future work, we will consider the develop of new measures to evaluate the performance of Nyquist-I pulses that consider only a distribution of the time jitter, and not its particular value. Also, we will probe that the optimization problem of minimize the BER subject to linear combination of Nyquist-I pulses is convex. This would imply that adding new pulses to the linear combination, would not affect negatively the BER.

Chapter 8

Annexes

Appendix A

8.1 Derivation of the Precise model for Co-channel Interference

Consider a base-band system impaired by ISI and CCI considering the Precise model. The signal at the output of the receiver filter ($y_a(t)$) assuming that a_0 is detected, can be written as

$$y_a = a_0 g_0^d + \sum_{\substack{k=-\infty \\ k\neq 0}}^{\infty} a_k g_k^d + \sum_{l=1}^{L} \eta_l + n, \tag{8.1}$$

where z represent the contribution from the ISI effect

$$z = \sum_{\substack{k=-\infty \\ k\neq 0}}^{\infty} a_k g_k^d = \sum_{\substack{k=-\infty \\ k\neq 0}}^{\infty} z_k, \tag{8.2}$$

and η_l the contribution from the lth interfering signal

$$\eta_l = \sum_{l=1}^{L} R_l[V_{c_l}\cos(\theta_l) - V_{d_l}\sin(\theta_l)], \tag{8.3}$$

$$\begin{aligned} V_{c_l} &= \sum_{k=-\infty}^{\infty} c_{k_l} g^i(t - kT - \upsilon_l), \\ V_{d_l} &= \sum_{k=-\infty}^{\infty} d_{k_l} g^i(t - kT - \upsilon_l). \end{aligned} \tag{8.4}$$

By symmetry, the average probability of error $\mathbb{P}_e$ assuming that the bit $a_0 = -1$ was transmitted for the in-phase component is given by

$$\mathbb{P}_e = \mathbb{P}(y_a > 0 \mid a_0 = -1), \tag{8.5}$$

then, the equation 8.1 turns in to

$$y_a = -g_0^d + z + \eta + n. \tag{8.6}$$

Let the probability density function (pdf) of the noise n denoted by $f(\cdot)$ and the complementary cumulative distribution function (cdf) denoted by $G(\cdot)$. The probability of error conditioned on $z + \eta$ is,

$$\begin{aligned} \mathbb{P}_{e|z+\eta} &= \mathbb{P}(-g_o^d + z + \eta + n > 0) \\ &= \mathbb{P}(n > g_o^d - z - \eta) \\ &= G(g_o^d - z - \eta). \end{aligned} \tag{8.7}$$

The calculation of the exact value of $\mathbb{P}_e$ is very complex because the distribution function of the RV $z + \eta$ is difficult to obtain. Let the pdf of $z + \eta$ be denoted $f_{z+\eta}(z + \eta)$. Averaging the conditional probability (8.7) over the distribution of all values of $z + \eta$

$$\mathbb{P}_e = \int_{-\infty}^{\infty} f_{z+\eta}(z + \eta) G(g_o^d - z - \eta) d(z + \eta), \tag{8.8}$$

assuming that $G(x)$ can be represented by a Fourier series, in the form

$$G(x) = \sum_{m=-\infty}^{\infty} c_m e^{jmwx} + \epsilon(x), \tag{8.9}$$

being $\epsilon(x)$ an error term and w the angular frequency. The expression in (8.9) says that the cdf $G(x)$ of the noise process can be expressed approximately and exactly (if $\epsilon(x) = 0$) by a Fourier series. Combining (8.8) with (8.9)

$$\begin{aligned} \mathbb{P}_e &= \int_{-\infty}^{\infty} f_{z+\eta}(z + \eta) \Big[\sum_{m=-\infty}^{\infty} c_m e^{jmw(g_o^d - z - \eta)} + \epsilon(g_o^d - z - \eta) \Big] d(z + \eta) \\ &= \sum_{m=-\infty}^{\infty} c_m e^{jmw(g_o^d)} \int_{-\infty}^{\infty} f_{z+\eta}(z + \eta) e^{-jmw(z+\eta)} d(z + \eta) \\ &+ \int_{-\infty}^{\infty} f_{z+\eta}(z + \eta) \epsilon(g_o^d - z - \eta) d(z + \eta). \end{aligned} \tag{8.10}$$

The interchange of the order of integration and summation in (8.10) is valid when the series (8.9) converges uniformly to a limit $G(x) - \epsilon(x)$. Let's name

$$\gamma = \int_{-\infty}^{\infty} f_{z+\eta}(z + \eta) \epsilon(g_o^d - z - \eta) d(z + \eta), \tag{8.11}$$

and

$$\Phi_{z+\eta}(w) = \mathbb{E}[e^{jw(z+\eta)}] = \int_{-\infty}^{\infty} f_{z+\eta}(z+\eta)e^{jw(z+\eta)}d(z+\eta), \tag{8.12}$$

where $\mathbb{E}$ denotes expectation. The term γ represents the error of the approximation of the Fourier series and $\Phi_{z+\eta}(w)$ is the characteristic function of the RV $(z+\eta)$. Combining (8.10) with (8.11) and (8.12)

$$\mathbb{P}_e = \sum_{m=-\infty}^{\infty} c_m e^{jmw(g_o^d)}\Phi_{z+\eta}(-mw) + \gamma, \tag{8.13}$$

is assumed that z_m, z_n, η_p and η_q ($-\infty \leq m \leq \infty$, $-\infty \leq n \leq \infty$, $1 \leq p \leq L$, $1 \leq q \leq L$, $z_m \neq z_q$ and $\eta_p \neq \eta_q$) are independent. Therefore

$$\begin{aligned}
\Phi_{z+\eta}(w) =& \mathbb{E}\Big[e^{jw(\cdots+z_{-1},z_1\cdots+\eta_1+\cdots+\eta_L)}\Big] = \mathbb{E}\Big[\prod_{\substack{k=-\infty\\k\neq 0}}^{\infty}\prod_{l=1}^{L} e^{jw(z_k+\eta_l)}\Big] \\
&= \mathbb{E}\Big[\prod_{\substack{k=-\infty\\k\neq 0}}^{\infty} e^{jw(z_k)} \times \prod_{l=1}^{L} e^{jw(\eta_l)}\Big] \\
&= \prod_{\substack{k=-\infty\\k\neq 0}}^{\infty} \mathbb{E}[e^{jw(z_k)}] \times \prod_{l=1}^{L} \mathbb{E}[e^{jw(\eta_l)}] \\
&= \prod_{\substack{k=-\infty\\k\neq 0}}^{\infty} \Phi_{z_k}(w) \times \prod_{l=1}^{L} \Phi_{\eta_l}(w).
\end{aligned} \tag{8.14}$$

Here the RV z_k can take two possible values, $\{-g_k, g_k\}$, with equal probability and consequently z_k follows a Rademacher distribution, with characteristic function given by

$$\Phi_{z_k}(w) = \frac{1}{2}(e^{jw} + e^{-jw}) = \cos(w). \tag{8.15}$$

For the Precise interfering model, assuming that the number of symbols from each co-channel interfering is $2 \times P + 1$ the characteristic function is

$$\begin{aligned}
\Phi_{\eta_l}(w) &= \mathbb{E}[\exp(w[V_{c_l}\cos(\theta_l) - V_{d_l}\sin(\theta_l)])] \\
&= \mathbb{E}\Big[\exp\Big(\sum_{j=-P}^{P} w[c_{k_l}\cos(\theta_l) - d_{k_l}\sin(\theta_l)]g^i(-\upsilon_l - jT)\Big)\Big] \\
&= \mathbb{E}\Big[\prod_{j=-P}^{P} \exp\Big(w[c_{j_l}\cos(\theta_l) - d_{j_l}\sin(\theta_l)]g^i(-\upsilon_l - jT)\Big)\Big] \\
&= \frac{1}{2\pi T}\int_0^{2\pi}\int_0^{T}\Big(\prod_{j=-P}^{P}[cos(wg_{j_l}^i\cos(\theta_l))cos(wg_{j_l}^i\sin(\theta_l))]\Big)d\upsilon_l d\theta_l,
\end{aligned} \tag{8.16}$$

defining

$$d_l(x) = \frac{1}{2\pi T}\int_0^{2\pi}\int_0^{T}\Big(\prod_{j=-P}^{P}[\cos(xg_{j_l}^i\cos(\theta_l))\cos(xg_{j_l}^i\sin(\theta_l))])\; d\upsilon_l\; d\theta_l\Big). \tag{8.17}$$

Combining (8.13), 8.16 and (8.15)

$$\begin{aligned}\mathbb{P}_e &= \sum_{m=-\infty}^{\infty} c_m e^{jmw(g_o^d)} \prod_{\substack{k=-\infty \\ k\neq 0}}^{\infty} cos(mwg_k^d) \prod_{l=1}^{L} d_l(mwR_l) + \gamma \\ &= c_o + \sum_{m=1}^{\infty} \{c_m e^{jmw(g_o^d)} + c_{-m} e^{-jmw(g_o^d)}\} \prod_{\substack{k=-\infty \\ k\neq 0}}^{\infty} cos(mwg_k^d) \prod_{l=1}^{L} d_l(mwR_l) + \gamma.\end{aligned} \tag{8.18}$$

Let M be a positive integer chosen so that "negligible" error results when the infinite series (8.18) is truncated after M terms.

$$\mathbb{P}_e = c_o + \sum_{m=1}^{M} \{c_m e^{jmw(g_o^d)} + c_{-m} e^{-jmw(g_o^d)}\} \prod_{\substack{k=-\infty \\ k\neq 0}}^{\infty} cos(mwg_k^d) \prod_{l=1}^{L} d_l(mwR_l) + \gamma + R_M, \tag{8.19}$$

where

$$R_M = \sum_{m=M+1}^{\infty} \{c_m e^{jmw(g_o^d)} + c_{-m} e^{-jmw(g_o^d)}\} \prod_{\substack{k=-\infty \\ k\neq 0}}^{\infty} cos(mwg_k^d) \prod_{l=1}^{L} d_l(mwR_l). \tag{8.20}$$

If (8.9) can be found that has good convergence properties, it means, only small number of terms M is needed in (8.19), then the effort to calculate $\mathbb{P}_e$ is proportional to $M(N-1)$ where N is number of symbols. In general, the coefficients of an exact Fourier series of $G(x)$ need to be determined by numerical integration. In this way we will use and approximate Fourier series, based on approximate the noise pdf, by a periodic square wave. Using the method explained in [6] the expression in (8.19) turns in to,

$$\mathbb{P}_e = \frac{1}{2} - \frac{2}{\pi} \sum_{\substack{m=1 \\ m\ odd}}^{M} \frac{\exp(-m^2w^2/2) sin(mwg_o^d)}{m} \prod_{\substack{k=-\infty \\ k\neq 0}}^{\infty} cos(mwg_k^d) \prod_{l=1}^{L} d_l(mwR_l) + \gamma + R_M. \tag{8.21}$$

Finally, if we consider finite number of interfering symbols, the limit of the product sequence due to ISI can be limited to $N1 + N2 - 1$ interfering symbols.

$$\mathbb{P}_e = \frac{1}{2} - \frac{2}{\pi} \sum_{\substack{m=1 \\ m\ odd}}^{M} \frac{\exp(-m^2w^2/2) sin(mwg_o^d)}{m} \prod_{\substack{k=N_1 \\ k\neq 0}}^{N_2} cos(mwg_k^d) \prod_{l=1}^{L} d_l(mwR_l) + \gamma + R_M + \beta, \tag{8.22}$$

with

$$\begin{aligned}\beta = &- \frac{2}{\pi} \sum_{\substack{m=1 \\ m\ odd}}^{M} \frac{\exp(-m^2w^2/2) sin(mwg_o^d)}{m} \prod_{\substack{k=N_1 \\ k\neq 0}}^{N_2} cos(mwg_k^d) \\ &\Big[\prod_{\substack{k=-\infty \\ k\neq 0}}^{N_1-1} cos(mwg_k^d) \prod_{\substack{k=N_2+1 \\ k\neq 0}}^{\infty} cos(mwg_k^d) - 1 \Big] \prod_{l=1}^{L} d_l(mwR_l).\end{aligned} \tag{8.23}$$

All the error terms are bounded and for details refers to [6]. Finally the expression to compute the BER is

$$\mathbb{P}_e = \frac{1}{2} - \frac{2}{\pi} \sum_{\substack{m=1 \\ m\ odd}}^{M} \frac{\exp(-m^2w^2/2) sin(mwg_o^d)}{m} \prod_{\substack{k=N_1 \\ k\neq 0}}^{N_2} cos(mwg_k^d) \prod_{l=1}^{L} d_l(mwR_l). \tag{8.24}$$

Appendix B

8.2 Numerical Results

α	Pulse	$t/T = 0.05$	$t/T = 0.10$	$t/T = 0.20$
0.25	RC	6.1303E-02	6.7453E-02	9.3014E-02
	BtRC	6.0466E-02	6.6013E-02	8.9572E-02
	SPLCP	5.7414E-02	6.1577E-02	8.0583E-02
	IPLCP	5.5936E-02	6.0194E-02	**7.9691E-02**
	ELP ($\beta = 1$)	5.4752E-02	5.9460E-02	8.0829E-02
	ELP ($\beta = 0.5$)	5.6585E-02	6.0769E-02	7.9927E-02
	IDJ1	5.3841E-02	**5.9198E-02**	8.3395E-02
	IDJLC	**5.2658E-02**	5.9254E-02	8.8999E-02
0.35	RC	6.0547E-02	6.6151E-02	8.9901E-02
	BtRC	5.9426E-02	6.4337E-02	8.5780E-02
	SPLCP	5.6944E-02	6.1049E-02	7.9898E-02
	IPLCP	5.5612E-02	5.9940E-02	7.9733E-02
	ELP ($\beta = 1$)	5.4575E-02	5.9384E-02	8.1183E-02
	ELP ($\beta = 0.5$)	5.6289E-02	6.0487E-02	**7.9727E-02**
	IDJ1	**5.3563E-02**	**5.9169E-02**	8.4498E-02
	IDJLC	5.3682E-02	6.9377E-02	1.4264E-01
0.5	RC	5.9464E-02	6.4400E-02	8.5928E-02
	BtRC	5.7972E-02	6.2249E-02	8.1607E-02
	SPLCP	5.6079E-02	6.0189E-02	**7.9139E-02**
	IPLCP	5.4994E-02	5.9525E-02	8.0163E-02
	ELP ($\beta = 1$)	**5.4224E-02**	5.9259E-02	8.2040E-02
	ELP ($\beta = 0.5$)	5.5720E-02	6.0001E-02	7.9604E-02
	IDJ1	5.3129E-02	**5.9185E-02**	8.6609E-02
	IDJLC	9.2186E-02	1.5782E-01	3.7760E-01

Table 8.1: BER considering ISI and CCI using the Precise Interference Model, for the ideal impulse response of the pulses and SNR=5dB, SIR=10dB, L=2.

α	Pulse	$t/T = 0.05$	$t/T = 0.10$	$t/T = 0.20$
0.25	RC	4.6483E-02	5.2466E-02	7.8009E-02
	BtRC	4.6061E-02	5.1398E-02	7.4683E-02
	SPLCP	4.4719E-02	4.8536E-02	6.6480E-02
	IPLCP	4.4247E-02	**4.8091E-02**	6.6208E-02
	ELP ($\beta = 1$)	4.3953E-02	4.8190E-02	6.7943E-02
	ELP ($\beta = 0.5$)	4.4446E-02	4.8245E-02	**6.6160E-02**
	IDJ1	4.3790E-02	4.8628E-02	7.1041E-02
	IDJLC	**4.3671E-02**	4.9707E-02	7.7555E-02
0.35	RC	4.6101E-02	5.1500E-02	7.4998E-02
	BtRC	4.5565E-02	5.0218E-02	7.1092E-02
	SPLCP	4.4549E-02	4.8288E-02	6.5969E-02
	IPLCP	4.4155E-02	**4.8054E-02**	6.6401E-02
	ELP ($\beta = 1$)	4.3916E-02	4.8245E-02	6.8395E-02
	ELP ($\beta = 0.5$)	4.4351E-02	4.8151E-02	**6.6084E-02**
	IDJ1	**4.3751E-02**	4.8823E-02	7.2320E-02
	IDJLC	4.5815E-02	6.0859E-02	1.3339E-01
0.5	RC	4.5583E-02	5.0263E-02	7.1232E-02
	BtRC	4.4932E-02	4.8887E-02	6.7312E-02
	SPLCP	4.4262E-02	**4.7969E-02**	**6.5567E-02**
	IPLCP	4.3995E-02	4.8069E-02	6.7139E-02
	ELP ($\beta = 1$)	4.3849E-02	4.8387E-02	6.9454E-02
	ELP ($\beta = 0.5$)	4.4181E-02	4.8038E-02	6.6216E-02
	IDJ1	**4.3701E-02**	4.9198E-02	7.4721E-02
	IDJLC	6.9170E-02	1.3856E-01	3.7550E-01

Table 8.2: BER considering ISI and CCI using the Precise Interference Model, for the ideal impulse response of the pulses and SNR=5dB, SIR=15dB, L=2.

α	Pulse	$t/T = 0.05$	$t/T = 0.10$	$t/T = 0.20$
0.25	RC	4.1755E-02	4.7642E-02	7.3064E-02
	BtRC	4.1471E-02	4.6705E-02	6.9789E-02
	SPLCP	4.0687E-02	4.4372E-02	6.1889E-02
	IPLCP	4.0538E-02	**4.4232E-02**	6.1827E-02
	ELP ($\beta = 1$)	**4.0528E-02**	4.4597E-02	6.3756E-02
	ELP ($\beta = 0.5$)	4.0594E-02	4.4249E-02	**6.1684E-02**
	IDJ1	4.0604E-02	4.5258E-02	6.7023E-02
	IDJLC	4.0821E-02	4.6661E-02	7.3825E-02
0.35	RC	4.1498E-02	4.6793E-02	7.0099E-02
	BtRC	4.1153E-02	4.5694E-02	6.6283E-02
	SPLCP	4.0614E-02	**4.4215E-02**	**6.1440E-02**
	IPLCP	**4.0521E-02**	4.4265E-02	6.2070E-02
	ELP ($\beta = 1$)	4.0536E-02	4.4694E-02	6.4240E-02
	ELP ($\beta = 0.5$)	4.0563E-02	4.4216E-02	6.1650E-02
	IDJ1	4.0640E-02	4.5524E-02	6.8358E-02
	IDJLC	4.3315E-02	5.8118E-02	1.3035E-01
0.5	RC	4.1166E-02	4.5733E-02	6.6419E-02
	BtRC	4.0788E-02	4.4618E-02	6.2653E-02
	SPLCP	4.0513E-02	**4.4072E-02**	**6.1159E-02**
	IPLCP	**4.0507E-02**	4.4417E-02	6.2909E-02
	ELP ($\beta = 1$)	4.0559E-02	4.4921E-02	6.5362E-02
	ELP ($\beta = 0.5$)	4.0520E-02	4.4224E-02	6.1868E-02
	IDJ1	4.0712E-02	4.6013E-02	7.0849E-02
	IDJLC	6.1405E-02	1.3185E-01	3.7488E-01

Table 8.3: BER considering ISI and CCI using the Precise Interference Model, for the ideal impulse response of the pulses and SNR=5dB, SIR=20dB, L=2.

α	Pulse	$t/T = 0.05$	$t/T = 0.10$	$t/T = 0.20$
0.25	RC	6.1224E-02	6.7353E-02	9.2856E-02
	BtRC	6.0392E-02	6.5918E-02	8.9417E-02
	SPLCP	5.7360E-02	6.1507E-02	8.0449E-02
	IPLCP	5.5894E-02	6.0136E-02	**7.9570E-02**
	ELP ($\beta = 1$)	5.4719E-02	5.9411E-02	8.0719E-02
	ELP ($\beta = 0.5$)	5.6538E-02	6.0705E-02	7.9800E-02
	IDJ1	5.3816E-02	**5.9157E-02**	8.3294E-02
	IDJLC	**5.2641E-02**	5.9225E-02	8.8918E-02
0.35	RC	6.0473E-02	6.6055E-02	8.9745E-02
	BtRC	5.9358E-02	6.4250E-02	8.5631E-02
	SPLCP	5.6893E-02	6.0983E-02	7.9768E-02
	IPLCP	5.5573E-02	5.9885E-02	7.9615E-02
	ELP ($\beta = 1$)	5.4544E-02	5.9337E-02	8.1074E-02
	ELP ($\beta = 0.5$)	5.6244E-02	6.0426E-02	**7.9602E-02**
	IDJ1	**5.3539E-02**	**5.9131E-02**	8.4401E-02
	IDJLC	5.3673E-02	6.9358E-02	1.4260E-01
0.5	RC	5.9396E-02	6.4312E-02	8.5778E-02
	BtRC	5.7914E-02	6.2174E-02	8.1469E-02
	SPLCP	5.6035E-02	6.0130E-02	**7.9017E-02**
	IPLCP	5.4959E-02	5.9474E-02	8.0050E-02
	ELP ($\beta = 1$)	5.4195E-02	5.9215E-02	8.1935E-02
	ELP ($\beta = 0.5$)	5.5680E-02	5.9944E-02	7.9485E-02
	IDJ1	**5.3108E-02**	**5.9150E-02**	8.6517E-02
	IDJLC	9.2061E-02	1.5769E-01	3.7762E-01

Table 8.4: BER considering ISI and CCI using the Precise Interference Model, for the ideal impulse response of the pulses and SNR=5dB, SIR=10dB, L=6.

α	Pulse	$t/T = 0.05$	$t/T = 0.10$	$t/T = 0.20$
0.25	RC	4.6481E-02	5.2460E-02	7.7994E-02
	BtRC	4.6059E-02	5.1393E-02	7.4668E-02
	SPLCP	4.4718E-02	4.8533E-02	6.6468E-02
	IPLCP	4.4246E-02	**4.8089E-02**	6.6197E-02
	ELP ($\beta = 1$)	4.3952E-02	4.8187E-02	6.7933E-02
	ELP ($\beta = 0.5$)	4.4446E-02	4.8242E-02	**6.6149E-02**
	IDJ1	4.3790E-02	4.8626E-02	7.1032E-02
	IDJLC	**4.3670E-02**	4.9705E-02	7.7547E-02
0.35	RC	4.6099E-02	5.1494E-02	7.4983E-02
	BtRC	4.5563E-02	5.0214E-02	7.1078E-02
	SPLCP	4.4548E-02	4.8285E-02	6.5958E-02
	IPLCP	4.4155E-02	**4.8052E-02**	6.6390E-02
	ELP ($\beta = 1$)	4.3916E-02	4.8243E-02	6.8385E-02
	ELP ($\beta = 0.5$)	4.4350E-02	4.8148E-02	**6.6073E-02**
	IDJ1	**4.3750E-02**	4.8821E-02	7.2311E-02
	IDJLC	4.5815E-02	6.0858E-02	1.3339E-01
0.5	RC	4.5581E-02	5.0259E-02	7.1218E-02
	BtRC	4.4930E-02	4.8884E-02	6.7300E-02
	SPLCP	4.4261E-02	**4.7966E-02**	**6.5557E-02**
	IPLCP	4.3995E-02	4.8067E-02	6.7129E-02
	ELP ($\beta = 1$)	4.3848E-02	4.8385E-02	6.9444E-02
	ELP ($\beta = 0.5$)	4.4180E-02	4.8035E-02	6.6206E-02
	IDJ1	**4.3701E-02**	4.9196E-02	7.4712E-02
	IDJLC	6.9159E-02	1.3854E-01	3.7550E-01

Table 8.5: BER considering ISI and CCI using the Precise Interference Model, for the ideal impulse response of the pulses and SNR=5dB, SIR=15dB, L=6.

α	Pulse	$t/T = 0.05$	$t/T = 0.10$	$t/T = 0.20$
0.25	RC	4.1755E-02	4.7642E-02	7.3063E-02
	BtRC	4.1471E-02	4.6704E-02	6.9788E-02
	SPLCP	4.0687E-02	4.4372E-02	6.1888E-02
	IPLCP	4.0539E-02	**4.4231E-02**	6.1826E-02
	ELP ($\beta = 1$)	**4.0528E-02**	4.4597E-02	6.3756E-02
	ELP ($\beta = 0.5$)	4.0594E-02	4.4249E-02	**6.1683E-02**
	IDJ1	4.0604E-02	4.5257E-02	6.7022E-02
	IDJLC	4.0822E-02	4.6661E-02	7.3824E-02
0.35	RC	4.1498E-02	4.6793E-02	7.0098E-02
	BtRC	4.1154E-02	4.5694E-02	6.6281E-02
	SPLCP	4.0614E-02	**4.4215E-02**	**6.1439E-02**
	IPLCP	**4.0521E-02**	4.4265E-02	6.2069E-02
	ELP ($\beta = 1$)	4.0536E-02	4.4694E-02	6.4239E-02
	ELP ($\beta = 0.5$)	4.0563E-02	4.4216E-02	6.1649E-02
	IDJ1	4.0640E-02	4.5523E-02	6.8357E-02
	IDJLC	4.3315E-02	5.8118E-02	1.3035E-01
0.5	RC	4.1166E-02	4.5733E-02	6.6418E-02
	BtRC	4.0788E-02	4.4617E-02	6.2652E-02
	SPLCP	4.0513E-02	**4.4072E-02**	**6.1158E-02**
	IPLCP	**4.0507E-02**	4.4417E-02	6.2908E-02
	ELP ($\beta = 1$)	4.0559E-02	4.4921E-02	6.5361E-02
	ELP ($\beta = 0.5$)	4.0520E-02	4.4223E-02	6.1867E-02
	IDJ1	4.0712E-02	4.6013E-02	7.0849E-02
	IDJLC	6.1404E-02	1.3185E-01	3.7488E-01

Table 8.6: BER considering ISI and CCI using the Precise Interference Model, for the ideal impulse response of the pulses and SNR=5dB, SIR=20dB, L=6.

α	Pulse	$t/T = 0.05$	$t/T = 0.10$	$t/T = 0.20$
0.25	RC	6.1198E-02	6.7321E-02	9.2810E-02
	BtRC	6.0367E-02	6.5887E-02	8.9371E-02
	SPLCP	5.7341E-02	6.1483E-02	8.0408E-02
	IPLCP	5.5879E-02	6.0117E-02	**7.9533E-02**
	ELP ($\beta = 1$)	5.4708E-02	5.9395E-02	8.0685E-02
	ELP ($\beta = 0.5$)	5.6521E-02	6.0684E-02	7.9762E-02
	IDJ1	5.3806E-02	**5.9144E-02**	8.3263E-02
	IDJLC	**5.2635E-02**	5.9215E-02	8.8894E-02
0.35	RC	6.0448E-02	6.6025E-02	8.9699E-02
	BtRC	5.9336E-02	6.4222E-02	8.5586E-02
	SPLCP	5.6876E-02	6.0961E-02	7.9728E-02
	IPLCP	5.5559E-02	5.9866E-02	7.9579E-02
	ELP ($\beta = 1$)	5.4533E-02	5.9321E-02	8.1041E-02
	ELP ($\beta = 0.5$)	5.6228E-02	6.0406E-02	**7.9565E-02**
	IDJ1	**5.3531E-02**	**5.9119E-02**	8.4371E-02
	IDJLC	5.3671E-02	6.9353E-02	1.4259E-01
0.5	RC	5.9373E-02	6.4284E-02	8.5733E-02
	BtRC	5.7894E-02	6.2149E-02	8.1427E-02
	SPLCP	5.6020E-02	6.0110E-02	**7.8979E-02**
	IPLCP	5.4947E-02	5.9458E-02	8.0016E-02
	ELP ($\beta = 1$)	5.4185E-02	5.9201E-02	8.1903E-02
	ELP ($\beta = 0.5$)	5.5665E-02	5.9926E-02	7.9448E-02
	IDJ1	**5.3101E-02**	**5.9139E-02**	8.6490E-02
	IDJLC	9.2024E-02	1.5766E-01	3.7762E-01

Table 8.7: BER considering ISI and CCI using the Precise Interference Model, for the ideal impulse response of the pulses and SNR=5dB, SIR=10dB, L=15.

α	Pulse	$t/T = 0.05$	$t/T = 0.10$	$t/T = 0.20$
0.25	RC	4.6480E-02	5.2458E-02	7.7989E-02
	BtRC	4.6058E-02	5.1392E-02	7.4663E-02
	SPLCP	4.4717E-02	4.8532E-02	6.6464E-02
	IPLCP	4.4246E-02	**4.8088E-02**	6.6194E-02
	ELP ($\beta = 1$)	4.3952E-02	4.8187E-02	6.7930E-02
	ELP ($\beta = 0.5$)	4.4445E-02	4.8241E-02	**6.6145E-02**
	IDJ1	4.3790E-02	4.8625E-02	7.1029E-02
	IDJLC	**4.3670E-02**	4.9705E-02	7.7545E-02
0.35	RC	4.6099E-02	5.1493E-02	7.4978E-02
	BtRC	4.5562E-02	5.0212E-02	7.1074E-02
	SPLCP	4.4547E-02	4.8284E-02	**6.5955E-02**
	IPLCP	4.4154E-02	**4.8051E-02**	6.6387E-02
	ELP ($\beta = 1$)	4.3916E-02	4.8242E-02	6.8382E-02
	ELP ($\beta = 0.5$)	4.4350E-02	4.8147E-02	6.6070E-02
	IDJ1	**4.3750E-02**	4.8820E-02	7.2309E-02
	IDJLC	4.5815E-02	6.0857E-02	1.3339E-01
0.5	RC	4.5581E-02	5.0257E-02	7.1214E-02
	BtRC	4.4930E-02	4.8883E-02	6.7296E-02
	SPLCP	4.4261E-02	**4.7965E-02**	**6.5553E-02**
	IPLCP	4.3994E-02	4.8066E-02	6.7126E-02
	ELP ($\beta = 1$)	4.3848E-02	4.8384E-02	6.9441E-02
	ELP ($\beta = 0.5$)	4.4180E-02	4.8035E-02	6.6203E-02
	IDJ1	**4.3701E-02**	4.9196E-02	7.4710E-02
	IDJLC	6.9156E-02	1.3854E-01	3.7550E-01

Table 8.8: BER considering ISI and CCI using the Precise Interference Model, for the ideal impulse response of the pulses and SNR=5dB, SIR=15dB, L=15.

α	Pulse	$t/T = 0.05$	$t/T = 0.10$	$t/T = 0.20$
0.25	RC	4.1755E-02	4.7642E-02	7.3062E-02
	BtRC	4.1471E-02	4.6704E-02	6.9787E-02
	SPLCP	4.0687E-02	4.4372E-02	6.1887E-02
	IPLCP	4.0539E-02	**4.4231E-02**	6.1826E-02
	ELP ($\beta = 1$)	**4.0529E-02**	4.4597E-02	6.3755E-02
	ELP ($\beta = 0.5$)	4.0594E-02	4.4249E-02	**6.1682E-02**
	IDJ1	4.0604E-02	4.5257E-02	6.7022E-02
	IDJLC	4.0822E-02	4.6660E-02	7.3824E-02
0.35	RC	4.1498E-02	4.6793E-02	7.0097E-02
	BtRC	4.1154E-02	4.5694E-02	6.6281E-02
	SPLCP	4.0614E-02	**4.4215E-02**	**6.1438E-02**
	IPLCP	**4.0521E-02**	4.4265E-02	6.2069E-02
	ELP ($\beta = 1$)	4.0536E-02	4.4694E-02	6.4239E-02
	ELP ($\beta = 0.5$)	4.0563E-02	4.4216E-02	6.1649E-02
	IDJ1	4.0640E-02	4.5523E-02	6.8357E-02
	IDJLC	4.3315E-02	5.8118E-02	1.3034E-01
0.5	RC	4.1166E-02	4.5733E-02	6.6418E-02
	BtRC	4.0788E-02	4.4617E-02	6.2652E-02
	SPLCP	4.0513E-02	**4.4072E-02**	**6.1158E-02**
	IPLCP	**4.0507E-02**	4.4417E-02	6.2908E-02
	ELP ($\beta = 1$)	4.0559E-02	4.4921E-02	6.5361E-02
	ELP ($\beta = 0.5$)	4.0520E-02	4.4223E-02	6.1867E-02
	IDJ1	4.0712E-02	4.6013E-02	7.0848E-02
	IDJLC	6.1404E-02	1.3185E-01	3.7488E-01

Table 8.9: BER considering ISI and CCI using the Precise Interference Model, for the ideal impulse response of the pulses and SNR=5dB, SIR=20dB, L=15.

α	Pulse	$t/T = 0.05$	$t/T = 0.10$	$t/T = 0.20$
0.25	RC	1.4413E-03	3.5098E-03	1.9568E-02
	BtRC	1.1534E-03	2.6904E-03	1.5308E-02
	SPLCP	4.6545E-04	8.5911E-04	4.9738E-03
	IPLCP	2.9962E-04	5.0309E-04	2.9109E-03
	ELP ($\beta = 1$)	2.1619E-04	3.5082E-04	2.0241E-03
	ELP ($\beta = 0.5$)	3.6339E-04	6.3675E-04	3.7147E-03
	IDJ1	1.7294E-04	2.8696E-04	**1.7287E-03**
	IDJLC	**1.4255E-04**	**2.7787E-04**	1.9881E-03
0.35	RC	1.1794E-03	2.7638E-03	1.5701E-02
	BtRC	8.5833E-04	1.8724E-03	1.0832E-02
	SPLCP	4.0279E-04	7.1352E-04	4.1121E-03
	IPLCP	2.7283E-04	4.4982E-04	2.5858E-03
	ELP ($\beta = 1$)	2.0659E-04	3.3532E-04	1.9399E-03
	ELP ($\beta = 0.5$)	3.3236E-04	5.6958E-04	3.3067E-03
	IDJ1	**1.6231E-04**	**2.7328E-04**	**1.6889E-03**
	IDJLC	2.6615E-04	1.6159E-03	3.5259E-02
0.5	RC	8.6775E-04	1.8985E-03	1.0983E-02
	BtRC	5.5305E-04	1.0708E-03	6.2203E-03
	SPLCP	3.0981E-04	5.1027E-04	2.8798E-03
	IPLCP	2.2976E-04	3.6932E-04	2.0933E-03
	ELP ($\beta = 1$)	1.8930E-04	3.0874E-04	1.8037E-03
	ELP ($\beta = 0.5$)	2.8104E-04	4.6376E-04	2.6579E-03
	IDJ1	**1.4762E-04**	**2.5639E-04**	**1.6789E-03**
	IDJLC	2.3220E-02	9.5759E-02	3.7189E-01

Table 8.10: BER considering ISI and CCI using the Precise Interference Model, for the ideal impulse response of the pulses and SNR=15dB, SIR=10dB, L=2.

α	Pulse	$t/T = 0.05$	$t/T = 0.10$	$t/T = 0.20$
0.25	RC	2.3141E-05	1.6729E-04	5.0368E-03
	BtRC	1.6959E-05	1.0287E-04	2.9686E-03
	SPLCP	5.6038E-06	1.7299E-05	3.4229E-04
	IPLCP	3.5762E-06	8.5723E-06	1.4955E-04
	ELP ($\beta = 1$)	2.6459E-06	5.6026E-06	8.9039E-05
	ELP ($\beta = 0.5$)	4.3399E-06	1.1650E-05	2.1750E-04
	IDJ1	2.1904E-06	**4.6168E-06**	**7.2404E-05**
	IDJLC	**1.9704E-06**	5.4645E-06	1.0513E-04
0.35	RC	1.7479E-05	1.0781E-04	3.1303E-03
	BtRC	1.1537E-05	5.5862E-05	1.4504E-03
	SPLCP	4.7884E-06	1.3353E-05	2.4993E-04
	IPLCP	3.2651E-06	7.4388E-06	1.2526E-04
	ELP ($\beta = 1$)	2.5429E-06	5.3386E-06	8.3980E-05
	ELP ($\beta = 0.5$)	3.9602E-06	1.0042E-05	1.8112E-04
	IDJ1	**2.0795E-06**	**4.4406E-06**	**7.0463E-05**
	IDJLC	6.7985E-06	1.3393E-04	1.7469E-02
0.5	RC	1.1695E-05	5.6947E-05	1.4804E-03
	BtRC	6.7997E-06	2.3892E-05	5.1690E-04
	SPLCP	3.6481E-06	8.4776E-06	1.4220E-04
	IPLCP	2.7787E-06	5.8479E-06	9.1865E-05
	ELP ($\beta = 1$)	2.3589E-06	4.9090E-06	7.6003E-05
	ELP ($\beta = 0.5$)	3.3519E-06	7.6899E-06	1.2973E-04
	IDJ1	**1.9269E-06**	**4.2646E-06**	**7.0848E-05**
	IDJLC	3.0642E-03	6.2992E-02	3.6769E-01

Table 8.11: BER considering ISI and CCI using the Precise Interference Model, for the ideal impulse response of the pulses and SNR=15dB, SIR=15dB, L=2.

α	Pulse	$t/T = 0.05$	$t/T = 0.10$	$t/T = 0.20$
0.25	RC	1.1473E-06	1.8367E-05	1.9825E-03
	BtRC	8.2559E-07	9.7526E-06	9.1173E-04
	SPLCP	2.7769E-07	1.2016E-06	5.1475E-05
	IPLCP	1.8771E-07	5.6918E-07	1.9602E-05
	ELP ($\beta = 1$)	1.4831E-07	3.7277E-07	1.1107E-05
	ELP ($\beta = 0.5$)	2.2180E-07	7.8914E-07	3.0334E-05
	IDJ1	**1.3059E-07**	**3.1920E-07**	**9.1021E-06**
	IDJLC	1.3146E-07	4.5622E-07	1.6165E-05
0.35	RC	8.5174E-07	1.0338E-05	9.8185E-04
	BtRC	5.5802E-07	4.6083E-06	3.3450E-04
	SPLCP	2.4021E-07	9.0299E-07	3.5150E-05
	IPLCP	1.7396E-07	4.9037E-07	1.6003E-05
	ELP ($\beta = 1$)	1.4414E-07	3.5677E-07	1.0452E-05
	ELP ($\beta = 0.5$)	2.0459E-07	6.7218E-07	2.4425E-05
	IDJ1	**1.2645E-07**	**3.1228E-07**	**8.9244E-06**
	IDJLC	7.0492E-07	2.8327E-05	1.1585E-02
0.5	RC	5.6533E-07	4.6960E-06	3.4038E-04
	BtRC	3.3314E-07	1.7401E-06	8.8409E-05
	SPLCP	1.8839E-07	5.4916E-07	1.7964E-05
	IPLCP	1.5286E-07	3.8309E-07	1.1304E-05
	ELP ($\beta = 1$)	1.3682E-07	3.3194E-07	9.4421E-06
	ELP ($\beta = 0.5$)	1.7734E-07	5.0554E-07	1.6570E-05
	IDJ1	**1.2098E-07**	**3.0976E-07**	**9.1556E-06**
	IDJLC	4.1406E-04	4.6557E-02	3.6512E-01

Table 8.12: BER considering ISI and CCI using the Precise Interference Model, for the ideal impulse response of the pulses and SNR=15dB, SIR=20dB, L=2.

α	Pulse	$t/T = 0.05$	$t/T = 0.10$	$t/T = 0.20$
0.25	RC	2.4688E-03	4.6240E-03	1.9957E-02
	BtRC	2.1321E-03	3.8011E-03	1.5896E-02
	SPLCP	1.1430E-03	1.6975E-03	6.2133E-03
	IPLCP	7.9628E-04	1.1313E-03	4.0873E-03
	ELP ($\beta = 1$)	5.7722E-04	8.2037E-04	3.0516E-03
	ELP ($\beta = 0.5$)	9.3811E-04	1.3575E-03	4.9394E-03
	IDJ1	4.4027E-04	6.4847E-04	**2.6252E-03**
	IDJLC	**3.0792E-04**	**5.2243E-04**	2.6792E-03
0.35	RC	2.1635E-03	3.8762E-03	1.6267E-02
	BtRC	1.7533E-03	2.9331E-03	1.1712E-02
	SPLCP	1.0237E-03	1.4855E-03	5.3583E-03
	IPLCP	7.3156E-04	1.0328E-03	3.7269E-03
	ELP ($\beta = 1$)	5.4862E-04	7.8282E-04	2.9422E-03
	ELP ($\beta = 0.5$)	8.7150E-04	1.2479E-03	4.5142E-03
	IDJ1	4.0351E-04	**6.0442E-04**	**2.5445E-03**
	IDJLC	**3.6072E-04**	1.7921E-03	3.5173E-02
0.5	RC	1.7660E-03	2.9620E-03	1.1850E-02
	BtRC	1.2964E-03	1.9826E-03	7.4101E-03
	SPLCP	8.2693E-04	1.1577E-03	4.0752E-03
	IPLCP	6.1861E-04	8.6939E-04	3.1531E-03
	ELP ($\beta = 1$)	4.9486E-04	7.1396E-04	2.7548E-03
	ELP ($\beta = 0.5$)	7.5290E-04	1.0616E-03	3.8119E-03
	IDJ1	**3.5039E-04**	**5.4246E-04**	**2.4697E-03**
	IDJLC	2.3552E-02	9.5507E-02	3.7178E-01

Table 8.13: BER considering ISI and CCI using the Precise Interference Model, for the ideal impulse response of the pulses and SNR=15dB, SIR=10dB, L=6.

α	Pulse	$t/T = 0.05$	$t/T = 0.10$	$t/T = 0.20$
0.25	RC	4.1208E-05	2.2371E-04	5.1776E-03
	BtRC	3.1886E-05	1.4724E-04	3.1402E-03
	SPLCP	1.2163E-05	3.1276E-05	4.3921E-04
	IPLCP	7.7766E-06	1.6376E-05	2.0560E-04
	ELP ($\beta = 1$)	5.5213E-06	1.0659E-05	1.2554E-04
	ELP ($\beta = 0.5$)	9.4715E-06	2.1784E-05	2.8997E-04
	IDJ1	4.2880E-06	**8.3781E-06**	**1.0087E-04**
	IDJLC	**3.3392E-06**	8.4584E-06	1.3190E-04
0.35	RC	3.2694E-05	1.5332E-04	3.3001E-03
	BtRC	2.3057E-05	8.7055E-05	1.6198E-03
	SPLCP	1.0487E-05	2.4814E-05	3.3058E-04
	IPLCP	7.0585E-06	1.4303E-05	1.7443E-04
	ELP ($\beta = 1$)	5.2534E-06	1.0098E-05	1.1845E-04
	ELP ($\beta = 0.5$)	8.6453E-06	1.9009E-05	2.4539E-04
	IDJ1	**3.9715E-06**	**7.8873E-06**	**9.7281E-05**
	IDJLC	8.3231E-06	1.4465E-04	1.7460E-02
0.5	RC	2.3328E-05	8.8576E-05	1.6516E-03
	BtRC	1.4517E-05	4.1508E-05	6.3429E-04
	SPLCP	8.0102E-06	1.6406E-05	1.9802E-04
	IPLCP	5.8884E-06	1.1265E-05	1.3028E-04
	ELP ($\beta = 1$)	4.7626E-06	9.1418E-06	1.0699E-04
	ELP ($\beta = 0.5$)	7.2737E-06	1.4803E-05	1.8052E-04
	IDJ1	**3.5228E-06**	**7.2758E-06**	**9.5804E-05**
	IDJLC	3.1841E-03	6.2750E-02	3.6765E-01

Table 8.14: BER considering ISI and CCI using the Precise Interference Model, for the ideal impulse response of the pulses and SNR=15dB, SIR=15dB, L=6.

α	Pulse	$t/T = 0.05$	$t/T = 0.10$	$t/T = 0.20$
0.25	RC	1.4425E-06	2.0522E-05	2.0027E-03
	BtRC	1.0555E-06	1.1182E-05	9.3195E-04
	SPLCP	3.6652E-07	1.4806E-06	5.6308E-05
	IPLCP	2.4510E-07	7.0818E-07	2.1833E-05
	ELP ($\beta = 1$)	1.8911E-07	4.5980E-07	1.2405E-05
	ELP ($\beta = 0.5$)	2.9146E-07	9.7854E-07	3.3517E-05
	IDJ1	1.6176E-07	**3.8536E-07**	**1.0081E-05**
	IDJLC	**1.5380E-07**	5.1845E-07	1.7249E-05
0.35	RC	1.0873E-06	1.1827E-05	1.0024E-03
	BtRC	7.2527E-07	5.4399E-06	3.4912E-04
	SPLCP	3.1692E-07	1.1201E-06	3.8799E-05
	IPLCP	2.2611E-07	6.1030E-07	1.7876E-05
	ELP ($\beta = 1$)	1.8275E-07	4.3858E-07	1.1663E-05
	ELP ($\beta = 0.5$)	2.6827E-07	8.3552E-07	2.7108E-05
	IDJ1	**1.5500E-07**	**3.7369E-07**	**9.8446E-06**
	IDJLC	7.4191E-07	2.8905E-05	1.1586E-02
0.5	RC	7.3418E-07	5.5421E-06	3.5532E-04
	BtRC	4.3898E-07	2.1193E-06	9.5179E-05
	SPLCP	2.4681E-07	6.8713E-07	2.0122E-05
	IPLCP	1.9637E-07	4.7539E-07	1.2667E-05
	ELP ($\beta = 1$)	1.7178E-07	4.0521E-07	1.0511E-05
	ELP ($\beta = 0.5$)	2.3103E-07	6.2992E-07	1.8516E-05
	IDJ1	**1.4566E-07**	**3.6480E-07**	**1.0020E-05**
	IDJLC	4.2673E-04	4.6481E-02	3.6511E-01

Table 8.15: BER considering ISI and CCI using the Precise Interference Model, for the ideal impulse response of the pulses and SNR=15dB, SIR=20dB, L=6.

α	Pulse	$t/T = 0.05$	$t/T = 0.10$	$t/T = 0.20$
0.25	RC	2.7603E-03	4.9073E-03	2.0049E-02
	BtRC	2.4182E-03	4.0899E-03	1.6037E-02
	SPLCP	1.3748E-03	1.9543E-03	6.5036E-03
	IPLCP	9.8200E-04	1.3444E-03	4.3845E-03
	ELP ($\beta = 1$)	7.2080E-04	9.9117E-04	3.3299E-03
	ELP ($\beta = 0.5$)	1.1448E-03	1.5911E-03	5.2374E-03
	IDJ1	5.4987E-04	7.8421E-04	2.8772E-03
	IDJLC	**3.7430E-04**	**6.1156E-04**	**2.8747E-03**
0.35	RC	2.4502E-03	4.1646E-03	1.6403E-02
	BtRC	2.0270E-03	3.2204E-03	1.1917E-02
	SPLCP	1.2424E-03	1.7302E-03	5.6564E-03
	IPLCP	9.0631E-04	1.2350E-03	4.0213E-03
	ELP ($\beta = 1$)	6.8567E-04	9.4694E-04	3.2161E-03
	ELP ($\beta = 0.5$)	1.0689E-03	1.4725E-03	4.8130E-03
	IDJ1	5.0286E-04	**7.2933E-04**	**2.7868E-03**
	IDJLC	**3.8943E-04**	1.8430E-03	3.5147E-02
0.5	RC	2.0402E-03	3.2495E-03	1.2052E-02
	BtRC	1.5424E-03	2.2514E-03	7.6851E-03
	SPLCP	1.0190E-03	1.3766E-03	4.3764E-03
	IPLCP	7.7167E-04	1.0496E-03	3.4375E-03
	ELP ($\beta = 1$)	6.1888E-04	8.6463E-04	3.0189E-03
	ELP ($\beta = 0.5$)	9.3162E-04	1.2677E-03	4.1079E-03
	IDJ1	**4.3401E-04**	**6.5049E-04**	**2.6953E-03**
	IDJLC	2.3622E-02	9.5424E-02	3.7176E-01

Table 8.16: BER considering ISI and CCI using the Precise Interference Model, for the ideal impulse response of the pulses and SNR=15dB, SIR=10dB, L=15.

α	Pulse	$t/T = 0.05$	$t/T = 0.10$	$t/T = 0.20$
0.25	RC	4.9485E-05	2.4368E-04	5.2156E-03
	BtRC	3.9009E-05	1.6381E-04	3.1871E-03
	SPLCP	1.5718E-05	3.7752E-05	4.7105E-04
	IPLCP	1.0109E-05	2.0255E-05	2.2575E-04
	ELP ($\beta = 1$)	7.1033E-06	1.3221E-05	1.3937E-04
	ELP ($\beta = 0.5$)	1.2299E-05	2.6679E-05	3.1499E-04
	IDJ1	5.4057E-06	1.0245E-05	**1.1179E-04**
	IDJLC	**3.9967E-06**	**9.7815E-06**	1.4146E-04
0.35	RC	3.9927E-05	1.7021E-04	3.3464E-03
	BtRC	2.8825E-05	9.9572E-05	1.6682E-03
	SPLCP	1.3615E-05	3.0285E-05	3.5801E-04
	IPLCP	9.1678E-06	1.7753E-05	1.9245E-04
	ELP ($\beta = 1$)	6.7381E-06	1.2507E-05	1.3158E-04
	ELP ($\beta = 0.5$)	1.1239E-05	2.3405E-05	2.6803E-04
	IDJ1	**4.9649E-06**	**9.5771E-06**	**1.0755E-04**
	IDJLC	8.8365E-06	1.4793E-04	1.7457E-02
0.5	RC	2.9142E-05	1.0124E-04	1.7003E-03
	BtRC	1.8623E-05	4.9360E-05	6.7129E-04
	SPLCP	1.0446E-05	2.0379E-05	2.1823E-04
	IPLCP	7.6112E-06	1.4024E-05	1.4482E-04
	ELP ($\beta = 1$)	6.0651E-06	1.1272E-05	1.1889E-04
	ELP ($\beta = 0.5$)	9.4562E-06	1.8374E-05	1.9907E-04
	IDJ1	**4.3369E-06**	**8.7134E-06**	**1.0526E-04**
	IDJLC	3.2176E-03	6.2690E-02	3.6764E-01

Table 8.17: BER considering ISI and CCI using the Precise Interference Model, for the ideal impulse response of the pulses and SNR=15dB, SIR=15dB, L=15.

α	Pulse	$t/T = 0.05$	$t/T = 0.10$	$t/T = 0.20$
0.25	RC	1.5618E-06	2.1270E-05	2.0085E-03
	BtRC	1.1501E-06	1.1693E-05	9.3795E-04
	SPLCP	4.0464E-07	1.5909E-06	5.7926E-05
	IPLCP	2.6962E-07	7.6427E-07	2.2606E-05
	ELP ($\beta = 1$)	2.0621E-07	4.9487E-07	1.2861E-05
	ELP ($\beta = 0.5$)	3.2131E-07	1.0543E-06	3.4605E-05
	IDJ1	1.7448E-07	**4.1150E-07**	**1.0424E-05**
	IDJLC	**1.6234E-07**	5.4137E-07	1.7612E-05
0.35	RC	1.1840E-06	1.2358E-05	1.0084E-03
	BtRC	7.9530E-07	5.7491E-06	3.5363E-04
	SPLCP	3.4990E-07	1.2069E-06	4.0040E-05
	IPLCP	2.4832E-07	6.5883E-07	1.8531E-05
	ELP ($\beta = 1$)	1.9908E-07	4.7168E-07	1.2090E-05
	ELP ($\beta = 0.5$)	2.9553E-07	9.0122E-07	2.8033E-05
	IDJ1	**1.6654E-07**	**3.9774E-07**	**1.0167E-05**
	IDJLC	7.5366E-07	2.9082E-05	1.1586E-02
0.5	RC	8.0497E-07	5.8566E-06	3.5992E-04
	BtRC	4.8419E-07	2.2667E-06	9.7392E-05
	SPLCP	2.7206E-07	7.4329E-07	2.0875E-05
	IPLCP	2.1473E-07	5.1276E-07	1.3147E-05
	ELP ($\beta = 1$)	1.8623E-07	4.3447E-07	1.0888E-05
	ELP ($\beta = 0.5$)	2.5394E-07	6.8027E-07	1.9196E-05
	IDJ1	**1.5544E-07**	**3.8599E-07**	**1.0320E-05**
	IDJLC	4.3063E-04	4.6460E-02	3.6510E-01

Table 8.18: BER considering ISI and CCI using the Precise Interference Model, for the ideal impulse response of the pulses and SNR=15dB, SIR=20dB, L=15.

Appendix C

8.3 Codes

All the codes used in this work are available in the following link:

`https://github.com/LaboratorioTICs-UChile/`

Appendix D

8.4 List of Publications

Conference

1. **J. Aranda Cubillo**, C. Azurdia, S. Montejo-Sanchez, I. Jirón, and R. Demo Souza, "Error probability analysis of Nyquist-I pulses in intersymbol and cochannel interference," in 2018 *IEEE Symposium on Computers and Communications (ISCC)*, Natal, Brazil, Jun. 2018.

2. S. Montejo-Sanchez, C. Azurdia, **J. Aranda Cubillo**, R. Demo Souza , E Garcia Fernandez and I.Soto, "Energy-Efficient Transmission Strategies with Multiple Radios in Cognitive Radio: Beyond Rendezvous," *2018 IEEE 11th Colombian Conference on Communications and Computing (COLCOM)*, Medellín, Colombia, May. 2018.

3. **J. Aranda Cubillo**, C. A. Azurdia-Meza, S. Montejo-Sánchez, F. M. Maciel-Barboza and I. Jirón, "Analysis of the exponential linear pulse in baseband digital communication systems," *2017 IEEE 9th Latin-American Conference on Communications (LATINCOM)*, Guatemala City, Nov. 2017, pp. 1-6. doi: 10.1109/LATINCOM.2017.8240170.

Bibliography

[1] J. Rodriguez, *Fundamentals of 5G mobile networks*. John Wiley & Sons, 2015.

[2] N. C. Beaulieu and M. O. Damen, "Parametric construction of Nyquist-I pulses," *IEEE Transactions on Communications*, vol. 52, pp. 2134–2142, Dec 2004.

[3] C. Azurdia-Meza, K. Lee, and K. Lee, "ISI-free linear combination pulses with better performance," *IEICE transactions on communications*, vol. 96, no. 2, pp. 635–638, 2013.

[4] H. F. Arraño and C. Azurdia-Meza, "ICI reduction in OFDM systems using a new family of Nyquist-I pulses," in *2014 IEEE Latin-America Conference on Communications (LATINCOM)*, pp. 1–6, Nov 2014.

[5] D. Zabala-Blanco, G. Campuzano, C. A. Azurdia-Meza, and S. Montejo-Sánchez, "Performance enhancement in OFDM systems with ICI utilizing the improved double jump linear combination pulse," in *Communications (LATINCOM), 2017 IEEE 9th Latin-American Conference on*, pp. 1–6, IEEE, 2017.

[6] N. C. Beaulieu, "The evaluation of error probabilities for intersymbol and cochannel interference," *IEEE Transactions on Communications*, vol. 39, no. 12, pp. 1740–1749, 1991.

[7] N. D. Alexandru and A. L. O. Balan, "Improved nyquist filters with piece-wise parabolic frequency characteristics," *IEEE Communications Letters*, vol. 15, no. 5, pp. 473–475, 2011.

[8] C. A. Azurdia-Meza, C. Estevez, A. D. Firoozabadi, and I. Soto, "Evaluation of the sinc parametric linear combination pulse in digital communication systems," in *2016 8th IEEE Latin-American Conference on Communications (LATINCOM)*, pp. 1–5, Nov 2016.

[9] A. L. Balan and N. D. Alexandru, "Construction of new ISI-free pulses using a linear combination of two polynomial pulses," *Telecommunication Systems*, vol. 59, no. 4, pp. 469–476, 2015.

[10] N. C. Beaulieu and A. A. Abu-Dayya, "Bandwidth efficient QPSK in cochannel interference and fading," *IEEE Transactions on Communications*, vol. 43, no. 9, pp. 2464–2474, 1995.

[11] S.-C. Lin and S.-T. Chiang, "Performance of diversity reception for QPSK with cochannel interference in a flat Rayleigh fading channel [mobile radio]," in *Vehicular Technology Conference, 2004. VTC2004-Fall. 2004 IEEE 60th*, vol. 3, pp. 1825–1829, IEEE, 2004.

[12] J. Cheng, N. C. Beaulieu, and X. Zhang, "Precise BER analysis of dual-channel reception of QPSK in Nakagami fading and cochannel interference," *IEEE Communications letters*, vol. 9, no. 4, pp. 316–318, 2005.

[13] D. Zabala-Blanco, G. Campuzano, and C. A. Azurdia-Meza, "General Nyquist-I pulses to mitigate carrier frequency offset in DVB-C-OFDM systems," in *Electronics, Electrical Engineering and Computing (INTERCON), 2017 IEEE XXIV International Conference on*, pp. 1–4, IEEE, 2017.

[14] S. Kamal, C. Azurdia-Meza, and K. Lee, "Nyquist-I pulses designed to suppress the effect of ICI power in OFDM systems," in *Wireless Communications and Mobile Computing Conference (IWCMC), 2015 International*, pp. 1412–1417, IEEE, 2015.

[15] H. Nyquist, "Certain topics in telegraph transmission theory," *Transactions of the American Institute of Electrical Engineers*, vol. 47, pp. 617–644, April 1928.

[16] N. C. Beaulieu, "Introduction to "Certain topics in telegraph transmission theory"," *Proceedings of the IEEE*, vol. 90, no. 2, pp. 276–279, 2002.

[17] P. Sandeep, S. Chandan, and A. K. Chaturvedi, "ISI-free pulses with reduced sensitivity to timing errors," *IEEE Communications Letters*, vol. 9, no. 4, pp. 292–294, 2005.

[18] C. A. Azurdia-Meza, K. Lee, and K. Lee, "PAPR Reduction in SC-FDMA by Pulse Shaping Using Parametric Linear Combination Pulses," *IEEE Communications Letters*, vol. 16, pp. 2008–2011, December 2012.

[19] S. Chandan, P. Sandeep, and A. K. Chaturvedi, "A family of ISI-free polynomial pulses," *IEEE Communications Letters*, vol. 9, no. 6, pp. 496–498, 2005.

[20] A. L. Balan and N. D. Alexandru, "Two improved Nyquist filters with piece-wise rectangular-polynomial frequency characteristics," *AEU-International Journal of Electronics and Communications*, vol. 66, no. 11, pp. 880–883, 2012.

[21] J. Aranda-Cubillo, C. A. Azurdia-Meza, S. Montejo-Sánchez, F. M. Maciel-Barboza, and I. Jiron, "Analysis of the exponential linear pulse in baseband digital communication systems," in *2017 IEEE 9th Latin-American Conference on Communications (LATINCOM)*, pp. 1–6, Nov 2017.

[22] C. A. Azurdia-Meza, C. Estevez, A. D. Firoozabadi, and I. Soto, "Evaluation of the sinc parametric linear combination pulse in digital communication systems," in *Communications (LATINCOM), 2016 8th IEEE Latin-American Conference on*, pp. 1–5, IEEE, 2016.

[23] H. F. Arrano and C. A. A. Meza, "ICI reduction in OFDM systems using a new family of Nyquist-I pulses," *IEEE Latin America Transactions*, vol. 13, pp. 3556–3561, Nov 2015.

[24] N. D. Alexandru and N. Cleju, "Implementation considerations regarding improved Nyquist filters," in *Electronics, Computers and Artificial Intelligence (ECAI), 2013 International Conference on*, pp. 1–4, IEEE, 2013.

[25] A. L. Balan and N. D. Alexandru, "Improved Nyquist pulses produced by a filter with senary piece-wise polynomial frequency characteristic," *Advances in Electrical and Computer Engineering*, vol. 14, no. 2, pp. 129–134, 2014.

[26] S. Kamal, C. A. A. Meza, N. H. Tran, and K. Lee, "Low-PAPR hybrid filter for SC-FDMA," *IEEE Communications Letters*, vol. 21, no. 4, pp. 905–908, 2017.

[27] D. Zabala-Blanco, C. A. Azurdia-Meza, , and G. Campuzano, "BER reduction in OFDM systems susceptible to ICI using the exponential linear pulse," *Proc. XXIV International Congress of Electrical Engineering, Electronics and Computing*, Aug. 2017.

[28] J. Proakis, "Digital communications," *McGraw-Hill, New York*, 2000.

[29] C.-Y. Yao, "A design method of hybrid analog/asymmetrical-FIR pulse-shaping filters with an eye-opening control option against receiver timing jitter," *ETRI journal*, vol. 32, no. 6, pp. 911–920, 2010.

[30] M. Bobula, A. Prokes, and K. Danek, "Nyquist filters with alternative balance between time- and frequency-domain parameters," *EURASIP J. Adv. Sig. Proc.*, vol. 2010, Dec. 2010.

[31] N. D. Alexandru and A. L. Balan, "Investigation of the mechanism of improvement in improved nyquist filters," *IET Signal Processing*, vol. 8, pp. 95–105, Feb 2014.

[32] P. Tan and N. C. Beaulieu, "Analysis of the effects of Nyquist pulse-shaping on the performance of OFDM systems with carrier frequency offset," *Transactions on Emerging Telecommunications Technologies*, vol. 20, no. 1, pp. 9–22, 2009.

[33] S. Kamal, C. A. Azurdia-Meza, and K. Lee, "Family of Nyquist-I pulses to enhance orthogonal frequency division multiplexing system performance," *IETE Technical Review*, vol. 33, no. 2, pp. 187–198, 2016.

[34] H. G. Myung, J. Lim, and D. J. Goodman, "Peak-to-average power ratio of single carrier FDMA signals with pulse shaping," in *Personal, Indoor and Mobile Radio Communications, 2006 IEEE 17th International Symposium on*, pp. 1–5, IEEE, 2006.

[35] C. An and H.-G. Ryu, "Design and performance comparison of W-OFDM under the nonlinear HPA environment," *Wireless Personal Communications*, vol. 98, no. 1, pp. 983–999, 2018.

[36] N. C. Beaulieu and J. Cheng, "Precise error-rate analysis of bandwidth-efficient BPSK in Nakagami fading and cochannel interference," *IEEE Transactions on Communications*, vol. 52, no. 1, pp. 149–158, 2004.

[37] R. C. Palat, A. Annamalai, and J. H. Reed, "Precise error rate analysis of bandlim-

ited BPSK system with timing errors and cochannel interference under generalized fast fading channels," in *Vehicular Technology Conference, 2008. VTC Spring 2008. IEEE*, pp. 1306–1310, IEEE, 2008.

[38] C. A. Azurdia-Meza, A. Falchetti, H. F. Arraño, S. Kamal, and K. S. Lee, "Evaluation of the improved parametric linear combination pulse in digital baseband communication systems," in *2015 International Conference on Information and Communication Technology Convergence (ICTC)*, pp. 485–487, IEE, 2015.

[39] C. A. Azurdia-Meza, "Evaluation of ISI-free parametric linear combination pulses in digital communication systems," *Wireless Pers. Commun*, vol. 84, pp. 1591–1598, Sep. 2015.

[40] D. Zabala-Blanco, G. Campuzano, and C. A. Azurdia-Meza, "Mitigated ICI in DVB-C2-OFDM systems utilizing the optimal improved double jump 1 filter," in *Electrical, Electronics Engineering, Information and Communication Technologies (CHILECON), 2017 CHILEAN Conference on*, pp. 1–4, IEEE, 2017.

[41] N. D. Alexandru and A. Balan, "ISI-free pulses produced by improved Nyquist filter with piece-wise linear characteristic," *Electronics Letters*, vol. 47, no. 4, pp. 256–257, 2011.

[42] N. D. Alexandru and A. L. Balan, "Design and Optimization of Modified K-Exponential Filter," in *2018 International Conference on Communications (COMM)*, pp. 71–74, IEEE, 2018.

[43] A. Assalini and A. M. Tonello, "Improved nyquist pulses," *IEEE Communications Letters*, vol. 8, no. 2, pp. 87–89, 2004.

[44] Y.-D. Wei and Y.-F. Chen, "Peak-to-average power ratio (PAPR) reduction by pulse shaping using the K-exponential filter," *IEICE transactions on communications*, vol. 93, no. 11, pp. 3180–3183, 2010.

[45] M. Avriel, *Nonlinear programming: analysis and methods*. Courier Corporation, 2003.

[46] B. Châtelain and F. Gagnon, "Peak-to-average power ratio and intersymbol interference reduction by nyquist pulse optimization," in *Vehicular Technology Conference, 2004. VTC2004-Fall. 2004 IEEE 60th*, vol. 2, pp. 954–958, IEEE, 2004.

[47] A. Boonkajay, T. Obara, T. Yamamoto, and F. Adachi, "Excess-bandwidth transmit filtering based on minimization of variance of instantaneous transmit power for low-PAPR SC-FDE," *IEICE Transactions on Communications*, vol. 98, no. 4, pp. 673–685, 2015.

[48] P. Tan and N. C. Beaulieu, "A novel pulse-shaping for reduced ICI in OFDM systems," in *Vehicular Technology Conference, 2004. VTC2004-Fall. 2004 IEEE 60th*, vol. 1, pp. 456–459, IEEE, 2004.

[49] P. K. Yadav, V. K. Dwivedi, V. Karwal, and J. Gupta, "A new windowing function to

reduce ICI in OFDM systems," *International Journal of Electronics Letters*, vol. 2, no. 1, pp. 2–7, 2014.

[50] V. Kumbasar and O. Kucur, "ICI reduction in OFDM systems by using improved sinc power pulse," *Digital Signal Processing*, vol. 17, no. 6, pp. 997–1006, 2007.

[51] S. Kamal, C. A. Azurdia-Meza, and K. Lee, "Suppressing the effect of ICI power using dual sinc pulses in OFDM-based systems," *AEU-International Journal of Electronics and Communications*, vol. 70, no. 7, pp. 953–960, 2016.

[52] M. Mohri and M. Hamamura, "ISI-free power roll-off pulse," *IEICE transactions on fundamentals of electronics, communications and computer sciences*, vol. 92, no. 10, pp. 2495–2497, 2009.

[53] S. Kamal, C. A. Azurdia-Meza, and K. Lee, "Subsiding OOB emission and ICI power using iPOWER pulse in OFDM systems," *Adv. Electr. Comput. Eng*, vol. 16, no. 1, pp. 79–86, 2016.